Asymptotic optimal detection for MIMO communication systems

Djelili Radji

Department of Electrical & Computer Engineering
McGill University
Montreal, Canada

December 2013

A thesis submitted to McGill University in partial fulfillment of the requirements for the degree of Master of Engineering.

2013/12/10

Abstract

The high complexity of optimal detection for spatial multiplexing MIMO systems motivates the need for more practical alternatives. Among many suboptimal schemes reported in the literature, very few can be proven to provide close to optimal performance with low fixed complexity. In this thesis, we consider a class of list-based detectors that first generate a list of candidate decision vectors, and then the best candidate in the list is chosen as the final decision. First, we perform a diversity analysis of such schemes and derive sufficient conditions for achieving optimal performance asymptotically. We then introduce the Sel-MMSE-OSIC algorithm that employs list-based detection and a diversity maximizing channel partition procedure that yields asymptotic optimality. Then we propose the MMSE-ISTP scheme which is an improved asymptotically optimal fixed complexity algorithm that provides substantial complexity reductions over Sel-MMSE-OSIC. This scheme is based on simplified channel partition and efficient tree based list detection. Simulations results show that Sel-MMSE-OSIC and MMSE-ISTP yield performances that are nearly indistinguishable from optimal at almost all SNR levels for space uncorrelated systems. To achieve further reductions in complexity for large constellation sizes, a variable complexity version of the MMSE-ISTP scheme is proposed. The resulting algorithm is a variable complexity scheme that operates on a very small subset of candidates, and employs an improved channel partition preprocessing that not only reduces complexity but also guarantees high SNR optimality over space uncorrelated channels. Simulations results confirm that the proposed scheme provides significant complexity reductions over conventional variable complexity detection schemes.

Sommaire

La haute complexité associée à la méthode optimale de détection pour les systèmes MIMO utilisant le multiplexage spatial motive la recherche d'alternatives plus pratiques. Parmi les nombreuses méthodes non optimales proposées dans la littérature, très peu peuvent théoriquement guarantir une performance quasi-optimale avec une complexité fixe et relativement basse. Dans cette thèse, nous considérons une classe de détecteurs utilisant une liste, qui premièrement génèrent une liste de vecteurs candidats et ensuite choisissent le meilleur candidat dans cette liste comme décision finale. Dans un premier temps nous faisons une analyse de diversité pour ces méthodes et dérivons des conditions suffisantes pour atteindre asymptotiquement une performance optimale. Nous introduisons ensuite l'algorithme Sel-MMSE-OSIC qui emploie une méthode de détection utilisant une liste et une méthode de partition du canal à diversité maximale permettant l'optimalité asymptotique. Après, nous proposons l'algorithme MMSE-ISTP qui apporte des réductions substantielles de complexité comparé à l'algorithme Sel-MMSE-OSIC tout en ayant une complexité fixe et étant asymptotiquement optimal. Cette méthode est basée sur une simplification de la partition du canal et une méthode de détection efficace utilisant une liste générée à partir d'un arbre de détection. Les résultats des simulations par ordinateur démontrent que Sel-MMSE-OSIC et MMSE-ISTP délivrent des performances pratiquement indissociables de la performance optimale pour tous les rapports signal-sur-bruit pour des canaux non corrélés dans l'espace. Pour atteindre des réductions additionnelles de complexité pour les grandes constellations, une version de MMSE-ISTP à complexité variable est ensuite proposée. L'algorithme qui en résulte est un algorithme à complexité variable qui opère sur un nombre réduit de candidats et emploie une méthode de partition du canal améliorée qui non seulement réduit la complexité mais aussi guarantit l'optimalité pour des

rapports signal-sur-bruit élevés pour des canaux non corrélés dans l'espace. Les résultats des simulations par ordinateur confirment que l'algorithme proposé permet des réductions significatives de la complexité comparé aux techniques à complexité variable conventionnelles.

Acknowledgements

First and foremost, I would like to thank my supervisor Professor Harry Leib for his guidance, discussions, and financial support during the course of my master's degree. His patience and critical insight were instrumental in the completion of this work.

I also would like to thank my fellow graduate students from Prof. Leib's laboratory for the insightful discussions and most importantly for their friendship. In particular, I am grateful to Wenjing Lin, Yi Wang, Scott Monk, Xiaofei Shao, Reza Mohajerani, Sahabul Alam, Habibul Islam, Andres Contreras, Tomas Sollund, Yischeng Chen, Bharathram Sivasubramanian, Usa Vilaipornsawai, Marthe Kassouf and Isabel Deslauriers.

Then I want to express my deep gratitude to my parents, my wife's parents, my brother and my sister for their continued support. Finally, I thank my beautiful wife for being by my side through these years. This work would not have been possible without her.

Contents

List of Figures

List of Tables

List of Acronyms

MIMO	Multiple-Input Multiple-Output
CSCG	Circular Symmetric Complex Gaussian
ML	Maximum Likelihood
SD	Sphere Decoding
V-BLAST	Vertical Bell Labs Space-Time
QAM	Quadrature Amplitude Modulation
PSK	Phase Shift Keying
QPSK	Quadrature PSK
SNR	Signal-to-Noise Ratio
ZF	Zero-Forcing
MMSE	Minimum Mean Square Error
SIC	Successive Interference Cancellation
OSIC	Ordered SIC

Notational convention

$(.)^T$	Transposition
$(.)^H$	Conjugate transpose
$\mathcal{E}[.]$	Expectation operation
$\|.\|$	Euclidean norm
$\mathbf{b}$	Column vector $\mathbf{b}$
$\mathbf{A}$	Matrix $\mathbf{A}$
$\mathbf{a}_i$	$= [\mathbf{A}]_i$, i-th column vector of matrix $\mathbf{A}$
$\mathbf{b}_{(i:j)}$	column vector composed of the i-th through j-th elements of vector $\mathbf{b}$
$\mathbf{A}_{(i:j,k:l)}$	matrix composed of the elements between the i-th through j-th rows and k-th through l-th column of matrix $\mathbf{A}$
$\mathbf{I}_N$	$N \times N$ identity matrix
$\mathbf{e}_i$	i-th unit vector of appropriate dimension
$\mathbf{0}$	zero vector or matrix of appropriate dimension
$\mathcal{A}$	set $\mathcal{A}$
$\|\mathcal{A}\|$	cardinality of set $\mathcal{A}$
$f_X(x)$	Probability density function (PDF) of random variable X
$F_X(x)$	Cumulative distribution function (CDF) of random variable X
$\Pr(A)$	Probability that the event A occurs

Chapter 1

Introduction

The use of multiple antennas at the transmitter and receiver yields significant capacity gains [1]. Suitable assignment of signal dimensions to transmit antennas and associated transmission power allocation result in important bandwidth efficiency gains with various system complexities [2]. The Vertical Bell Laboratories Layered Space-Time (V-BLAST) architecture [3, 4] launched a multiple-input-multiple-output (MIMO) wireless communications technology providing high bandwidth efficiency through spatial multiplexing (SM) [4,5]. In this architecture, for each channel usage, each transmit antenna transmits an independent symbol. However the optimal receiver, which implements maximum likelihood (ML) detection, solves a minimization problem over a candidates set with a cardinality that grows exponentially with the number of transmit antennas [6]. Hence ML detection using an exhaustive search approach has a complexity that is prohibitively large for most practical applications. To alleviate this problem, suboptimal approaches based on successive interference cancellation (SIC), using the zero-forcing (ZF) or the minimum mean-squared error (MMSE) criteria with optimized ordering, are commonly employed [3, 4, 7]. Analytical and numerical results have shown that because of the diversity loss incurred,

such schemes perform rather poorly compared to ML detection [8–10]. Therefore, other alternatives capable of bridging this performance gap with reasonable complexity are of significant interest for practical applications.

Sphere decoding (SD) [11, 12] is a detection technique that exploits the lattice structure of the system model to provide significant complexity reductions with respect to the exhaustive ML receiver without any performance degradation. However, SD has a variable complexity that depends on the channel realization and operating SNR. Furthermore, its expected complexity remains exponential in the number of transmit antennas for any finite SNR [13], making its integration into practical communication systems problematic. Many variants of the SD algorithm, providing various performance-complexity tradeoffs, have been reported in the literature. These include depth-first [14–16], breadth-first [17–19] and best-first [20–22] search schemes. The "fixed-complexity sphere decoder" (FSD) of [23–25] relieves the problems associated with variations in complexity while guaranteeing high SNR optimality. In addition, the FSD, unlike the SD, has a parallelizable structure that can be exploited to provide higher throughputs [23]. In its basic form SD is not applicable to under-determined systems, i.e systems with more transmit than receive antennas. However, a regularized SD technique operating on an extended channel matrix [11, 20, 26–28] can be employed for arbitrary number of transmit and receive antennas.

Several other alternatives have been proposed to improve the performance of the conventional V-BLAST receivers. Among them, is the class of list-based detectors, which are analogous to the Chase decoding algorithm in the sense that they first generate a list of candidate decision vectors, and then the best candidate in the list is chosen as the final decision [29–32]. Despite good error rate performances assessed through computer simulations only, no analytical results proving close to optimal performance were reported. For example, in [33] we showed that compared to ML detection, the "Generalized parallel

interference cancellation" (GPIC) algorithm of [30] performs poorly for under-determined systems and incurs a diversity loss at high SNR for over-determined systems.

1.1 Thesis contribution

In this thesis, we propose new low complexity list-based detectors with guaranteed asymptotic optimality for space uncorrelated channels. We first perform a diversity analysis of a class of list-based detectors which includes the GPIC algorithm from [30] that employ channel matrix partition and standard ZF/MMSE-OSIC detection techniques for candidates list generation. From this we obtain sufficient conditions for such receivers to provide optimal ML performance at high SNR.

We then introduce the "Selection based MMSE-OSIC" (Sel-MMSE-OSIC) scheme which builds on GPIC but employs a smaller list size and an improved channel partition technique that yields asymptotic optimal performance for all systems configurations on space uncorrelated channels. Although Sel-MMSE-OSIC has better performance and lower complexity than GPIC, it increases the complexity with respect to FSD [23, 25] by a factor of 2 to 3 [33]. Hence, next we propose the "MMSE-Incremental Selection and Tree based Processing" (MMSE-ISTP) algorithm which has lower complexity than the FSD and Sel-MMSE-OSIC schemes and has guaranteed high SNR optimality over space uncorrelated channels for all systems configurations. It improves over the Sel-MMSE-OSIC scheme in two aspects: first, it employs a simplified channel partition technique based on "incremental" antenna selection. This partition method not only has lower complexity than the method used by Sel-MMSE-OSIC but it also yields asymptotic optimality. Second, it employs an efficient tree based approach to lower the complexity of the candidates list generation. In addition, contrary to FSD which requires channel regularization to be appli-

cable for under-determined systems, the MMSE-ISTP is suitable with or without channel regularization for all system configurations, thus providing additional flexibility.

While the fixed complexity feature of the MMSE-ISTP scheme is very attractive for practical implementation since parallelism and pipelining may be exploited to increase throughput, a variable complexity alternative can be considered when the list size becomes large. Thus, we further develop a variable complexity version of the MMSE-ISTP scheme that achieves lower average complexity while maintaining same performance as the fixed complexity approach. The resulting algorithm is a variable complexity scheme with improved channel partition preprocessing, that not only reduces complexity but also guarantees high SNR optimality for all system configurations over space uncorrelated channels.

The material presented in this thesis is based on our publications in [33–36].

1.2 Thesis outline

The rest of this thesis is organized as follows: chapter 2 presents the MIMO V-BLAST system model, briefly reviews conventional receivers and through a detailed diversity analysis, obtains sufficient conditions for list-based detectors to perform asymptotically optimal. The fixed complexity asymptotically optimal Sel-MMSE-OSIC and MMSE-ISTP schemes are then introduced in chapter 3 along with a complexity analysis. After that in chapter 4, the MMSE-ISVTP scheme which is a variable complexity extension of MMSE-ISTP is considered. Computer simulations results on error rates, complexity and also including the impact of spatial correlation and channel estimation errors are presented in chapter 5. Conclusions and discussions are finally given in chapter 6.

Chapter 2

Performance analysis of list-based MIMO detectors

This chapter deals with a class of list-based detectors which analogous to the schemes from [29, 37–39] aim at improving the performance of the classical ZF/MMSE-OSIC receivers by first partitioning the channel matrix, then building a list of candidates vectors using classical techniques and finally choosing the best candidate among the list as the final decision. In this chapter, a detailed diversity analysis of such schemes is performed and sufficient conditions to guarantee optimal ML performance at high SNR are obtained. Part of this chapter was published in [33].

2.1 System model

We consider a MIMO communication system employing N_T transmit and N_R receive antennas over a Rayleigh flat fading channel that is time invariant over one use. As illustrated in Fig. 2.1, in the V-BLAST architecture, at the transmitter the incoming information stream is first demultiplexed into N_T substreams. Then for each substream, groups of n_c consecutive bits are mapped to symbols drawn from a zero-mean constellation $\mathcal{A}$ of size

$M = |\mathcal{A}| = 2^{n_c}$ and average symbol energy σ_s^2. Each transmit antenna then transmits an independent symbol for each channel usage. Let $\mathbf{x} = [x_1 \dots x_{N_T}]^T \in \mathcal{A}^{N_T}$ be the N_T-dimensional vector of transmitted symbols over one channel use. Then assuming perfect synchronization, the N_R-dimensional received vector $\mathbf{y} = [y_1 \dots y_{N_R}]^T \in \mathbb{C}^{N_R \times 1}$ is given by

$$\mathbf{y} = \mathbf{H}\mathbf{x} + \mathbf{n}\,, \tag{2.1}$$

where the channel matrix $\mathbf{H} \in \mathbb{C}^{N_R \times N_T}$ has independent identically distributed (i.i.d) circularly symmetric complex Gaussian (CSCG) zero mean entries of unit variance, with its (i,j)-th component $h_{i,j}$ being the fading coefficient from the j-th transmit antenna to the i-th receive antenna. Furthermore, $\mathbf{n} = [n_1 \dots n_{N_R}]^T \in \mathbb{C}^{N_R \times 1}$ is the additive noise vector whose components are i.i.d CSCG with zero mean and variance σ_n^2. The SNR is defined here as $\text{SNR} = \dfrac{\sigma_s^2}{\sigma_n^2}$.

Then given $\mathbf{y}$, using a certain decision rule, the MIMO detector at the receiver side obtains an estimate $\hat{\mathbf{x}} = [\hat{x}_1 \dots \hat{x}_{N_T}]^T \in \mathcal{A}^{N_T}$ for the transmitted vector $\mathbf{x}$. A constellation demapper then maps each component of $\hat{\mathbf{x}}$ to the corresponding bit sequence. The resulting N_T substreams are finally multiplexed to obtain the reconstructed information sequence.

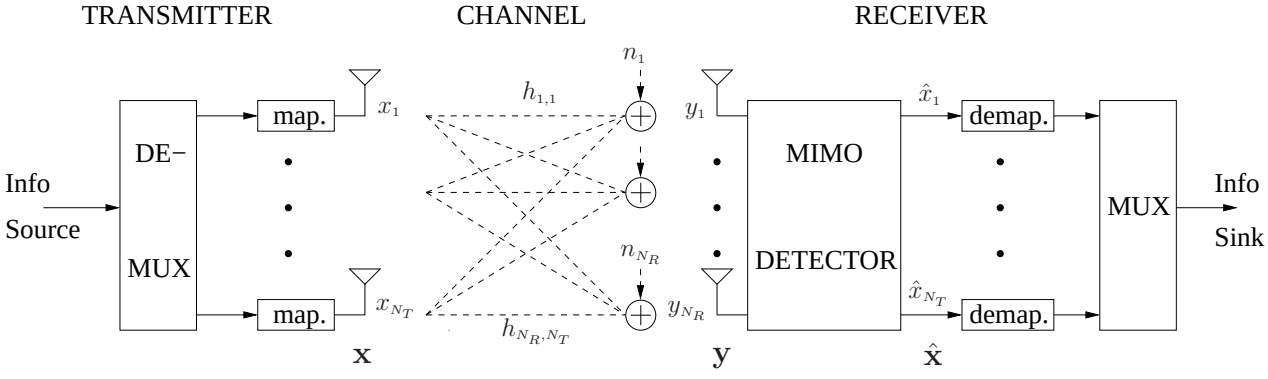

Fig. 2.1 MIMO V-BLAST system model

2.2 Maximum likelihood (ML) decision rule

The objective of the MIMO detector is to minimize the average probability of detection error $P_e(\mathrm{SNR})$, defined as the average probability that not all detected symbols are correct. With $\mathbf{H}$ known at the receiver and assuming that the components of the transmitted signal vector $\mathbf{x}$ are equally probable, the lowest average error probability is achieved by the maximum likelihood (ML) detector using a minimum Euclidean distance (MED) decision rule [6]

$$\hat{\mathbf{x}}^{\mathrm{ML}} = \arg \min_{\mathbf{d} \in \mathcal{A}^{N_T}} \|\mathbf{y} - \mathbf{H}\mathbf{d}\|^2 . \tag{2.2}$$

Since $|\mathcal{A}^{N_T}| = M^{N_T}$, which grows exponentially with N_T, an exhaustive search approach for solving (2.2) leads to impractically high complexity for large systems.

2.3 ZF/MMSE-OSIC detector

To alleviate the high complexity of exhaustive ML detection, suboptimal approaches employing ZF or MMSE based linear detection (LD) or their OSIC counterparts are commonly used [3,4,7]. For the LD case, the detected symbols are given by $\hat{x}_i = \mathcal{M}(\check{x}_i)\,,\ i = 1, \ldots, N_T$ where $\mathcal{M}(.)$ maps its argument to the closest element in $\mathcal{A}$ and $\check{x}_i$ is obtained as

$$\check{x}_i = \left[\left(\mathbf{H}^H \mathbf{H} + \beta^2 \mathbf{I}_{N_T} \right)^{-1} \mathbf{H}^H \mathbf{y} \right]_i , \quad i = 1, \ldots, N_T$$

where $\beta = \mathrm{SNR}^{-1/2}$ for MMSE and $\beta = 0$ for ZF. In SIC based detectors, the interference caused by previously detected symbols is cancelled prior to detecting the current symbol. However erroneous decisions on early layers yield imperfect interference cancellation on future layers, thus causing so-called error propagation. The error propagation issue can be mitigated by reordering the layers prior to detection. Clearly, different ordering rules yield different performance. The V-BLAST ordering rule is an optimized channel

dependent ordering rule that maximizes the smallest post-processing SNR among all layers [3, 4, 9, 10]. The ZF/MMSE-OSIC algorithm employing the V-BLAST optimal ordering can significantly improve the performance of LD and SIC with fixed ordering, i.e. channel independent ordering [9, 10]. Its main steps can be summarized as follows [7]:

1. Initialization: let $\mathbf{B}_{N_T} = \mathbf{H}$ and $\mathbf{z}_{N_T} = \mathbf{y}$, with $\mathbf{H}$ and $\mathbf{y}$ as defined in (2.1).
2. Recursion: for $i = N_T, \ldots, 1$,
   - Compute $\mathbf{Q}^{(i)} = \left(\mathbf{B}_i^H \mathbf{B}_i + \beta^2 \mathbf{I}_i\right)^{-1}$ with $\beta = \mathrm{SNR}^{-1/2}$ for MMSE and $\beta = 0$ for ZF.
   - Obtain $p_i = \arg\min_{l=1,\ldots,i} [\mathbf{Q}^{(i)}]_{(l,l)}$ and let $\mathbf{q}_{p_i}^{(i)}$ be the p_i-th column of $\mathbf{Q}^{(i)}$.
   - Obtain $\hat{x}_{p_i} = \mathcal{M}(\check{x}_{p_i})$ with $\check{x}_{p_i}$ obtained as: $\check{x}_{p_i} = \mathbf{q}_{p_i}^{(i),H} \mathbf{B}_i^H \mathbf{z}_i$.
   - If $i > 1$, compute $\mathbf{z}_{i-1} = \mathbf{z}_i - [\mathbf{B}_i]_{p_i} \hat{x}_{p_i}$
   - If $i > 1$, obtain $\mathbf{B}_{i-1}$ from $\mathbf{B}_i$ by removing its p_i-th column.

This algorithm can be efficiently implemented with $\mathcal{O}(N_T^3)$ complexity [7]. Thus compared to the exponential complexity of exhaustive ML detection, this scheme can provide tremendous complexity savings for large systems. However the achieved performance remains much poorer than ML detection [6, 8–10]. Next we introduce a class of MIMO detectors which build on these classical techniques and aim at providing close to ML performance with relatively low complexity.

2.4 List-based MIMO detectors

2.4.1 Alternative representation of the ML decision rule

Consider an alternative representation of the ML decision rule. Let the matrix $\mathbf{H}_1 \in \mathbb{C}^{N_R \times N}$ be composed of a subset of N $(1 \leq N \leq N_T)$ columns of $\mathbf{H}$, with the remaining columns forming $\mathbf{H}_2 \in \mathbb{C}^{N_R \times (N_T - N)}$. Clearly, there are a total of $N_U = \binom{N_T}{N}$ such possible subsets. Furthermore, let $\mathbf{x}_1$ denote the vector whose elements are symbols transmitted from the N antennas corresponding to $\mathbf{H}_1$ and $\mathbf{x}_2$ similarly defined for $\mathbf{H}_2$. Hence $\mathbf{H}\mathbf{x} = \mathbf{H}_1\mathbf{x}_1 + \mathbf{H}_2\mathbf{x}_2$.

Denote the elements of the sets $\mathcal{A}^N$ and $\mathcal{A}^{N_T-N}$ respectively as $\{\tilde{\mathbf{x}}_1^1, \tilde{\mathbf{x}}_1^2, \ldots, \tilde{\mathbf{x}}_1^K\}$ and $\{\tilde{\mathbf{x}}_2^1, \tilde{\mathbf{x}}_2^2, \ldots, \tilde{\mathbf{x}}_2^Q\}$. Hence $K = |\mathcal{A}^N| = M^N$ and $Q = |\mathcal{A}^{N_T-N}| = M^{N_T-N}$. The ML decision rule of (2.2) can now be rewritten as:

$$\hat{\mathbf{x}}_1^{\mathrm{ML}} = \tilde{\mathbf{x}}_1^{k^*}\,, \qquad \hat{\mathbf{x}}_2^{\mathrm{ML}} = \tilde{\mathbf{x}}_2^{q^*}\,, \tag{2.3}$$

where

$$(k^*,\, q^*) = \arg \min_{k\in\{1,2,\ldots,K\},\ \ q\in\{1,2,\ldots,Q\}} \|\mathbf{y} - \mathbf{H}_1\tilde{\mathbf{x}}_1^k - \mathbf{H}_2\tilde{\mathbf{x}}_2^q\|^2\,. \tag{2.4}$$

Defining

$$\mathbf{y}^k = \mathbf{y} - \mathbf{H}_1\tilde{\mathbf{x}}_1^k = \mathbf{H}_2\mathbf{x}_2 + \mathbf{H}_1\big(\mathbf{x}_1 - \tilde{\mathbf{x}}_1^k\big) + \mathbf{n}\,, \tag{2.5}$$

and

$$\mathbf{d}_2^k = \arg \min_{\mathbf{d}_2\in\{\tilde{\mathbf{x}}_2^1, \tilde{\mathbf{x}}_2^2, \ldots, \tilde{\mathbf{x}}_2^Q\}} \|\mathbf{y}^k - \mathbf{H}_2\mathbf{d}_2\|^2\,, \qquad k = 1, 2, \ldots, K\,, \tag{2.6}$$

we have the following equivalent representation of the ML decision rule:

$$\hat{\mathbf{x}}_1^{\mathrm{ML}} = \tilde{\mathbf{x}}_1^{k^*}\,, \qquad \hat{\mathbf{x}}_2^{\mathrm{ML}} = \tilde{\mathbf{x}}_2^{q^*} = \mathbf{d}_2^{k^*} \tag{2.7}$$

where

$$k^* = \arg \min_{k\in\{1,2,\ldots,K\}} \|\mathbf{y}^k - \mathbf{H}_2\mathbf{d}_2^k\|^2 \tag{2.8}$$

with $\mathbf{y}^k$ and $\mathbf{d}_2^k$ given by (2.5) and (2.6).

2.4.2 List-based detectors

The class of list-based detectors we shall consider are based on the following three steps:

1. **Channel partition :** A channel partition rule is employed to obtain $\mathbf{H}_1$, with the remaining columns of $\mathbf{H}$ composing $\mathbf{H}_2$. Clearly any partitioning scheme is applicable, resulting in different performances. It is thus desirable to derive a selection procedure that improves performance.

2. **Candidate vectors list generation :** Instead of using a MED rule to obtain the candidates $\mathbf{d}_2^k$ of (2.6), standard linear ZF/MMSE or ZF/MMSE-OSIC detectors [4,6,7] are employed to generate them. Clearly, a substantial reduction in complexity is achieved compared to using the MED rule which has a complexity that grows

exponentially with $N_T - N$. However, the candidates obtained in this manner may differ from those of (2.6) and consequently a certain amount of performance loss may be incurred as compared to ML detection.

3. **Final decision :** Among the list of M^N candidates vectors generated, the final decision is made following the MED rule of (2.8). The size of the candidates list grows exponentially with N, therefore it is important to make N as small as possible while minimizing the performance loss with respect to ML detection.

2.5 Performance analysis

In this section, we analyze the average probability of detection error $P_e(\mathrm{SNR})$, defined as the average probability that not all detected symbols are correct, i.e.

$$P_e(\mathrm{SNR}) = \Pr\big(\hat{\mathbf{x}} \neq \mathbf{x}\big)\,. \tag{2.9}$$

Specifically, our aim is to quantify the diversity gain provided, where we recall that a given scheme is said to provide a diversity gain d if [5]:

$$\lim_{\mathrm{SNR}\to\infty} \frac{\log P_e(\mathrm{SNR})}{\log \mathrm{SNR}} = -d\,. \tag{2.10}$$

Therefore at high SNR, we approximately have

$$P_e(\mathrm{SNR}) \propto \mathrm{SNR}^{-d}\,.$$

Hence the higher is d, the faster $P_e(\mathrm{SNR})$ decays to zero with increasing SNR. The relevance of our diversity analysis approach comes from the fact that the performance loss incurred by suboptimal schemes such as the linear ZF or MMSE algorithms and their OSIC counterparts, as compared to the ML algorithm, is due in part to a decrease in diversity gain. For a MIMO system that transmits independent data substreams on each antenna,

thereby providing maximal multiplexing gain [5], the diversity gain provided by the ML receiver is N_R [6, 40], whereas the suboptimal schemes cited above can only provide an $N_R - N_T + 1$ diversity gain [6, 8–10]. Hence a diversity analysis can indeed capture an essential part of the performance advantage provided by a specific scheme as compared to another. To evaluate (2.10), we use tight upper and lower bounds to $P_e(\text{SNR})$. To simplify notations, we refer to the average probability of error as P_e, where its dependence on SNR is not explicitly written unless necessary.

Denote by $\mathcal{S}(\mathbf{y}\,,\,\mathbf{H})$ the set of all candidate pairs $\{(\tilde{\mathbf{x}}_1^k\,,\,\mathbf{d}_2^k)\,,\ k = 1, 2, \ldots, K\}$ generated by the list-based detector for a given received vector $\mathbf{y}$ and a given channel matrix $\mathbf{H}$. Then the output of the list-based detector can be expressed as:

$$(\hat{\mathbf{x}}_1^{\text{GPIC}}, \hat{\mathbf{x}}_2^{\text{GPIC}}) = \arg \min_{(\tilde{\mathbf{x}}_1, \mathbf{d}_2) \in \mathcal{S}(\mathbf{y}\,,\,\mathbf{H})} \|\mathbf{y} - \mathbf{H}_1\tilde{\mathbf{x}}_1 - \mathbf{H}_2\mathbf{d}_2\|^2\,. \tag{2.11}$$

Comparison of (2.11) with (2.3), shows that the only difference between the ML and the list-based algorithms is that the latter searches for the optimal pair $(\hat{\mathbf{x}}_1, \hat{\mathbf{x}}_2)$ over a subset of the set used by the former. Hence,

$$(\hat{\mathbf{x}}_1^{\text{GPIC}}, \hat{\mathbf{x}}_2^{\text{GPIC}}) = (\hat{\mathbf{x}}_1^{\text{ML}}, \hat{\mathbf{x}}_2^{\text{ML}}) \Leftrightarrow (\hat{\mathbf{x}}_1^{\text{ML}}, \hat{\mathbf{x}}_2^{\text{ML}}) \in \mathcal{S}(\mathbf{y}\,,\,\mathbf{H})\,. \tag{2.12}$$

2.5.1 Upper bound on P_e

We first expand P_e as:

$$P_e = \mathcal{E}_{\mathbf{H}\,,\,\mathbf{x}}\big[\Pr\big(\hat{\mathbf{x}} \neq \mathbf{x}|\mathbf{H}\,,\,\mathbf{x}\big)\big] \tag{2.13}$$

We now further have:

$$\begin{aligned}\Pr\big(\hat{\mathbf{x}} \neq \mathbf{x}|\mathbf{H}\,,\,\mathbf{x}\big) \;=\; & \Pr\big(\hat{\mathbf{x}} \neq \mathbf{x}|\mathbf{H}\,,\,\mathbf{x}\,,\,\hat{\mathbf{x}}^{\text{ML}} \neq \mathbf{x}\big)\Pr\big(\hat{\mathbf{x}}^{\text{ML}} \neq \mathbf{x}|\mathbf{H}\,,\,\mathbf{x}\big) \\ & + \Pr\big(\hat{\mathbf{x}} \neq \mathbf{x}|\mathbf{H}\,,\,\mathbf{x}\,,\,\hat{\mathbf{x}}^{\text{ML}} = \mathbf{x}\big)\Pr\big(\hat{\mathbf{x}}^{\text{ML}} = \mathbf{x}|\mathbf{H}\,,\,\mathbf{x}\big)\,.\end{aligned} \tag{2.14}$$

The first term in the right side of (2.14) can be upper bounded as:

$$\Pr\big(\hat{\mathbf{x}} \neq \mathbf{x}|\mathbf{H}\,,\,\mathbf{x}\,,\,\hat{\mathbf{x}}^{\text{ML}} \neq \mathbf{x}\big)\Pr\big(\hat{\mathbf{x}}^{\text{ML}} \neq \mathbf{x}|\mathbf{H}\,,\,\mathbf{x}\big) \leq \Pr\big(\hat{\mathbf{x}}^{\text{ML}} \neq \mathbf{x}|\mathbf{H}\,,\,\mathbf{x}\big)\,. \tag{2.15}$$

To simplify the second term in the right side of (2.14), we first make the expansion:

$$\begin{aligned}\Pr\big(\hat{\mathbf{x}} \neq \mathbf{x}|\mathbf{H}\,,\,\mathbf{x}\,,\,\hat{\mathbf{x}}^{\mathrm{ML}} = \mathbf{x}\big) \;&=\; \Pr\big(\hat{\mathbf{x}} \neq \mathbf{x}|\mathbf{H}\,,\,\mathbf{x}\,,\,\hat{\mathbf{x}}^{\mathrm{ML}} = \mathbf{x}\,,\,(\mathbf{x}_1,\mathbf{x}_2) \in \mathcal{S}(\mathbf{y}\,,\,\mathbf{H})\big).\\ &\qquad \Pr\big((\mathbf{x}_1,\mathbf{x}_2) \in \mathcal{S}(\mathbf{y}\,,\,\mathbf{H})|\mathbf{H}\,,\,\mathbf{x}\,,\,\hat{\mathbf{x}}^{\mathrm{ML}} = \mathbf{x}\big)\\ &\quad + \Pr\big(\hat{\mathbf{x}} \neq \mathbf{x}|\mathbf{H}\,,\,\mathbf{x}\,,\,\hat{\mathbf{x}}^{\mathrm{ML}} = \mathbf{x}\,,\,(\mathbf{x}_1,\mathbf{x}_2) \notin \mathcal{S}(\mathbf{y}\,,\,\mathbf{H})\big).\\ &\qquad \Pr\big((\mathbf{x}_1,\mathbf{x}_2) \notin \mathcal{S}(\mathbf{y}\,,\,\mathbf{H})|\mathbf{H}\,,\,\mathbf{x}\,,\,\hat{\mathbf{x}}^{\mathrm{ML}} = \mathbf{x}\big)\;. \quad (2.16)\end{aligned}$$

Then we observe that

$$\Pr\big(\hat{\mathbf{x}} \neq \mathbf{x}|\mathbf{H}\,,\,\mathbf{x}\,,\,\hat{\mathbf{x}}^{\mathrm{ML}} = \mathbf{x}\,,\,(\mathbf{x}_1,\mathbf{x}_2) \notin \mathcal{S}(\mathbf{y}\,,\,\mathbf{H})\big) = 1 \quad (2.17)$$

since the transmitted pair $(\mathbf{x}_1, \mathbf{x}_2)$ is not an element of $\mathcal{S}(\mathbf{y}\,,\,\mathbf{H})$. Furthermore, from (2.12)

$$\Pr\big(\hat{\mathbf{x}}\neq\mathbf{x}|\mathbf{H},\mathbf{x},\hat{\mathbf{x}}^{\mathrm{ML}}=\mathbf{x},(\mathbf{x}_1,\mathbf{x}_2)\in\mathcal{S}(\mathbf{y},\mathbf{H})\big)=\Pr\big(\hat{\mathbf{x}}\neq\hat{\mathbf{x}}^{\mathrm{ML}}|\mathbf{H},\mathbf{x},\hat{\mathbf{x}}^{\mathrm{ML}}=\mathbf{x},(\hat{\mathbf{x}}_1^{\mathrm{ML}},\hat{\mathbf{x}}_2^{\mathrm{ML}})\in\mathcal{S}(\mathbf{y},\mathbf{H})\big)=0\,. \quad (2.18)$$

Substituting (2.17) and (2.18) into (2.16), we have:

$$\begin{aligned}\Pr\big(\hat{\mathbf{x}} \neq \mathbf{x}|\mathbf{H},\mathbf{x},\hat{\mathbf{x}}^{\mathrm{ML}} = \mathbf{x}\big) \;&=\; \Pr\big((\mathbf{x}_1,\mathbf{x}_2) \notin \mathcal{S}(\mathbf{y},\mathbf{H})|\mathbf{H},\mathbf{x},\hat{\mathbf{x}}^{\mathrm{ML}} = \mathbf{x}\big) &(2.19)\\ &=\; \Pr\big((\mathbf{x}_1,\mathbf{x}_2) \neq (\mathbf{x}_1,\mathbf{d}_2^{k_1})|\mathbf{H},\mathbf{x},\hat{\mathbf{x}}^{\mathrm{ML}} = \mathbf{x}\big) &(2.20)\\ &=\; \Pr\big(\mathbf{d}_2^{k_1} \neq \mathbf{x}_2|\mathbf{H},\mathbf{x},\hat{\mathbf{x}}^{\mathrm{ML}} = \mathbf{x}\big) &(2.21)\end{aligned}$$

where $\mathbf{x}_1 = \tilde{\mathbf{x}}_1^{k_1}$ for some $k_1 \in \{1, 2, \ldots, K\}$. Furthermore,

$$\begin{aligned}\Pr\big(\mathbf{d}_2^{k_1} \neq \mathbf{x}_2|\mathbf{H}\,,\,\mathbf{x}\big) \;&=\; \Pr\big(\mathbf{d}_2^{k_1} \neq \mathbf{x}_2|\mathbf{H}\,,\,\mathbf{x}\,,\,\hat{\mathbf{x}}^{\mathrm{ML}} = \mathbf{x}\big)\Pr\big(\hat{\mathbf{x}}^{\mathrm{ML}} = \mathbf{x}|\mathbf{H}\,,\,\mathbf{x}\big)\\ &\qquad + \Pr\big(\mathbf{d}_2^{k_1} \neq \mathbf{x}_2|\mathbf{H}\,,\,\mathbf{x}\,,\,\hat{\mathbf{x}}^{\mathrm{ML}} \neq \mathbf{x}\big)\Pr\big(\hat{\mathbf{x}}^{\mathrm{ML}} \neq \mathbf{x}|\mathbf{H}\,,\,\mathbf{x}\big)\\ &\geq\; \Pr\big(\mathbf{d}_2^{k_1} \neq \mathbf{x}_2|\mathbf{H}\,,\,\mathbf{x}\,,\,\hat{\mathbf{x}}^{\mathrm{ML}} = \mathbf{x}\big)\Pr\big(\hat{\mathbf{x}}^{\mathrm{ML}} = \mathbf{x}|\mathbf{H}\,,\,\mathbf{x}\big)\,. \quad (2.22)\end{aligned}$$

Using (2.21) in (2.22), we have:

$$\Pr\big(\mathbf{d}_2^{k_1} \neq \mathbf{x}_2|\mathbf{H}\,,\,\mathbf{x}\big) \geq \Pr\big(\hat{\mathbf{x}} \neq \mathbf{x}|\mathbf{H}\,,\,\mathbf{x}\,,\,\hat{\mathbf{x}}^{\mathrm{ML}} = \mathbf{x}\big)\Pr\big(\hat{\mathbf{x}}^{\mathrm{ML}} = \mathbf{x}|\mathbf{H}\,,\,\mathbf{x}\big)\,. \quad (2.23)$$

Recall that $\mathbf{d}_2^{k_1}$ is the output of the suboptimal algorithm used to generate the candidates for $\mathbf{x}_2$ when supplied with the received vector $\mathbf{y}^{k_1}$ given by:

$$\mathbf{y}^{k_1} = \mathbf{y} - \mathbf{H}_1\tilde{\mathbf{x}}_1^{k_1} = \mathbf{H}_2\mathbf{x}_2 + \mathbf{H}_1\big(\mathbf{x}_1 - \tilde{\mathbf{x}}_1^{k_1}\big) + \mathbf{n} = \mathbf{H}_2\mathbf{x}_2 + \mathbf{n}\,. \quad (2.24)$$

Thus we have

$$\Pr\big(\mathbf{d}_2^{k_1} \neq \mathbf{x}_2|\mathbf{H}\,,\,\mathbf{x}\big) = \Pr\big(\hat{\mathbf{x}}_2 \neq \mathbf{x}_2|\mathbf{H}_2\,,\,\mathbf{x}_2\big)\,. \quad (2.25)$$

The use of (2.15), (2.23) and (2.25) in (2.14) yields:

$$\Pr\big(\hat{\mathbf{x}} \neq \mathbf{x}|\mathbf{H}\,,\,\mathbf{x}\big) \leq \Pr\big(\hat{\mathbf{x}}^{\mathrm{ML}} \neq \mathbf{x}|\mathbf{H}\,,\,\mathbf{x}\big) + \Pr\big(\hat{\mathbf{x}}_2 \neq \mathbf{x}_2|\mathbf{H}_2\,,\,\mathbf{x}_2\big)\,. \tag{2.26}$$

Averaging both sides of (2.26) with respect to $\mathbf{H}$ and $\mathbf{x}$ yields the desired upper bound:

$$P_e \leq P_e^{\mathrm{ML}} + P_{e2} \tag{2.27}$$

where

$$P_e^{\mathrm{ML}} = \mathcal{E}_{\mathbf{H}\,,\mathbf{x}}\big[\Pr\big(\hat{\mathbf{x}}^{\mathrm{ML}} \neq \mathbf{x}|\mathbf{H}\,,\,\mathbf{x}\big)\big] \qquad \text{and} \qquad P_{e2} = \mathcal{E}_{\mathbf{H}_2\,,\mathbf{x}_2}\big[\Pr\big(\hat{\mathbf{x}}_2 \neq \mathbf{x}_2|\mathbf{H}_2\,,\,\mathbf{x}_2\big)\big]\,. \tag{2.28}$$

Since the reduced channel $\mathbf{H}_2$ corresponds to a smaller number of transmit antennas than the full channel $\mathbf{H}$, we are not constrained by $P_e^{\mathrm{ML}} < P_{e2}$.

2.5.2 Lower bound on P_e

Since the optimum receiver (i.e the one that achieves the lowest average probability of error) for our system implements the ML decision rule [6, 41], the average probability of error associated with this receiver is a lower bound to the one achieved by any other detection scheme. Thus we have:

$$P_e \geq P_e^{\mathrm{ML}}\,. \tag{2.29}$$

However, a less trivial lower bound can be obtained by rewriting (2.14) as

$$\begin{aligned}\Pr(\hat{\mathbf{x}} \neq \mathbf{x}|\mathbf{H}\,,\,\mathbf{x}) \;=\; & \Pr\big(\hat{\mathbf{x}} \neq \mathbf{x}|\mathbf{H},\mathbf{x},(\mathbf{x}_1,\mathbf{x}_2) \in \mathcal{S}(\mathbf{y},\mathbf{H})\big)\Pr\big((\mathbf{x}_1,\mathbf{x}_2) \in \mathcal{S}(\mathbf{y},\mathbf{H})|\mathbf{H},\mathbf{x}\big) \\ & + \Pr\big(\hat{\mathbf{x}} \neq \mathbf{x}|\mathbf{H},\mathbf{x},(\mathbf{x}_1,\mathbf{x}_2) \notin \mathcal{S}(\mathbf{y},\mathbf{H})\big)\Pr\big((\mathbf{x}_1,\mathbf{x}_2) \notin \mathcal{S}(\mathbf{y},\mathbf{H})|\mathbf{H},\mathbf{x}\big)\,.\end{aligned} \tag{2.30}$$

Clearly, we have

$$\Pr\big(\hat{\mathbf{x}} \neq \mathbf{x}|\mathbf{H}\,,\,\mathbf{x}\,,\,(\mathbf{x}_1,\mathbf{x}_2) \notin \mathcal{S}(\mathbf{y}\,,\,\mathbf{H})\big) = 1 \tag{2.31}$$

since $(\mathbf{x}_1,\mathbf{x}_2)$ is not an element of $\mathcal{S}(\mathbf{y}\,,\,\mathbf{H})$. Also, following similar steps as those used in the derivation of the upper bound (2.27), we have

$$\begin{aligned}\Pr\big((\mathbf{x}_1,\mathbf{x}_2) \notin \mathcal{S}(\mathbf{y}\,,\mathbf{H})|\mathbf{H}\,,\,\mathbf{x}\big) &= \Pr\big((\mathbf{x}_1\,,\,\mathbf{x}_2) \neq (\mathbf{x}_1\,,\,\mathbf{d}_2^{k_1})|\mathbf{H}\,,\,\mathbf{x}\big) && (2.32)\\ &= \Pr\big(\mathbf{d}_2^{k_1} \neq \mathbf{x}_2|\mathbf{H}\,,\,\mathbf{x}\big) && (2.33)\\ &= \Pr\big(\hat{\mathbf{x}}_2 \neq \mathbf{x}_2|\mathbf{H}_2\,,\,\mathbf{x}_2\big)\,. && (2.34)\end{aligned}$$

Hence from (2.30) with (2.31) and (2.34), we obtain:

$$\Pr(\hat{\mathbf{x}} \neq \mathbf{x}|\mathbf{H}\,,\,\mathbf{x}) \geq \Pr\big(\hat{\mathbf{x}}_2 \neq \mathbf{x}_2|\mathbf{H}_2\,,\,\mathbf{x}_2\big)\,. \tag{2.35}$$

Then averaging both sides of (2.35) with respect to $\mathbf{H}$ and $\mathbf{x}$, we obtain:

$$P_e \geq P_{e2}\,. \tag{2.36}$$

Combining (2.36) and (2.29), we get the desired lower bound:

$$P_e \geq \max\Big\{P_{e2}\,,\, P_e^{\mathrm{ML}}\Big\}\,. \tag{2.37}$$

2.5.3 Channel independent selection

The combination of (2.27) and (2.37) gives:

$$\max\{P_{e2}\,,\, P_e^{\mathrm{ML}}\} \leq P_e \leq P_e^{\mathrm{ML}} + P_{e2}\,. \tag{2.38}$$

Thus the overall performance of the list-based algorithm is determined by the relative values of P_{e2} and P_e^{ML}. However, for a given N, different channel partitioning schemes will result in different performances in terms of P_{e2}. In particular, we will see that the list-based method using any channel independent partitioning scheme yields a suboptimal diversity gain in P_{e2} leading to poor overall performance for small values of N. However, a diversity maximizing partitioning scheme yields an optimal diversity gain in P_{e2}, making possible to achieve maximal overall diversity gain with relatively small N.

Recall that the ML receiver achieves a diversity of order N_R, and hence at high SNR,

$$P_e^{\mathrm{ML}}(\mathrm{SNR}) \propto \mathrm{SNR}^{-N_R}\,. \tag{2.39}$$

As for P_{e2}, if the $L = N_T - N$ columns of the channel matrix $\mathbf{H}$ that form $\mathbf{H}_2$ are chosen at random without using any channel information, then from (2.24) and (2.28) P_{e2} is the average error probability of a given detection scheme for a MIMO flat Rayleigh fading channel with L transmit and N_R receive antennas. With the linear ZF/MMSE algorithms and their OSIC counterparts, the diversity gain is [6, 8–10]:

$$d^{\mathrm{indep}} = N_R - L + 1 = N_R - N_T + N + 1\,, \tag{2.40}$$

and at high SNR, we have

$$P_{e2} = P_{e2}^{\mathrm{LD/OSIC}} \propto \mathrm{SNR}^{-N_R+N_T-N-1}\,. \tag{2.41}$$

Clearly, if $N < N_T - 1$, then $N + 1 - N_T < 0$ and

$$\lim_{\mathrm{SNR}\to\infty} \frac{P_e^{\mathrm{ML}}(\mathrm{SNR})}{P_{e2}^{\mathrm{LD/OSIC}}(\mathrm{SNR})} = 0\,. \tag{2.42}$$

Hence, at high SNR, both sides of (2.38) are dominated by the term $P_{e2}^{\mathrm{LD/OSIC}}$, and

$$P_e(\mathrm{SNR}) \approx P_{e2}^{\mathrm{LD/OSIC}}(\mathrm{SNR}) \propto \mathrm{SNR}^{-(N_R - N_T + N + 1)}\,. \tag{2.43}$$

Thus channel independent partitioning increases the diversity gain by N as compared to the conventional V-BLAST receivers with no partitioning. However, from (2.43), achieving the same diversity order as the ML receiver in this case requires $N = N_T - 1$. Clearly with such a value of N, no significant reduction in complexity as compared to the ML algorithm can be achieved. We now show that using a diversity maximizing selection procedure, the list-based algorithm can provide optimal diversity with $N < N_T - 1$.

2.5.4 Diversity maximizing selection

The maximum achievable diversity gain with the LD or the OSIC algorithms can be bounded as [42]:

$$d_L \leq \tilde{d} \leq d_U \tag{2.44}$$

where

$$d_L = (N_T - L + 1)(N_R - L + 1) = (N + 1)(N_R - N_T + N + 1) \tag{2.45}$$

$$d_U = (N_T - L + 1)(N_R - 1) = (N + 1)(N_R - 1) \tag{2.46}$$

for $N_T \geq 2,\ N_R \geq 2$ and $1 \leq L = N_T - N \leq \min\{N_T, N_R\}$, i.e $\max\{0,\ N_T - N_R\} \leq N \leq N_T - 1$. Since we require N to be a strictly positive integer, then the range of allowable values for N with optimal selection is:

$$\max\{1,\ N_T - N_R\} \leq N \leq N_T - 1\,. \tag{2.47}$$

We note here that contrary to the standard ZF/MMSE receivers, (2.47) does not require $N_R \geq N_T$. Hence, this algorithm can handle the case $N_T > N_R$ provided that $N \geq N_T - N_R$.

Reverting back to the bounds in (2.44), we point out that the authors of [42] make the conjecture

$$\tilde{d} = d_L = (N+1)(N_R - N_T + N + 1)\,. \tag{2.48}$$

This conjecture is a generalization of a previous one made in [43], that was proven in [44] for the linear ZF/MMSE, the ZF-SIC with fixed/optimal ordering, and the MMSE-SIC with fixed ordering algorithms. However, to the best of our knowledge, the proof for the MMSE-SIC with optimal ordering is still lacking. We now proceed with the analysis of the list-based algorithm employing a diversity optimal selection, and show how to choose N to guarantee asymptotically optimal performance. From (2.44), at high SNR we have:

$$P_{e2} = P_{e2}^{\text{LD/OSIC}} \propto \text{SNR}^{-\tilde{d}}\,. \tag{2.49}$$

Using (2.38) and (2.39), we draw the following conclusions:

1. If $\tilde{d} > N_R$, and since from (2.39) and (2.49)

$$\frac{P_{e2}^{\text{LD/OSIC}}(\text{SNR})}{P_e^{\text{ML}}(\text{SNR})} \propto \text{SNR}^{-(\tilde{d}-N_R)} \tag{2.50}$$

we have

$$\lim_{\text{SNR}\to\infty} \frac{P_{e2}^{\text{LD/OSIC}}(\text{SNR})}{P_e^{\text{ML}}(\text{SNR})} = 0\,. \tag{2.51}$$

Using (2.51) with (2.38), we obtain:

$$\lim_{\text{SNR}\to\infty} \frac{P_e(\text{SNR})}{P_e^{\text{ML}}(\text{SNR})} = 1\,. \tag{2.52}$$

Hence, the list-based detector achieves optimal performance asymptotically.

2. If $\tilde{d} = N_R$, then, $P_{e2}^{\text{LD/OSIC}}(\text{SNR}) \propto \text{SNR}^{-N_R}$. Thus, from (2.38) and (2.39), at high SNR

$$P_e(\text{SNR}) \propto \text{SNR}^{-N_R} \tag{2.53}$$

showing that the list-based detector only achieves the same diversity gain as the ML algorithm.

3. If $\tilde{d} < N_R$, using (2.38) and (2.39) yields

$$\lim_{\mathrm{SNR}\to\infty} \frac{P_e(\mathrm{SNR})}{P_e^{\mathrm{LD/OSIC}}(\mathrm{SNR})} = 1\,, \tag{2.54}$$

and thus at high SNR, we have

$$P_e(\mathrm{SNR}) \propto \mathrm{SNR}^{-\tilde{d}} \tag{2.55}$$

showing that the list-based detector provides a diversity gain strictly lower than the ML's.

Define $f(N) = d_L - N_R$, and with (2.48) consider the following function:

$$f(s) = (s+1)(N_R - N_T + s + 1) - N_R\,, \quad s \in \mathbb{R}\,. \tag{2.56}$$

We seek the minimal integer N_{min}, such that when $N \geq N_{min}$ we have $f(N) > 0$. Since from (2.44) $\tilde{d} \geq d_L$, we have that $f(N) > 0 \Rightarrow \tilde{d} > N_R$. Therefore if $N \geq N_{min}$ then the list-based algorithm achieves optimal performance asymptotically. Thus, by analyzing the function (2.56), we can derive sufficient conditions for the list-based algorithm with diversity optimal channel partition to provide ML performance at high SNR. The two zeros of $f(s)$ are:

$$s_1 = \sqrt{N_R + \frac{1}{4}\big(N_R - N_T\big)^2} - \frac{1}{2}\big(N_R - N_T\big) - 1 \tag{2.57}$$

$$s_2 = -\sqrt{N_R + \frac{1}{4}\big(N_R - N_T\big)^2} - \frac{1}{2}\big(N_R - N_T\big) - 1 \tag{2.58}$$

and $f(s)$ is negative if and only if $s_2 < s < s_1$. Now consider the following:

1. Assume $N_R \geq 1$. If $N_R \geq N_T$, then $s_2 = -\Big(\sqrt{N_R + \frac{1}{4}\big(N_R - N_T\big)^2} + \frac{1}{2}\big(N_R - N_T\big) + 1\Big) < 0$. Now if $N_R < N_T$, then $s_2 = \frac{1}{2}\big(N_T - N_R\big)\Big(1 - \sqrt{1 + 4N_R\big(N_T - N_R\big)^{-2}}\Big) - 1 < -1 < 0$.

2. Assume $N_R \geq 1$ and $N_T \geq 2$, then $\frac{1}{4}\big(N_R + N_T\big)^2 - \frac{1}{4}\big(N_R - N_T\big)^2 = N_R N_T > N_R$. Thus $\sqrt{N_R + \frac{1}{4}\big(N_R - N_T\big)^2} < \frac{1}{2}\big(N_R + N_T\big)$. Therefore, $s_1 < \frac{1}{2}\big(N_R + N_T\big) - \frac{1}{2}\big(N_R - N_T\big) - 1 = N_T - 1$.

3. Assume $N_R \geq 1$ and $N_T \geq 2$.

- If $N_R = N_T$, then $s_1 = \sqrt{N_R} - 1 > \sqrt{2} - 1 > 0$.
- If $N_R < N_T$, then $s_1 = \frac{1}{2}\big(N_T - N_R\big)\Big(1 + \sqrt{1 + 4N_R\big(N_T - N_R\big)^{-2}}\Big) - 1 > \frac{2}{2}\big(N_T - N_R\big) - 1 = N_T - N_R - 1$.
- If $N_R > N_T$, then since $N_T \geq 2 > 1$, $N_R > N_R - N_T + 1$. Thus, $N_R + \frac{1}{4}\big(N_R - N_T\big)^2 > \frac{1}{4}\big(N_R - N_T\big)^2 + N_R - N_T + 1 = \Big(\frac{1}{2}\big(N_R - N_T\big) + 1\Big)^2$. Hence, $s_1 = \sqrt{N_R + \frac{1}{4}\big(N_R - N_T\big)^2} - \frac{1}{2}\big(N_R - N_T\big) - 1 > 0$.

Combining these results, we conclude that if $N_T \geq 2$ and $N_R \geq 1$, then

$$s_2 < 0 \quad \text{and} \quad \max\{0, N_T - N_R - 1\} < s_1 < N_T - 1\,. \tag{2.59}$$

Since $s_2 < 0$ for all system configurations of interest and $N > 0$,

$$f(N) > 0 \Leftrightarrow N > s_1 \Leftrightarrow N \geq \Big\lfloor s_1 + 1 \Big\rfloor = N_{min} \tag{2.60}$$

where $\lfloor A \rfloor$ stands for rounding to the nearest integer less than or equal to A, and the last inequality follows from the fact that N must be an integer. Hence

$$N_{min} = \Big\lfloor \sqrt{N_R + \frac{1}{4}\big(N_R - N_T\big)^2} - \frac{1}{2}\big(N_R - N_T\big) \Big\rfloor\,. \tag{2.61}$$

Using (2.59), we obtain

$$\max\{1,\, N_T - N_R\} \leq N_{min} \leq N_T - 1 \tag{2.62}$$

providing identical bounds as (2.47). Hence, the sufficient condition to guarantee that with optimum selection the list-based algorithm performs asymptotically optimum, is

$$N \geq N_{min}\,. \tag{2.63}$$

From (2.61), when $N_R = N_T$, we have $N_{min} = \Big\lfloor \sqrt{N_R} \Big\rfloor$. To get further insight into the behaviour of N_{min} for large under-determined or over-determined systems, let $N_R = N_T + \Delta_N$ where $\Delta_N \geq 1 - N_T$ is a constant integer. Then from (2.61), we have: $N_{min} = \Big\lfloor \sqrt{N_T + \Delta_N + \frac{1}{4}\Delta_N^2} - \frac{1}{2}\Delta_N \Big\rfloor$. Thus when $N_T \gg \Delta_N^2$, we get

$$N_{min} \approx \left\lfloor \sqrt{N_T} \right\rfloor . \tag{2.64}$$

Hence for large systems, the list-based algorithm provides optimal performance at high SNR, with a complexity that grows exponentially with $\left\lfloor \sqrt{N_T} \right\rfloor$ only as opposed to N_T for the exhaustive ML receiver. Furthermore, from (2.60), we have $N_{min} = 1$ if and only if $s_1 < 1$. It is straightforward to verify: $s_1 < 1 \Leftrightarrow N_R > 2N_T - 4 \Leftrightarrow N_R \geq 2N_T - 3$, where the last inequality follows because N_R is an integer. Thus we have shown

$$N_{min} = 1 \Leftrightarrow N_R \geq 2N_T - 3 . \tag{2.65}$$

Hence given N_T, we can always ensure $N_{min} = 1$ by selecting N_R sufficiently large.

Table 2.1 Values of N_{min} for various system configurations

N_R \ N_T	4	6	8	10	12
2	2	4	6	8	10
4	2	3	4	6	8
6	1	2	3	5	6
8	1	2	2	4	5
10	1	1	2	3	4
12	1	1	2	2	3
14	1	1	1	2	2
16	1	1	1	2	2
18	1	1	1	1	2
20	1	1	1	1	2
22	1	1	1	1	1

Table 2.1 provides the values of N_{min} for various system configurations. From this table, we observe that for $N_T = N_R = 12$, $N_{min} = 3$; hence confirming the fact that N_{min} is a relatively small integer even for large systems. Furthermore, we also observe that for $N_T = 6$, $N_{min} = 3$ for $N_R = 4$ and $N_{min} = 2$ for $N_R = 6$. Hence, in this case, increasing N_R by 2 not only increases the optimal diversity gain by 2 but also reduces N_{min}.

Chapter 3

The fixed complexity asymptotically optimal Sel-MMSE-OSIC and MMSE-ISTP algorithms

In the previous chapter, we derived sufficient conditions for list-based detectors to provide optimal performance asymptotically. We shall now propose specific schemes capable of delivering the promised performance. We first introduce the asymptotically optimal Sel-MMSE-OSIC scheme which employs a diversity maximizing selection procedure for channel partition and MMSE-OSIC for candidates list generation. Then we propose the lower complexity MMSE-ISTP scheme which improves over the Sel-MMSE-OSIC scheme in two aspects: first, it employs a simplified channel partition technique based on "incremental" antenna selection. This partition method not only has lower complexity than the one used by Sel-MMSE-OSIC but it also yields asymptotic optimality. Second, the proposed scheme employs an efficient tree based approach to lower the complexity of the candidates list generation. Part of this chapter was published in [33, 36].

3.1 The Sel-MMSE-OSIC algorithm

Let the set of all possible matrices $\mathbf{H}_2 \in \mathbb{C}^{N_R \times L}$ ($L = N_T - N$) resulting from the partition of the channel matrix $\mathbf{H}$ be denoted as $\{\mathbf{H}_2^{(1)}, \mathbf{H}_2^{(2)}, \ldots, \mathbf{H}_2^{(N_U)}\}$ ($N_U = \binom{N_T}{N}$). Then, from [42], for linear ZF/MMSE algorithms, the desired subset is $\mathbf{H}_2^{(t)}$ with t given by :

$$t = \arg \min_{1 \leq j \leq N_U} (Z_j) \tag{3.1}$$

where

$$Z_j = \begin{cases} \max_{k=1,\ldots,L} \left\{ \left(\mathbf{H}_2^{(j)H} \mathbf{H}_2^{(j)} \right)^{-1}_{kk} \right\}, & \text{for ZF} \\ \max_{k=1,\ldots,L} \left\{ \left(\mathbf{H}_2^{(j)H} \mathbf{H}_2^{(j)} + \mathrm{SNR}^{-1} \mathbf{I}_L \right)^{-1}_{kk} \right\}, & \text{for MMSE} \end{cases} \tag{3.2}$$

In [9, 10, 45], it was shown that LD and SIC algorithms based on the MMSE criterion can achieve significant performance gains over their ZF based counterparts. Therefore we focus here on the MMSE criterion, and we now consider a scheme that employs the diversity maximizing selection procedure of (3.1), with MMSE-OSIC rather than linear MMSE for detection in the candidates list generation. Given a selected channel $\mathbf{H}_2 \in \mathbb{C}^{N_R \times L}$, the diversity gain achieved using linear MMSE detection is given by [42]

$$d^{\mathrm{LD}} = - \lim_{\mathrm{SNR} \to \infty} \frac{\log \Pr \left(R_{min}^{\mathrm{LD}} \leq 1 \right)}{\log \mathrm{SNR}}, \tag{3.3}$$

where

$$R_{min}^{\mathrm{LD}} = \min_{k=1 \ldots L} \frac{\mathrm{SNR}}{\left(\mathbf{H}_2^H \mathbf{H}_2 + \mathrm{SNR}^{-1} \mathbf{I}_L \right)^{-1}_{kk}} - 1, \tag{3.4}$$

and the one achieved using MMSE-SIC with any ordering rule is given by [42]

$$d^{\mathrm{SIC}} = - \lim_{\mathrm{SNR} \to \infty} \frac{\log \Pr \left(R_{min}^{\mathrm{SIC}} \leq 1 \right)}{\log \mathrm{SNR}} \tag{3.5}$$

where

$$R_{min}^{\mathrm{SIC}} = \min_{k=1 \ldots L} \frac{\mathrm{SNR}}{\left(\mathbf{H}_{2,k}^H \mathbf{H}_{2,k} + \mathrm{SNR}^{-1} \mathbf{I}_k \right)^{-1}_{\pi(k)\pi(k)}} - 1, \tag{3.6}$$

with $\mathbf{H}_{2,k}$ being a submatrix obtained from $\mathbf{H}_2$ by removing the $k-1$ columns corresponding to the $k-1$ substreams previously detected, and $\pi(k)$ being the index of that column of

$\mathbf{H}_{2,k}$ that corresponds to the substream chosen for detection. It can be shown that [45]

$$R_{min}^{\text{SIC}} \geq R_{min}^{\text{LD}} \qquad \text{with probability one (w.p.1).} \tag{3.7}$$

Hence, from Appendix A, we get:

$$\log \Pr\left(R_{min}^{\text{LD}} \leq 1\right) \geq \log \Pr\left(R_{min}^{\text{SIC}} \leq 1\right), \tag{3.8}$$

and thus we have:

$$d^{\text{LD}} = -\lim_{\text{SNR}\to\infty} \frac{\log \Pr\left(R_{min}^{\text{LD}} \leq 1\right)}{\log \text{SNR}} \leq -\lim_{\text{SNR}\to\infty} \frac{\log \Pr\left(R_{min}^{\text{SIC}} \leq 1\right)}{\log \text{SNR}} = d^{\text{SIC}}. \tag{3.9}$$

Furthermore, from (2.48) and [44], for LD algorithms, this selection procedure provides optimum diversity, i.e $d^{\text{LD}} = \tilde{d} = d_L$. Hence, for SIC with any ordering rule, the provided diversity gain d^{SIC} satisfies: $d^{\text{SIC}} \geq d_L$. Therefore, from the previous analysis of list-based detectors, we conclude that if $N \geq N_{min}$ (cf. (2.61)), then asymptotic optimality is guaranteed. Hence, we propose the asymptotically optimal Sel-MMSE-OSIC algorithm, which employs (3.1) for channel partition and MMSE-OSIC with V-BLAST ordering for candidates list generation. Although for SIC, column ordering rules that perform better than V-BLAST ordering have been proposed in the literature [46, 47], these ordering strategies are significantly more complex than conventional V-BLAST ordering. In addition, as we shall see in chapter 5, Sel-MMSE-OSIC with V-BLAST ordering actually performs virtually same as ML at all SNR levels for space uncorrelated channels. Thus no significant performance gains can be expected from employing more complex column ordering strategies with Sel-MMSE-OSIC.

Assume that $\mathbf{H}$ and $\mathbf{x}$ are respectively partitioned as $\mathbf{H} = [\mathbf{H}_2\ \mathbf{H}_1]$ and $\mathbf{x} = [x_1 \dots x_{N_T}]^T = [\mathbf{x}_2^T\ \mathbf{x}_1^T]^T$ with $\mathbf{x}_1 = [x_{L+1} \dots x_{N_T}]^T \in \mathcal{A}^N$ and $\mathbf{x}_2 = [x_1 \dots x_L]^T \in \mathcal{A}^L$. The Sel-MMSE-OSIC algorithm can then be summarized as follows:

Algorithm: Sel-MMSE-OSIC

1. **Channel partition**: obtain $\mathbf{H}_2 = \mathbf{H}_2^{(t)}$ as in (3.1) and let $\mathbf{H}_1$ be composed of the remaining N columns of $\mathbf{H}$.

2. **MMSE-OSIC weight vectors**: compute

$$\mathbf{Q}^{(i)} = \left(\mathbf{B}_i^H \mathbf{B}_i + \mathrm{SNR}^{-1}\mathbf{I}_i\right)^{-1}, \quad i = L, \ldots, 1, \tag{3.10}$$

$$p_i = \arg \min_{l=1,\ldots,i} [\mathbf{Q}^{(i)}]_{(l,l)}, \quad i = L, \ldots, 1 \tag{3.11}$$

and

$$\mathbf{w}_i = \mathbf{B}_i \mathbf{q}_{p_i}^{(i)}, \quad i = L, \ldots, 1 \tag{3.12}$$

where $\mathbf{B}_L = \mathbf{H}_2$ and $\mathbf{B}_i$ is obtained from $\mathbf{B}_{i+1}$ by removing its p_{i+1}-th column. The algorithm of [48] can be used to compute all $\mathbf{w}_i$ efficiently.

3. **Candidates vectors list generation**: for each candidate vector $\tilde{\mathbf{x}}_1^k = [\tilde{x}_{L+1}^{(k)} \ldots \tilde{x}_{N_T}^{(k)}]^T \in \mathcal{A}^N$ for $\mathbf{x}_1$ (k=1, ..., M^N), compute $\mathbf{y}^k = \mathbf{y} - \mathbf{H}_1 \tilde{\mathbf{x}}_1^k$. Then, an associated candidate vector $\hat{\mathbf{d}}_2^k = [\hat{d}_1^{(k)} \ldots \hat{d}_L^{(k)}]^T \in \mathcal{A}^L$ for $\mathbf{x}_2$ is generated, with $\hat{d}_i^{(k)} = \mathcal{M}(\check{d}_i^{(k)})$, $\check{d}_i^{(k)}$ obtained using MMSE-SIC

$$\check{d}_i^{(k)} = \mathbf{w}_i^H \mathbf{z}_i^k, \quad i = L, \ldots, 1 \tag{3.13}$$

where

$$\mathbf{z}_i^k = \mathbf{z}_{i+1}^k - [\mathbf{B}_{i+1}]_{p_{i+1}} \hat{d}_{i+1}^{(k)}, \quad i = L, \ldots, 1 \tag{3.14}$$

with $\mathbf{z}_L^k = \mathbf{y}^k$ and $\mathcal{M}(.)$ maps its argument to the closest element in $\mathcal{A}$.

4. **MED rule**: for the final decision, choose the pair $(\tilde{\mathbf{x}}_1^{k^*}, \hat{\mathbf{d}}_2^{k^*})$ where

$$k^* = \arg \min_{k \in \{1,2,\ldots,M^N\}} \|\mathbf{y}^k - \mathbf{H}_2 \mathbf{d}_2^k\|^2 = \arg \min_{k \in \{1,2,\ldots,M^N\}} \|\mathbf{z}_1^k - [\mathbf{B}_1]_1 \hat{d}_1^{(k)}\|^2 . \tag{3.15}$$

Although the description above is based on the MMSE criterion, a ZF-based version that is suitable for all system configurations with the same asymptotic optimality guarantees can be straightforwardly obtained.

The channel partition procedure used in the Sel-MMSE-OSIC scheme requires the inversion of $N_U = \binom{N_T}{N}$ matrices of dimension $L = N_T - N$. Thus, the overall cost of this approach can be very high for large systems. Thus we now consider a simplified procedure that also yields asymptotic optimality.

3.2 Simplified channel partition

First (2.1) is rewritten as follows:

$$\breve{\mathbf{y}} = \breve{\mathbf{H}}\mathbf{x} + \breve{\mathbf{n}}\,, \tag{3.16}$$

with

$$\breve{\mathbf{y}} = [\mathbf{y}^T\ \mathbf{0}]^T\,, \qquad \breve{\mathbf{H}} = [\mathbf{H}^T\ \beta\mathbf{I}_{N_T}]^T\,, \qquad \breve{\mathbf{n}} = [\mathbf{n}^T\ -\beta\mathbf{x}^T]^T \tag{3.17}$$

where $\beta = \mathrm{SNR}^{-1/2}$. Contrary to $\mathbf{H}$, $\breve{\mathbf{H}}$ has full column rank with probability one (w.p.1) irrespective of the number of transmit and receive antennas [20], and corresponds to MMSE regularization [26]. Let $\breve{\mathbf{H}}$ and $\breve{\mathbf{y}}$ be as defined in (3.17). Then for channel partition, we employ the low complexity antenna selection rule of [42] with $\breve{\mathbf{H}}$. The partitioned matrix and its QR decomposition are given by

$$\tilde{\mathbf{H}} = \breve{\mathbf{H}}\tilde{\mathbf{\Pi}} = [\tilde{\mathbf{H}}_2\ \tilde{\mathbf{H}}_1] = \tilde{\mathbf{Q}}\,[\tilde{\mathbf{R}}^T\ \mathbf{0}]^T \tag{3.18}$$

where $\tilde{\mathbf{\Pi}} \in \mathbb{C}^{N_T \times N_T}$ is the column permutation matrix induced by the selection rule, $\tilde{\mathbf{R}} \in \mathbb{C}^{N_T \times N_T}$ is upper triangular with positive diagonal elements, and $\tilde{\mathbf{Q}} \in \mathbb{C}^{(N_R+N_T)\times(N_R+N_T)}$ is unitary. Furthermore, $\tilde{\mathbf{H}}_2 = [\breve{\mathbf{h}}_{k_1}\ \breve{\mathbf{h}}_{k_2}\ \ldots\ \breve{\mathbf{h}}_{k_L}]$ with $k_1 = \arg\max_{l=1,\ldots,N_T} \|\breve{\mathbf{h}}_l\|^2$, and

$$k_i = \arg \max_{l \notin \{k_1,\ldots,k_{i-1}\}} \frac{1}{\left([\breve{\mathbf{H}}_{i-1}\ \breve{\mathbf{h}}_l]^H[\breve{\mathbf{H}}_{i-1}\ \breve{\mathbf{h}}_l]\right)^{-1}_{(i,i)}}\,, \quad i = 2,\ldots,L \tag{3.19}$$

where $\breve{\mathbf{H}}_{i-1} = [\breve{\mathbf{h}}_{k_1} \ldots \breve{\mathbf{h}}_{k_{i-1}}]$. Using same terminology as in [42,49], this is an "incremental" selection rule that selects at each step the column with the largest projection on the space spanned by the previously selected columns [42]. Analogous to the Greedy QR algorithm of [50,51], we obtain the matrices $\tilde{\mathbf{\Pi}}$ and $\tilde{\mathbf{R}}$ in (3.18) and the vector $\tilde{\mathbf{y}} = \tilde{\mathbf{Q}}^H\breve{\mathbf{y}}$ by applying a Householder transformations based QR decomposition with column pivoting to $\breve{\mathbf{H}}$ and $\breve{\mathbf{y}}$ [52]. The resulting algorithm is detailed in Appendix B.

A transmit antenna selection based on the procedure above is considered in [42] that employs a decision feedback receiver where the symbol corresponding to $\breve{\mathbf{h}}_{k_L}$ is detected first, then the one corresponding to $\breve{\mathbf{h}}_{k_{L-1}}$ is detected next, and this process continues until the symbol corresponding to $\breve{\mathbf{h}}_{k_1}$ is detected. For such an ordering rule we have

Theorem 1. *Let ρ_i be the post processing* SNR *associated with the i-th ($1 \leq i \leq L$) detected layer using the detection order of [42]. Then we have $\rho_1 \leq \rho_2 \leq \cdots \leq \rho_L$.*

Proof. For the i-th ($1 \leq i \leq L$) detected layer, ρ_i is given by [42]:

$$\rho_i = \frac{\text{SNR}}{\left([\breve{\mathbf{h}}_{k_1} \ \ldots \ \breve{\mathbf{h}}_{k_j}]^H[\breve{\mathbf{h}}_{k_1} \ \ldots \ \breve{\mathbf{h}}_{k_j}]\right)^{-1}_{(j,j)}} - 1\,, \tag{3.20}$$

where $j = L - i + 1$. Using (3.18), we have: $[\breve{\mathbf{h}}_{k_1} \ \ldots \ \breve{\mathbf{h}}_{k_j}]^H[\breve{\mathbf{h}}_{k_1} \ \ldots \ \breve{\mathbf{h}}_{k_j}] = \tilde{\mathbf{R}}^H_{(1:j,1:j)}\tilde{\mathbf{R}}_{(1:j,1:j)}$. Then, since $\tilde{\mathbf{R}}_{(1:j,1:j)}$ is upper triangular, we obtain

$$\rho_i = \beta^{-2}\,\tilde{r}^2_{j,j} - 1\,, \tag{3.21}$$

where $\tilde{r}_{j,j} = \tilde{\mathbf{R}}_{(j,j)}$ with $\tilde{\mathbf{R}}$ defined in (3.18) and $\beta = \text{SNR}^{-1/2}$. Similarly, for the $i+1$-th detected layer, we obtain

$$\rho_{i+1} = \beta^{-2}\,\tilde{r}^2_{j-1,j-1} - 1\,. \tag{3.22}$$

Now since $\tilde{\mathbf{R}}$ was obtained through QR decomposition with column pivoting, we have [52]:

$$\tilde{r}^2_{j-1,j-1} \geq \tilde{r}^2_{j,j}\,. \tag{3.23}$$

From (3.23), (3.21) and (3.22), we get $\rho_{i+1} \geq \rho_i$, from which we obtain $\rho_1 \leq \ldots \leq \rho_L$. □

Thus the layers with smaller post-processing SNRs are detected before those with larger ones. Hence, the detector suffers significantly from error propagation. Therefore, after obtaining $\tilde{\mathbf{H}}_1$ and $\tilde{\mathbf{H}}_2$ through the Greedy QR algorithm, we further apply the V-BLAST ordering rule to $\tilde{\mathbf{H}}_2$ for improved performance [7, 48]. The proposed simplified channel partition can now be summarized as follows:

Algorithm: Simplified channel partition

1. Use the MMSE based Greedy QR algorithm of Appendix B to obtain $\tilde{\mathbf{\Pi}}$, $\tilde{\mathbf{R}}$ and $\tilde{\mathbf{y}} = \tilde{\mathbf{Q}}^H \breve{\mathbf{y}}$, with $\tilde{\mathbf{\Pi}}$, $\tilde{\mathbf{R}}$ and $\tilde{\mathbf{Q}}$ defined in (3.18).

2. Obtain $(\mathbf{B}_L^H \mathbf{B}_L)^{-1} = \left(\tilde{\mathbf{H}}_2^H \tilde{\mathbf{H}}_2\right)^{-1} = \tilde{\mathbf{R}}_{(1:L,1:L)}^{-1} \left(\tilde{\mathbf{R}}_{(1:L,1:L)}^{-1}\right)^H$ and use the algorithm of [48] to obtain $\hat{\mathbf{\Pi}} \in \mathbb{C}^{L \times L}$, the column permutation matrix corresponding to the V-BLAST order associated with $\tilde{\mathbf{H}}_2$.

3. Let $\bar{\mathbf{\Pi}} = [\mathbf{e}_{p_1} \ \ldots \ \mathbf{e}_{p_{N_T}}] = \tilde{\mathbf{\Pi}} \begin{bmatrix} \hat{\mathbf{\Pi}} & \mathbf{0} \\ \mathbf{0} & \mathbf{I}_N \end{bmatrix}$ be the N_T-dimensional column permutation matrix induced by the selection and ordering rules on the columns of $\breve{\mathbf{H}}$ defined in (3.17). The ordered set $\{p_1 \ldots p_{N_T}\}$ is a permutation of integers $1,\ldots,N_T$. Then use the Givens QR algorithm from [52] to obtain

$$\bar{\mathbf{H}} = [\breve{\mathbf{h}}_{p_1} \ \ldots \ \breve{\mathbf{h}}_{p_{N_T}}] = \breve{\mathbf{H}}\bar{\mathbf{\Pi}} = [\tilde{\mathbf{H}}_2\hat{\mathbf{\Pi}} \ \ \tilde{\mathbf{H}}_1] = \bar{\mathbf{Q}}\,[\bar{\mathbf{R}}^T \ \mathbf{0}]^T \qquad \text{and} \qquad \bar{\mathbf{y}} = \bar{\mathbf{Q}}^H \breve{\mathbf{y}} \tag{3.24}$$

where $\bar{\mathbf{R}} \in \mathbb{C}^{N_T \times N_T}$ is upper triangular with $\bar{\mathbf{R}}_{(i,i)} > 0$, $\forall i$.

The MMSE-ISTP scheme is a list based detection algorithm that employs the proposed channel partition. The significance of the proposed partition technique is two folds: first, it has much lower complexity than the exhaustive search approach used for Sel-MMSE-OSIC. Second, as far as performance is concerned, similar to Sel-MMSE-OSIC, we have

Theorem 2. *If N is chosen such that $(N+1)\,(N_R - N_T + N + 1) = N_R$, then the MMSE-ISTP scheme provides full diversity gain. Furthermore, $N \geq N_{min}$, with N_{min} given by (2.61), is a sufficient condition for MMSE-ISTP to provide optimal performance at high* SNR.

Proof. Same as for the Sel-MMSE-OSIC scheme, we have [42]:

$$\tilde{d} = -\lim_{\mathrm{SNR}\to\infty} \frac{\log \Pr\left(R_{min}^{\mathrm{SIC}} \leq 1\right)}{\log \mathrm{SNR}}\,, \tag{3.25}$$

with

$$R_{min}^{\mathrm{SIC}} = \min_{i=1\ldots L} \rho_i\,, \tag{3.26}$$

and ρ_i defined in (3.20). Then from (3.9), we have

$$\tilde{d} \geq d^{\mathrm{LD}} \tag{3.27}$$

with d^{LD} defined as in (3.3) but with R_{min}^{LD} defined here as

$$R_{min}^{\text{LD}} = \min_{k=1\ldots L} \frac{\text{SNR}}{\left(\tilde{\mathbf{H}}_2^H \tilde{\mathbf{H}}_2\right)_{kk}^{-1}} - 1\,, \tag{3.28}$$

Let $\tilde{\lambda}_1 \geq \tilde{\lambda}_2 \geq \cdots \geq \tilde{\lambda}_L > 0$ be the singular values of $\tilde{\mathbf{H}}_2$. Similarly, let $\breve{\lambda}_1 \geq \breve{\lambda}_2 \geq \cdots \geq \breve{\lambda}_{N_T} > 0$ be the singular values of $\breve{\mathbf{H}}$. Then, from [51], we have:

$$\breve{\lambda}_i^2 \prod_{j=1}^{i} \frac{1}{(N_R + N_T - j + 1)(N_T - j + 1)} \leq \tilde{\lambda}_i^2 \leq \breve{\lambda}_i^2, \quad i = 1, \ldots, L \tag{3.29}$$

In particular, we have

$$\alpha \breve{\lambda}_L^2 \leq \tilde{\lambda}_L^2 \leq \breve{\lambda}_L^2 \tag{3.30}$$

where $\alpha = \prod_{j=1}^{L} \frac{1}{(N_R+N_T-j+1)(N_T-j+1)} > 0$ is a positive constant. Now let let $\tilde{\mathbf{H}}_2^H \tilde{\mathbf{H}}_2 = \mathbf{U}^H \mathbf{\Lambda} \mathbf{U}$ where $\mathbf{U} \in \mathbb{C}^{L \times L}$ is unitary and $\mathbf{\Lambda} = \text{diag}(\tilde{\lambda}_1^2, \ldots, \tilde{\lambda}_L^2)$ be the eigenvalue decomposition of $\tilde{\mathbf{H}}_2^H \tilde{\mathbf{H}}_2$. Then, we straightforwardly obtain:

$$\left(\tilde{\mathbf{H}}_2^H \tilde{\mathbf{H}}_2\right)_{i,i}^{-1} = \sum_{j=1}^{L} \tilde{\lambda}_j^{-2} |u_{j,i}|^2 \leq \tilde{\lambda}_L^{-2} \sum_{j=1}^{L} |u_{j,i}|^2 = \tilde{\lambda}_L^{-2} \tag{3.31}$$

Thus using (3.31) in (3.28), we get

$$R_{min}^{\text{LD}} \geq \text{SNR} \tilde{\lambda}_L^2 - 1 \geq \alpha \text{SNR} \breve{\lambda}_L^2 - 1\,. \tag{3.32}$$

where we used (3.30) to obtain the second inequality in (3.32). Observe from (3.17) that

$$\breve{\mathbf{H}}^H \breve{\mathbf{H}} = \mathbf{H}^H \mathbf{H} + \beta^2 \mathbf{I}_{N_T}\,. \tag{3.33}$$

Furthermore, given our Rayleigh fading model, the rank of $\mathbf{H}$ is N_{RT} w.p.1, with

$$N_{RT} = \min\{N_R, N_T\}\,. \tag{3.34}$$

Now let $\lambda_1 \geq \lambda_2 \geq \cdots \geq \lambda_{N_{RT}} > 0$ be the strictly positive singular values of $\mathbf{H}$. Then using (3.33), we straightforwardly get

$$\breve{\lambda}_i^2 = \begin{cases} \lambda_i^2 + \beta^2 & \text{if } 1 \leq i \leq N_{RT} \\ \beta^2 & \text{if } N_{RT} + 1 \leq i \leq N_T \end{cases} \tag{3.35}$$

Since $L \leq N_{RT}$, from (3.35) we have

$$\breve{\lambda}_L^2 = \lambda_L^2 + \beta^2 \geq \lambda_L^2\,. \tag{3.36}$$

Hence using (3.36) in (3.32), we obtain

$$R_{min}^{\text{LD}} \geq \alpha \text{SNR} \lambda_L^2 - 1 \tag{3.37}$$

Therefore, using the result of Appendix A, we get

$$\Pr\left(R_{min}^{\text{LD}} \leq 1\right) \leq \Pr\left(\alpha \,\text{SNR}\, \lambda_L^2 \leq 2\right) \tag{3.38}$$

Then using (3.38) in (3.3), we get:

$$\begin{aligned} d^{\text{LD}} &\geq \lim_{\text{SNR}\to\infty} \frac{\log \Pr\left(\alpha \,\text{SNR}\, \lambda_L^2 \leq 2\right)}{\log \text{SNR}^{-1}} \\ &= \lim_{\text{SNR}\to\infty} \frac{\log \Pr\left(\lambda_L^2 \leq 2\alpha^{-1}\text{SNR}^{-1}\right)}{\log \text{SNR}^{-1}} \\ &= \lim_{\epsilon\to 0} \frac{\log \Pr\left(\lambda_L^2 \leq \epsilon\right)}{\log \epsilon} \\ &= \left(N_{\scriptscriptstyle T} - L + 1\right)\left(N_{\scriptscriptstyle R} - L + 1\right) = d_L \end{aligned} \tag{3.39}$$

where (3.39) follows from [50]. Finally using (3.39) in (3.27), we get

$$\tilde{d} \geq \left(N_{\scriptscriptstyle T} - L + 1\right)\left(N_{\scriptscriptstyle R} - L + 1\right) = \left(N + 1\right)\left(N_{\scriptscriptstyle R} - N_{\scriptscriptstyle T} + N + 1\right) . \tag{3.40}$$

The theorem then follows from (3.40) and the performance analysis from Chapter 2. □

The same conclusions hold for the ZF criterion based ISTP scheme (see [34]). The ZF based FSD scheme [23,25] on the other hand is not applicable for under-determined systems. It is possible to apply the FSD algorithm on the regularized matrix $\breve{\mathbf{H}}$ so that the resulting scheme, which we refer to as MMSE-FSD, is applicable for all systems configurations. Note however that MMSE regularization requires knowledge of the operating SNR which is not known a priori and thus must be estimated. Hence the ISTP scheme provides additional flexibility over the FSD scheme.

3.3 Tree based list detection

Similar to Sel-MMSE-OSIC, for each $\tilde{\mathbf{s}}=[\tilde{s}_{L+1}\ldots\tilde{s}_{N_T}]^T\in\mathcal{A}^N$ a vector $\hat{\mathbf{s}}=[\hat{s}_1\ldots\hat{s}_L]^T\in\mathcal{A}^L$ is generated, with

$$\hat{s}_i = \mathcal{M}(\check{s}_i)\,, \quad i = L,\ldots,1\,, \tag{3.41}$$

$\check{s}_i$ obtained using MMSE-SIC

$$\check{s}_i = \left[\left([\mathbf{h}_{p_1} \ \ldots \ \mathbf{h}_{p_i}]^H [\mathbf{h}_{p_1} \ \ldots \ \mathbf{h}_{p_i}] + \mathrm{SNR}^{-1} \mathbf{I}_i \right)^{-1} [\mathbf{h}_{p_1} \ \ldots \ \mathbf{h}_{p_i}]^H \left(\mathbf{y} - \sum_{j=L+1}^{N_T} \mathbf{h}_{p_j} \tilde{s}_j - \sum_{j=i+1}^{L} \mathbf{h}_{p_j} \hat{s}_j \right) \right]_{(i)}, \quad (3.42)$$

where $\mathbf{h}_{p_j}, (j{=}1, \ldots, N_T)$ is the p_j-th column of $\mathbf{H}$ with p_j defined in step 3) of the proposed channel partition. Now observing that

$$\breve{\mathbf{h}}_{p_j} = [\mathbf{h}_{p_j}^T \ \beta \, \mathbf{e}_{p_j}^T]^T \quad (3.43)$$

and noting that for $i \neq j$, $\mathbf{e}_i^H \mathbf{e}_j = 0$, we obtain

$$\left([\mathbf{h}_{p_1} \ \ldots \ \mathbf{h}_{p_i}]^H [\mathbf{h}_{p_1} \ \ldots \ \mathbf{h}_{p_i}] + \mathrm{SNR}^{-1} \mathbf{I}_i \right) = \left([\breve{\mathbf{h}}_{p_1} \ \ldots \ \breve{\mathbf{h}}_{p_i}]^H [\breve{\mathbf{h}}_{p_1} \ \ldots \ \breve{\mathbf{h}}_{p_i}] \right) \quad (3.44)$$

where we used the fact that $\beta^2 = \mathrm{SNR}^{-1}$. Furthermore, for $j \notin \{1, \ldots, i\}$, we obtain

$$[\mathbf{h}_{p_1} \ \ldots \ \mathbf{h}_{p_i}]^H \mathbf{h}_{p_j} = [\breve{\mathbf{h}}_{p_1} \ \ldots \ \breve{\mathbf{h}}_{p_i}]^H \breve{\mathbf{h}}_{p_j} \quad (3.45)$$

In addition, we also have

$$[\mathbf{h}_{p_1} \ \ldots \ \mathbf{h}_{p_i}]^H \mathbf{y} = [\breve{\mathbf{h}}_{p_1} \ \ldots \ \breve{\mathbf{h}}_{p_i}]^H \breve{\mathbf{y}} \quad (3.46)$$

with $\breve{\mathbf{y}}$ defined in (3.17). Then using (3.44), (3.45) and (3.46) in (3.42) yields

$$\check{s}_i = \left[\left([\breve{\mathbf{h}}_{p_1} \ \ldots \ \breve{\mathbf{h}}_{p_i}]^H [\breve{\mathbf{h}}_{p_1} \ \ldots \ \breve{\mathbf{h}}_{p_i}] \right)^{-1} [\breve{\mathbf{h}}_{p_1} \ \ldots \ \breve{\mathbf{h}}_{p_i}]^H \left(\breve{\mathbf{y}} - \sum_{j=L+1}^{N_T} \breve{\mathbf{h}}_{p_j} \tilde{s}_j - \sum_{j=i+1}^{L} \breve{\mathbf{h}}_{p_j} \hat{s}_j \right) \right]_{(i)}. \quad (3.47)$$

Now we observe that (3.24) implies that

$$\breve{\mathbf{h}}_{p_j} = \bar{\mathbf{Q}} \, [\bar{\mathbf{r}}_j^T \ \mathbf{0}]^T, \quad j = 1, \ldots, N_T. \quad (3.48)$$

From (3.48), we obtain

$$[\breve{\mathbf{h}}_{p_1} \ \ldots \ \breve{\mathbf{h}}_{p_i}] = \bar{\mathbf{Q}} \, [\bar{\mathbf{R}}_{(1:N_T,1:i)}^T \mathbf{0}]^T = \bar{\mathbf{Q}} \, [\bar{\mathbf{R}}_{(1:i,1:i)}^T \mathbf{0}]^T \quad (3.49)$$

where the second equality in (3.49) follows because $\bar{\mathbf{R}}$ is upper triangular. Furthermore, $\bar{\mathbf{R}}_{(1:i,1:i)}$ is invertible since it is an upper triangular matrix with positive diagonal elements.

Hence, from (3.49) we straightforwardly obtain

$$\left([\breve{\mathbf{h}}_{p_1} \ \dots \ \breve{\mathbf{h}}_{p_i}]^H[\breve{\mathbf{h}}_{p_1} \ \dots \ \breve{\mathbf{h}}_{p_i}]\right)^{-1}[\breve{\mathbf{h}}_{p_1} \ \dots \ \breve{\mathbf{h}}_{p_i}]^H = [\bar{\mathbf{R}}^{-1}_{(1:i,1:i)}\,\mathbf{0}]\,\bar{\mathbf{Q}}^H\,. \tag{3.50}$$

Using (3.50) and (3.48) in (3.47) yields

$$\begin{aligned}\check{s}_i &= \left[\bar{\mathbf{R}}^{-1}_{(1:i,1:i)}\Big(\bar{\mathbf{y}}_{(1:i)} - \sum_{j=L+1}^{N_T}\bar{\mathbf{R}}_{(1:i,j)}\tilde{s}_j - \sum_{j=i+1}^{L}\bar{\mathbf{R}}_{(1:i,j)}\hat{s}_j\Big)\right]_{(i)} &(3.51)\\ &= \mathbf{e}_i^H\bar{\mathbf{R}}^{-1}_{(1:i,1:i)}\Big(\bar{\mathbf{y}}_{(1:i)} - \sum_{j=L+1}^{N_T}\bar{\mathbf{R}}_{(1:i,j)}\tilde{s}_j - \sum_{j=i+1}^{L}\bar{\mathbf{R}}_{(1:i,j)}\hat{s}_j\Big) &(3.52)\end{aligned}$$

with $\bar{\mathbf{y}}$ defined in (3.24). Now since $\bar{\mathbf{R}}^{-1}_{(1:i,1:i)}$ is upper triangular, we have $\mathbf{e}_i^H\bar{\mathbf{R}}^{-1}_{(1:i,1:i)} = \left(\bar{\mathbf{R}}^{-1}_{(1:i,1:i)}\right)_{(i,i)}\mathbf{e}_i^H$. Furthermore, since $\left(\bar{\mathbf{R}}^{-1}_{(1:i,1:i)}\right)_{(i,i)} = \left(\bar{\mathbf{R}}_{(i,i)}\right)^{-1}$, (3.52) becomes

$$\check{s}_i = \frac{1}{\bar{r}_{i,i}}\Big(\bar{y}_i - \sum_{j=L+1}^{N_T}\bar{r}_{i,j}\tilde{s}_j - \sum_{j=i+1}^{L}\bar{r}_{i,j}\hat{s}_j\Big) \tag{3.53}$$

where $\bar{r}_{i,j} = \bar{\mathbf{R}}_{(i,j)}$ and $\bar{y}_i = \bar{\mathbf{y}}_{(i)}$. Now regarding the MMSE-ISTP's final output, first define $\mathbf{d}{=}[\hat{\mathbf{s}}^T\,\tilde{\mathbf{s}}^T]^T \in \mathcal{A}^{N_T}$ for each candidate pair $(\tilde{\mathbf{s}}\,,\,\hat{\mathbf{s}})$. Then let $\mathcal{S}(\mathbf{y},\mathbf{H})$ be the set of all M^N candidate vectors generated. Then similar to Sel-MMSE-OSIC, the MMSE-ISTP's output is obtained as

$$\hat{\mathbf{d}} = \arg\min_{\mathbf{d}\in\mathcal{S}(\mathbf{y},\mathbf{H})}\left(\Big\|\mathbf{y} - [\mathbf{h}_{p_1} \ \dots \ \mathbf{h}_{p_{N_T}}]\,\mathbf{d}\Big\|^2\right)\,. \tag{3.54}$$

Observe that

$$\left\|\breve{\mathbf{y}} - \bar{\mathbf{H}}\mathbf{d}\right\|^2 = \Big\|\mathbf{y} - [\mathbf{h}_{p_1} \ \dots \ \mathbf{h}_{p_{N_T}}]\,\mathbf{d}\Big\|^2 + \beta^2\|\mathbf{d}\|^2\,. \tag{3.55}$$

Thus (3.54) is equivalent to

$$\hat{\mathbf{d}} = \arg\min_{\mathbf{d}\in\mathcal{S}(\mathbf{y},\mathbf{H})}\left(\left\|\breve{\mathbf{y}} - \bar{\mathbf{H}}\mathbf{d}\right\|^2 - \beta^2\left\|\mathbf{d}\right\|^2\right)\,. \tag{3.56}$$

Now using the QR decomposition of (3.24), we have

$$\left\|\breve{\mathbf{y}} - \bar{\mathbf{H}}\mathbf{d}\right\|^2 = \left\|\bar{\mathbf{Q}}^H\breve{\mathbf{y}} - \begin{bmatrix}\bar{\mathbf{R}}\\ \mathbf{0}\end{bmatrix}\mathbf{d}\right\|^2 = \left\|\bar{\mathbf{y}}_{(1:N_T)} - \bar{\mathbf{R}}\mathbf{d}\right\|^2 + \left\|\bar{\mathbf{y}}_{(N_T+1:N_R+N_T)}\right\|^2\,. \tag{3.57}$$

Since the last term in (3.57) is independent of $\mathbf{d}$, (3.56) is equivalent to:

$$\hat{\mathbf{d}} = \arg\min_{\mathbf{d}\in\mathcal{S}(\mathbf{y},\mathbf{H})}\left(\left\|\bar{\mathbf{y}}_{(1:N_T)} - \bar{\mathbf{R}}\mathbf{d}\right\|^2 - \beta^2\left\|\mathbf{d}\right\|^2\right)\,. \tag{3.58}$$

The corresponding decisions for the symbols transmitted from the antennas composing $\tilde{\mathbf{H}}_1$ and $\tilde{\mathbf{d}}_2$ are respectively $\hat{\mathbf{x}}_1$=$\hat{\mathbf{d}}_{(L+1:N_T)}$ and $\hat{\mathbf{x}}_2$=$\hat{\mathbf{d}}_{(1:L)}$. For constant modulus alphabets, as PSK, i.e $|z|^2=\sigma_s^2\,,\ \forall z\in\mathcal{A}$, we have $\|\mathbf{d}\|^2=N_T\sigma_s^2\,,\ \forall\mathbf{d}\in\mathcal{A}^{N_T}$, hence the second term in the objective function of (3.58) can be omitted. Defining

$$\xi_k(\mathbf{d}_{(k:N_T)})=\|\bar{\mathbf{y}}_{(k:N_T)}-\bar{\mathbf{R}}_{(k:N_T,k:N_T)}\mathbf{d}_{(k:N_T)}\|^2-\beta^2\left\|\mathbf{d}_{(k:N_T)}\right\|^2\,,\quad k=1,\ldots,N_T\,, \tag{3.59}$$

(3.58) is then equivalent to $\hat{\mathbf{d}}=\arg\min_{\mathbf{d}\in\mathcal{S}(\mathbf{y},\mathbf{H})}\xi_1(\mathbf{d}_{(1:N_T)})$. It is easily verified that

$$\xi_k(\mathbf{d}_{(k:N_T)})=\xi_{k+1}(\mathbf{d}_{(k+1:N_T)})+\gamma_k(\mathbf{d}_{(k:N_T)}) \tag{3.60}$$

with $\xi_{k+1}(\mathbf{d}_{(k+1:N_T)})=0$ if $k=N_T$ and

$$\gamma_k(\mathbf{d}_{(k:N_T)})=\bar{r}_{k,k}^2|\zeta_k(\mathbf{d}_{(k+1:N_T)})-d_k|^2-\beta^2|d_k|^2\,, \tag{3.61}$$

where

$$\zeta_k(\mathbf{d}_{(k+1:N_T)})=\begin{cases}\bar{r}_{k,k}^{-1}\left(\bar{y}_k-\bar{\mathbf{R}}_{(k,k+1:N_T)}\mathbf{d}_{(k+1:N_T)}\right) & \text{if } 1\le k<N_T\\ \bar{r}_{k,k}^{-1}\bar{y}_k & \text{if } k=N_T\end{cases}\,. \tag{3.62}$$

Furthermore, recalling that $\mathbf{d}_{(1:L)}=\hat{\mathbf{s}}$ and $\mathbf{d}_{(L+1:N_T)}=\tilde{\mathbf{s}}$, if $k\le L$,, we get

$$\zeta_k(\mathbf{d}_{(k+1:N_T)})=\bar{r}_{k,k}^{-1}\left(\bar{y}_k-\bar{\mathbf{R}}_{(k,k+1:N_T)}\mathbf{d}_{(k+1:N_T)}\right)=\bar{r}_{k,k}^{-1}\left(\bar{y}_k-\sum_{j=L+1}^{N_T}\bar{r}_{k,j}\tilde{s}_j-\sum_{j=k+1}^{L}\bar{r}_{k,j}\hat{s}_j\right)\,. \tag{3.63}$$

Comparing (3.63) with (3.53) and using (3.41), we conclude

$$d_k=\mathcal{M}\Big(\zeta_k(\mathbf{d}_{(k+1:N_T)})\Big)\,,\quad k\le L\,. \tag{3.64}$$

We can now derive a tree based implementation of the list detection. The tree has N_T layers, with a total of V_k nodes at layer k ($k=1,\ldots,N_T$). Similar to FSD [23], V_k is given by:

$$V_k=\begin{cases}M^{N_T-k+1} & \text{if } L+1\le k\le N_T\\ M^N & \text{otherwise}\end{cases} \tag{3.65}$$

Thus the N layers closest to the root are fully expanded, and a single child node is generated per parent node for the remaining layers. Denote the i-th node at the k-th layer as $v_k^{(i)}$ (i=$0,\ldots,V_k$−1). Also, associated with $v_k^{(i)}$ is the partial vector $\mathbf{d}_{(k:N_T)}^{(i)}=[d_k^{(i)}\,d_{k+1}^{(i)}\ldots d_{N_T}^{(i)}]^T$. Letting $\mathcal{A}=\{a_0\ \ldots\ a_{M-1}\}$ and assuming that N_T>L+1, we proceed as follows:

Algorithm: Tree based list detection

1. Let $k = N_T$.
   Compute $\zeta_k(\mathbf{d}_{(k+1:N_T)})$ using (3.62).
   Generate the M nodes $v_k^{(0)}, \ldots, v_k^{(M-1)}$ associated respectively with $\mathbf{d}_{(k:N_T)}^{(0)}=[a_0], \ldots, \mathbf{d}_{(k:N_T)}^{(M-1)}=[a_{M-1}]$.
   For each node $v_k^{(j)}$, $j=0, \ldots, M-1$, compute $\gamma_k(\mathbf{d}_{(k:N_T)}^{(j)})$ and $\xi_k(\mathbf{d}_{(k:N_T)}^{(j)})$ using (3.61) and (3.60) respectively.

2. For layers $k = N_T, \ldots, L+2$, for each node $v_k^{(i)}$,
   Compute $\zeta_{k-1}(\mathbf{d}_{(k:N_T)}^{(i)})$ using (3.62).
   Generate the M child nodes $v_{k-1}^{(iM)}$, $v_{k-1}^{(iM+1)}$, $\ldots$, $v_{k-1}^{(iM+M-1)}$ at layer $k-1$, associated respectively with $\mathbf{d}_{(k-1:N_T)}^{(iM)} = [a_0\, \mathbf{d}_{(k:N_T)}^{(i)\,T}]^T$, $\mathbf{d}_{(k-1:N_T)}^{(iM+1)} = [a_1\, \mathbf{d}_{(k:N_T)}^{(i)\,T}]^T, \ldots, \mathbf{d}_{(k-1:N_T)}^{(iM+M-1)} = [a_{M-1}\, \mathbf{d}_{(k:N_T)}^{(i)\,T}]^T$.
   For each node $v_{k-1}^{(j)}$, $j=iM, \ldots, iM+M-1$, compute $\gamma_{k-1}(\mathbf{d}_{(k-1:N_T)}^{(j)})$ and $\xi_{k-1}(\mathbf{d}_{(k-1:N_T)}^{(j)})$ using (3.61) and (3.60) respectively.

3. For layers $k = L+1, \ldots, 2$, for each node $v_k^{(i)}$,
   Compute $\zeta_{k-1}(\mathbf{d}_{(k:N_T)}^{(i)})$ using (3.62).
   Obtain $d_{k-1}^{(i)}$ using (3.64).
   Generate the child node $v_{k-1}^{(i)}$ at layer $k-1$, associated with $\mathbf{d}_{(k-1:N_T)}^{(i)} = [d_{k-1}^{(i)}\, \mathbf{d}_{(k:N_T)}^{(i)\,T}]^T$.
   For this node $v_{k-1}^{(i)}$, compute $\gamma_{k-1}(\mathbf{d}_{(k-1:N_T)}^{(i)})$ and $\xi_{k-1}(\mathbf{d}_{(k-1:N_T)}^{(i)})$ using (3.61) and (3.60) respectively.

4. Compute
$$i^* = \arg \min_{i \in \{0,\ldots,M^N-1\}} \xi_1(\mathbf{d}_{(1:N_T)}^{(i)}) \tag{3.66}$$
   and the final decision is $\mathbf{d}_{(1:N_T)}^{(i^*)}$.

If N_T=L+1, i.e N=1, then step 2) is skipped. The MMSE-ISTP tree is illustrated in Fig. 3.1.

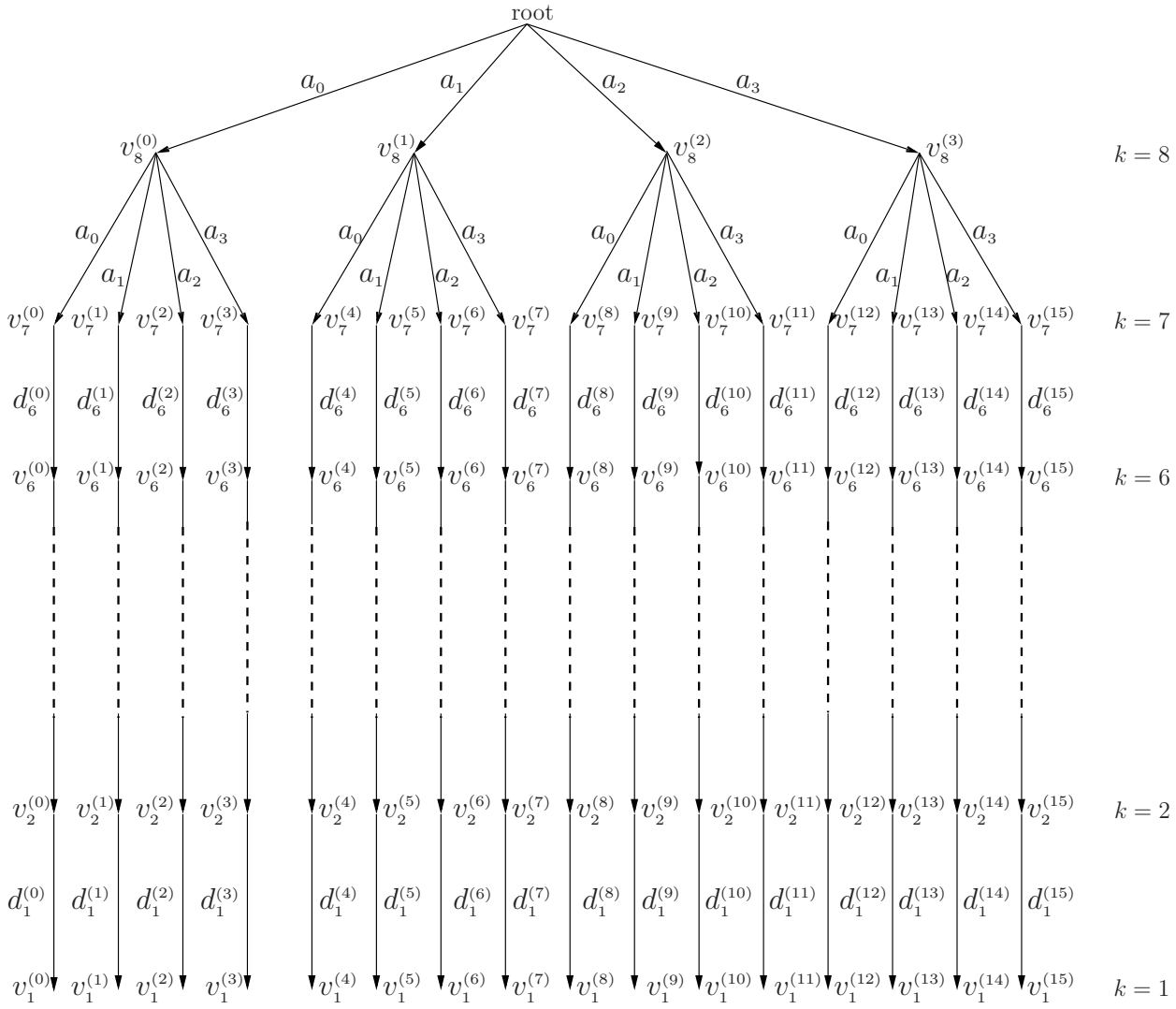

Fig. 3.1 Illustration of the MMSE-ISTP tree for $N_T = 8$, $N = 2$, $M = 4$

Observe that for this configuration, the MMSE-ISTP tree contains overall only 4+7×16=116 nodes (excluding the root) while the corresponding tree for an exhaustive search contains $\sum_{i=1}^{N_T} 4^i$=87380 nodes. In principle, to provide further complexity reductions, same as in [53], we could apply techniques from the K-Best algorithm [17] to the MMSE-ISTP tree. However, such an approach does not guarantee finding the MMSE-ISTP's output and hence the theoretical high SNR optimality is not preserved. Therefore, we employ here a different technique that exploits the structure of the MMSE-ISTP tree to lower the cost of computing (3.62) with no performance loss. Assuming that

$k \in \{2,\ldots,N_T\}$, for any node $v_k^{(i)}$ ($i \in \{0,\ldots,V_k{-}1\}$), from (3.62) we have:

$$\zeta_{k-1}(\mathbf{d}^{(i)}_{(k:N_T)}) = \bar{r}^{-1}_{k-1,k-1}\left(\bar{y}_{k-1} - \bar{\mathbf{R}}_{(k-1,k:N_T)}\mathbf{d}^{(i)}_{(k:N_T)}\right) = \bar{r}^{-1}_{k-1,k-1}\left(\bar{y}_{k-1} - \sum_{j=k}^{N_T}\bar{r}_{k-1,j}d_j^{(i)}\right) . \quad (3.67)$$

Now assuming that $N > 1$, let $(m_{N-1,i} \ldots m_{0,i})$ be the base-M representation of i, i.e $i = m_{N-1,i}M^{N-1}+\cdots+m_{1,i}M+m_{0,i}$ with $m_{j,i} \in \{0,\ldots,M{-}1\}$. Thus for $k = L{+}1,\ldots,N_T$, the partial vector $\mathbf{d}^{(i)}_{(k:N_T)}$ is given by

$$\mathbf{d}^{(i)}_{(k:N_T)} = [a_{m_{0,i}} \ \ldots \ a_{m_{k_i-1,i}} \ a_{m_{k_i,i}} \ a_{m_{k_i+1,i}} \ \ldots \ a_{m_{N_T-k,i}}]^T . \quad (3.68)$$

Then assuming that $i \neq 0$, let k_i be such that $m_{j,i} = 0\,,\ \forall j < k_i$ and $m_{k_i,i} \neq 0$, and define $w(i) = i - m_{k_i,i}M^{k_i}$. Clearly $m_{k_i,w(i)}{=}0$ and the representations of i and $w(i)$ differ only in their $(k_i{+}1)$-th position. Hence using (3.68), for $k = L+1,\ldots,N_T$, we have

$$\mathbf{d}^{(w(i))}_{(k:N_T)} = [a_{m_{0,i}} \ \ldots \ a_{m_{k_i-1,i}} \ a_0 \ a_{m_{k_i+1,i}} \ \ldots \ a_{m_{N_T-k,i}}]^T . \quad (3.69)$$

Now using (3.67), we obtain

$$\zeta_{k-1}(\mathbf{d}^{(i)}_{(k:N_T)}) = \zeta_{k-1}(\mathbf{d}^{(w(i))}_{(k:N_T)}) + \bar{r}^{-1}_{k-1,k-1}\left(\bar{r}_{k-1,k+k_i}(a_0{-}a_{m_{k_i,i}})\right) , \quad L+1 \leq k \leq N_T\,,\ i \neq 0\,. \quad (3.70)$$

Since $w(i) \in \{0,\ldots,V_k{-}1\}$ and $w(i) < i$, $\zeta_{k-1}(\mathbf{d}^{(w(i))}_{(k:N_T)})$ is readily available when computing $\zeta_{k-1}(\mathbf{d}^{(i)}_{(k:N_T)})$. For the remaining layers, we also have:

$$\begin{aligned}\mathbf{d}^{(i)}_{(k:N_T)} &= [d_k^{(i)} \ d_{k+1}^{(i)} \ \ldots \ d_L^{(i)} \ a_{m_{0,i}} \ \ldots \ a_{m_{k_i-1,i}} \ a_{m_{k_i,i}} \ a_{m_{k_i+1,i}} \ldots \ a_{m_{N-1,i}}]^T \\ \mathbf{d}^{(w(i))}_{(k:N_T)} &= [d_k^{(w(i))} \ d_{k+1}^{(w(i))} \ \ldots \ d_L^{(w(i))} \ a_{m_{0,i}} \ \ldots \ a_{m_{k_i-1,i}} \ a_0 \ a_{m_{k_i+1,i}} \ \ldots \ a_{m_{N-1,i}}]^T .\end{aligned}$$

Then defining,

$$\boldsymbol{\Delta}^{(k)}_{i,w(i)} = [\delta_1^{i,w(i)} \ \ldots \ \delta_{L-k+1}^{i,w(i)}]^T = \mathbf{d}^{(w(i))}_{(k:L)} - \mathbf{d}^{(i)}_{(k:L)} = \begin{cases} [d_k^{(w(i))} - d_k^{(i)} \ \boldsymbol{\Delta}^{(k+1)\,T}_{i,w(i)}]^T & \text{if } 2 \leq k < L \\ d_L^{(w(i))} - d_L^{(i)} & \text{if } k = L \end{cases} \quad (3.71)$$

using (3.67), we get

$$\begin{aligned}\zeta_{k-1}(\mathbf{d}^{(i)}_{(k:N_T)}) &= \zeta_{k-1}(\mathbf{d}^{(w(i))}_{(k:N_T)}) \\ &+ \bar{r}^{-1}_{k-1,k-1}\left(\bar{r}_{k-1,L+k_i+1}(a_0{-}a_{m_{k_i,i}}) + \sum_{j=1,\ldots,L-k+1}\bar{r}_{k-1,k-1+j}\delta_j^{(i,w(i))}\right) , \quad 2 \leq k \leq L\,,\ i \neq 0\,.\end{aligned} \quad (3.72)$$

From (3.71), given $\mathbf{\Delta}_{i,w(i)}^{(k+1)}$, obtaining $\mathbf{\Delta}_{i,w(i)}^{(k)}$ requires only one complex addition. Furthermore, the elements of the set $\mathcal{A}'=\{a_0-a_1,\ldots,a_0-a_{M-1}\}$ are independent of $\bar{\mathbf{R}}$ and $\bar{\mathbf{y}}$, and hence can be precomputed. Observe now that the computation of $\left(\bar{y}_{k-1}-\sum_{j=k}^{N_T}\bar{r}_{k-1,j}d_j^{(i)}\right)$ in (3.67) involves N_T-k+2 terms, while the expressions within the main parentheses in (3.70) and (3.72) involve respectively 1 and $N_T-N-k+2$ terms. Finally, if $N=1$, then neither (3.70) nor (3.72) provide complexity reductions over (3.67).

In summary, assuming that $N>1$, $\zeta_{k-1}(\mathbf{d}_{(k:N_T)}^{(i)})$ is efficiently computed as follows:

Algorithm: Efficient computation of $\zeta_{k-1}(\mathbf{d}_{(k:N_T)}^{(i)})$

1. $\zeta_{k-1}(\mathbf{d}_{(k:N_T)}^{(0)})$ is computed using (3.67), $2\leq k\leq N_T$.
2. If $i\neq 0$, $\zeta_{k-1}(\mathbf{d}_{(k:N_T)}^{(i)})$ is computed using (3.70) if $L+1\leq k\leq N_T$ or (3.72) if $2\leq k\leq L$.
3. If $N=1$, then $\zeta_{k-1}(\mathbf{d}_{(k:N_T)}^{(i)})$ is computed from (3.67) for all nodes and all layers.

3.4 Complexity analysis and comparison

We will now analyze the total complexity of the Sel-MMSE-OSIC and MMSE-ISTP schemes. We count the number of floating point operations (FLOPS) required, where a complex addition/substraction costs 2 flops and a complex multiplication/division costs 6 flops [7].

3.4.1 Total complexity of Sel-MMSE-OSIC

The channel partition stage of the Sel-MMSE-OSIC scheme requires the computation of $N_U=\binom{N_T}{N}$ inverses of matrices of the form $\left(\mathbf{A}^H\mathbf{A}+\mathrm{SNR}^{-1}\mathbf{I}_L\right)$ where $\mathbf{A}$ is an $N_R\times(N_T-N)$ complex matrix. From the results presented in [48], each such inversion requires $\Big(4(N_T-N)^3+(N_T-N)^2(4N_R+1)+(N_T-N)(4N_R-6)+6\Big)$ flops . Using the results from [48], the generation of the L MMSE weight vectors $\mathbf{w}_i$ from (3.12) costs $\Big(4/3(N_T-N)^3+(N_T-$

$N)^2(4N_R+3)+(N_T-N)(2N_R-13/3)\Big)$ flops. Hence the total cost of the Sel-MMSE-OSIC's preprocessing stage, i.e. channel partition and weight vectors generation, is

$$C^{\text{preprocessing}}_{\text{Sel-MMSE-OSIC}} = \binom{N_T}{N}\Big(4(N_T-N)^3+(N_T-N)^2(4N_R+1)+(N_T-N)(4N_R-6)+6\Big) + \Big(4/3(N_T-N)^3+(N_T-N)^2(4N_R+3)+(N_T-N)(2N_R-13/3)\Big) \quad \text{flops}. \quad (3.73)$$

Then for each of the M^N candidate vectors, computing $\mathbf{y}^k$ costs $8NN_R$ flops. Then obtaining $\check{d}_i^{(k)}$ from (3.13) cost $8N_R-2$ flops for each i. We denote by q the cost of the mapping function $\mathcal{M}(.)$. The computation of $\mathbf{z}_i^k$ of (3.14) requires $8N_R$ flops for $i=L-1,\ldots,1$. Finally solving (3.15) costs $12M^NN_R-1$ flops. Hence the overall cost of list detection is

$$C^{\text{list}}_{\text{Sel-MMSE-OSIC}} = M^N\Big((N_T-N)(16N_R+q-2)+8NN_R+4N_R\Big)-1 \quad \text{flops}. \quad (3.74)$$

The total cost of the Sel-MMSE-OSIC scheme is then the sum of (3.73) and (3.74).

3.4.2 Total complexity of the MMSE-ISTP scheme

By a simple flops counting argument, we can show that the MMSE based Greedy QR algorithm of Appendix B costs $N_T\left(8N_TN_R+18N_R+\frac{19}{2}N_T+\frac{39}{2}\right)$ flops. Then computing $\check{\mathbf{R}}^{-1}_{(1:L,1:L)}$ costs (see. e.g. [52]) $\frac{4}{3}L^3-\frac{1}{2}L^2+\frac{1}{6}L$ flops. After that, computing $\tilde{\mathbf{R}}_2^{-1}\left(\tilde{\mathbf{R}}_2^{-1}\right)^H$ costs $\frac{4}{3}L^3-L^2+\frac{2}{3}L$ flops. Then obtaining the V-BLAST ordering using the algorithm of [48] costs $\frac{4}{3}L^3-\frac{1}{2}L^2+\frac{1}{6}L-1$ flops. Finally obtaining $\bar{\mathbf{R}}$ and $\bar{\mathbf{y}}$ by Givens QR (see. e.g [52]) costs $4L^3+15L^2-16L-14$ flops. Hence, the channel partition step costs overall

$$C^{\text{preprocessing}}_{\text{MMSE-ISTP}} = N_T\left(8N_T^2+8N_TN_R+18N_R-N_T\left(24N-\frac{45}{2}\right)+2N(12N-13)+\frac{9}{2}\right) - N(8N^2-13N-15)-15 \quad \text{flops}. \quad (3.75)$$

Now concerning the tree based list detection stage, we assume that $N>1$, $L>1$ and that $\alpha^2|z|^2$, $\forall z\in\mathcal{A}$ is readily available. Then in Step 1), given $\bar{r}^{-1}_{N_T,N_T}$ (which costs 1 flop to obtain), computing $\zeta_k(\mathbf{d}_{(k+1:N_T)})$ using (3.62), costs 2 flops. Then for each node $v_k^{(j)}$,

$j = 0, \ldots, M-1$, given $\bar{r}^2_{N_T,N_T}$ (which also costs 1 flop to obtain), computing $\gamma_k(\mathbf{d}^{(j)}_{(k:N_T)})$ using (3.61) costs 7 flops. Then obtaining $\xi_k(\mathbf{d}^{(j)}_{(k:N_T)})$ using (3.60) cost no additional flops. Hence the total cost of Step 1) is:

$$C_1 = 2 + 2 + 7M = 7M + 4 \text{ flops}. \tag{3.76}$$

As for Step 2), for each node $v^{(i)}_k$ at layer $k = N_T, \ldots, L+2$, if $i \neq 0$ then given the set $\mathcal{A}' = \{a_0 - a_1, \ldots, a_0 - a_{M-1}\}$ (which we assume has been precomputed), and given $\bar{r}^{-1}_{k-1,k-1}$, computing $\zeta_{k-1}(\mathbf{d}^{(i)}_{(k:N_T)})$ using (3.70) costs 10 flops. If $i = 0$ then computing $\zeta_{k-1}(\mathbf{d}^{(0)}_{(k:N_T)})$ using (3.67) costs $8(N_T - k + 1) + 2$ flops. Then for each $v^{(j)}_{k-1}$, $j = iM, \ldots, iM + M - 1$, given $\bar{r}^2_{k-1,k-1}$, computing $\gamma_{k-1}(\mathbf{d}^{(j)}_{(k-1:N_T)})$ using (3.61) costs 7 flops and finally obtaining $\xi_{k-1}(\mathbf{d}^{(j)}_{(k-1:N_T)})$ using (3.60) costs 1 additional flop. Hence the total cost associated with the k-th layer of Step 2) is:

$$\begin{aligned} C^{(k)}_2 &= 2 + 10(V_k - 1) + 8(N_T - k + 1) + 2 + V_k M(7+1) \\ &= (10 + 8M)V_k + 8(N_T - k) + 2 \text{ flops}. \end{aligned}$$

Hence, the total cost associated with Step 2) is:

$$\begin{aligned} C_2 &= \sum_{k=L+2}^{N_T} (10 + 8M)M^{N_T - k + 1} + 8(N_T - k) + 2 \\ &= 8M^N + 18\sum_{j=2}^{N-1} M^j + 10M + 2N(2N-5) + 6 \text{ flops}. \end{aligned} \tag{3.77}$$

Proceeding similarly, we obtain that the total cost associated with Step 3) is

$$C_3 = \Big(4(N_T - N)^2 + (16 + q)(N_T - N) - 2\Big)M^N + 8(N_T - N)(N-1) + 2 \quad \text{flops}. \tag{3.78}$$

where we assumed that the cost of obtaining d_k using (3.64) is q flops. Finally, obtaining the final output in Step 4) requires

$$C_4 = M^N - 1 \quad \text{flops}. \tag{3.79}$$

Hence using (3.76), (3.77), (3.78) and (3.79), the list detection stage costs overall

$$C^{\text{list}}_{\text{MMSE-ISTP}} = M^N\Big(4(N_T-N)^2+(N_T-N)(16+q)+7\Big)+18\sum_{k=2}^{N-1}M^k + 17M+8NN_T-8N_T-4N^2-2N+11 \quad \text{flops}\,. \quad (3.80)$$

The total cost of the MMSE-ISTP scheme is the sum of (3.75) and (3.80). If $N=1$, then

$$C^{\text{list}}_{\text{MMSE-ISTP, 1}} = M\left(4N_T^2+(6+q)N_T-q-2\right)+2N_T+1 \quad \text{flops}\,. \quad (3.81)$$

Comparing (3.75) with (3.80) we see that the former is cubic in N_T, and the latter is quadratic in N_T. Thus when M^N is relatively small, i.e small constellation size and small N, then the channel partition step dominates the total complexity.

3.4.3 Complexity comparison

In Table 3.1, we present the ratio of the total complexities of Sel-MMSE-OSIC [33], FSD [23] as well as MMSE-FSD and SFSD [53] to that of MMSE-ISTP. The total complexities of these schemes are easily obtained from the complexity analyzes given in [33] and [53]. Notice that FSD and SFSD are not suitable for under-determined systems. Regarding the cost q of obtaining d_k from (3.64), we consider square M-QAM constellations and set q as follows: $q=0$ if $M=4$, and $q=4$ otherwise. Further details are provided in Appendix C.

Table 3.1 Flops count of various fixed complexity algorithms relative to MMSE-ISTP

System \ M		4	16	64
$N_T=N_R=6$, $N=2$	Sel-MMSE-OSIC	3.39	3.36	3.38
	FSD	1.15	1.50	1.56
$N_T=N_R=8$, $N=2$	Sel-MMSE-OSIC	6.43	3.91	3.50
	FSD	1.08	1.46	1.53
	SFSD	0.92	0.55	0.28
$N_T=7$, $N_R=6$, $N=2$	Sel-MMSE-OSIC	4.46	3.14	2.96
	MMSE-FSD	1.15	1.51	1.56
$N_T=8$, $N_R=6$, $N=3$	Sel-MMSE-OSIC	6.0	3.22	3.17
	MMSE-FSD	1.66	1.90	1.91

As seen in Table 3.1, the MMSE-ISTP scheme has lower complexity than the Sel-MMSE-OSIC, FSD and MMSE-FSD schemes. Indeed, it lowers the complexity with respect to FSD by a factor of about 1.5, and up to 1.9 for MMSE-FSD. Compared to Sel-MMSE-OSIC, it lowers the complexity by a factor up to 6 for QPSK and up to 3.5 for 64QAM. The SFSD algorithm on the other hand can lower the complexity with respect to MMSE-ISTP by a factor of 1.8 and 3.6 for N_T=N_R=8 with 16QAM and 64QAM respectively. However, we will see in chapter 5 that while the MMSE-ISTP scheme has a performance nearly indistinguishable from ML in most cases, the SFSD scheme exhibits a diversity loss. Furthermore the latter requires adequate tuning of multiple parameters to reduce the performance degradation. This tuning is done through computer simulations and the appropriate settings were given in [53] for the N_T=N_R=8 system with QPSK and 16QAM only. For 64QAM, we found the setting to be (2048, 1024, 512, 256, 128) (see. [53] for more information). For such a large system, the tuning process is very time consuming.

Chapter 4

The variable complexity MMSE-ISVTP algorithm

In chapter 3, we proposed the fixed complexity asymptotically optimal Sel-MMSE-OSIC and MMSE-ISTP schemes. The latter was shown to be less complex than the former and its fixed complexity makes it very attractive for practical implementation, since very high throughput can be achieved through pipelining and paralleling (see. e.g. [54]). However for large constellation sizes or large systems, the list size becomes large and therefore the power and memory requirements associated with the fixed complexity strategy can become excessive. In such cases, one can tolerate some complexity variations in order to lower the average computational load. Hence in this chapter, we consider a variable complexity version of the MMSE-ISTP scheme. We first briefly review the classical sphere decoding (SD) algorithm which is a variable complexity tree search based algorithm for MIMO detection [11, 20]. Its basic principles are then leveraged to develop a variable complexity version of MMSE-ISTP, which finds the MMSE-ISTP's output without explicitly visiting all the nodes in the MMSE-ISTP's tree. Part of this chapter was published in [35, 36].

4.1 Sphere decoding (SD) algorithm

Assume for now that $\mathbf{H}$ has full column rank, implying $N_T \leq N_R$, and let the QR decomposition of $\mathbf{H}$ be :

$$\mathbf{H} = \mathbf{Q}\,[\mathbf{R}^T\,\mathbf{0}]^T \tag{4.1}$$

where $\mathbf{Q} \in \mathbb{C}^{N_R \times N_R}$ is unitary, i.e $\mathbf{Q}\mathbf{Q}^H = \mathbf{Q}^H\mathbf{Q} = \mathbf{I}_{N_R}$. $\mathbf{R}$ is an $N_T \times N_T$ upper triangular matrix with positive diagonal elements. Since $\mathbf{Q}$ is unitary, using (4.1), we have:

$$\|\mathbf{y} - \mathbf{H}\mathbf{d}\|^2 = \left\|\mathbf{y} - \mathbf{Q}\begin{bmatrix}\mathbf{R}\\ \mathbf{0}\end{bmatrix}\mathbf{d}\right\|^2 = \|\mathbf{z}_{(1:N_T)} - \mathbf{R}\mathbf{d}\|^2 + \|\mathbf{z}_{(N_T+1:N_R)}\|^2 \tag{4.2}$$

with

$$\mathbf{z} = \mathbf{Q}^H\mathbf{y}\,. \tag{4.3}$$

Using (4.2) in (2.2), the ML decision rule becomes:

$$\hat{\mathbf{x}}^{\mathrm{ML}} = \arg\min_{\mathbf{d}\in\mathcal{A}^{N_T}} \left(\|\mathbf{z}_{(1:N_T)} - \mathbf{R}\mathbf{d}\|^2 + \|\mathbf{z}_{N_T+1:N_R}\|^2\right)\,. \tag{4.4}$$

Finally since the second term in (4.4) is independent of $\mathbf{d}$, it doest not affect the solution of the minimization problem and therefore the ML decision rule in the QR domain is

$$\hat{\mathbf{x}}^{\mathrm{ML}} = \arg\min_{\mathbf{d}\in\mathcal{A}^{N_T}} \|\mathbf{z}_{(1:N_T)} - \mathbf{R}\mathbf{d}\|^2\,. \tag{4.5}$$

The SD algorithm searches for the optimal solution of (4.5) subject to a sphere constraint C_{SD}^2, i.e the search set is restricted to those points $\mathbf{d} \in \mathcal{A}^{N_T}$ that satisfy

$$\|\mathbf{z}_{(1:N_T)} - \mathbf{R}\mathbf{d}\|^2 \leq C_{SD}^2\,. \tag{4.6}$$

For the search set to be nonempty, the sphere radius C_{SD} must satisfy: $C_{SD}^2 \geq \min_{\mathbf{d}\in\mathcal{A}^{N_T}} \|\mathbf{z}_{(1:N_T)} - \mathbf{R}\mathbf{d}\|^2$. In practice, C_{SD} is generally initialized to a large value and is updated as the search progresses and new ML candidates are generated. Note that the sphere constraint does not entail any loss of optimality of SD since the minimizer of (4.5) must also satisfy (4.6). Given C_{SD}, the SD algorithm exploits the triangular structure

of $\mathbf{R}$ to find the points $\mathbf{d}$ that satisfy (4.6). Specifically,let

$$\xi'_k(\mathbf{d}_{(k:N_T)}) = \|\mathbf{z}_{(k:N_T)} - \mathbf{R}_{(k:N_T,k:N_T)}\mathbf{d}_{(k:N_T)}\|^2\,, \quad k = 1,\ldots,N_T\,. \tag{4.7}$$

Clearly, $\xi'_1(\mathbf{d}_{(1:N_T)}) = \|\mathbf{z}_{(1:N_T)} - \mathbf{R}\mathbf{d}\|^2$ and thus the radius constrained minimization solved by the SD algorithm is

$$\hat{\mathbf{x}}^{\mathrm{ML}} = \arg\min_{\mathbf{d}\in\mathcal{S}} \xi'_1(\mathbf{d}_{(1:N_T)}) \tag{4.8}$$

where $\mathcal{S} = \{\mathbf{d} \in \mathcal{A}^{N_T} : \xi'_1(\mathbf{d}_{(1:N_T)}) \le C^2_{SD}\}$. Observe now that

$$\|\mathbf{z}_{(k:N_T)} - \mathbf{R}_{(k:N_T,k:N_T)}\mathbf{d}_{(k:N_T)}\|^2 = \|\mathbf{z}_{(k+1:N_T)} - \mathbf{R}_{(k+1:N_T,k+1:N_T)}\mathbf{d}_{(k+1:N_T)}\|^2 + |z_k - r_{k,k}d_k - \mathbf{R}_{(k,k+1:N_T)}\mathbf{d}_{(k+1:N_T)}|^2\,, \tag{4.9}$$

where z_k and d_k are respectively the k-th component of $\mathbf{z}$ and $\mathbf{d}$, and $r_{k,k}$ is the k-th diagonal element of $\mathbf{R}$. Thus defining

$$\begin{aligned}\gamma'_k(\mathbf{d}_{(k:N_T)}) &= |z_k - r_{k,k}d_k - \mathbf{R}_{(k,k+1:N_T)}\mathbf{d}_{(k+1:N_T)}|^2 \\ &= r^2_{k,k}|\zeta_k(\mathbf{d}_{(k+1:N_T)}) - d_k|^2\,, \quad k = 1,\ldots,N_T\end{aligned} \tag{4.10}$$

with

$$\zeta'_k(\mathbf{d}_{(k+1:N_T)}) = \begin{cases} r^{-1}_{k,k}\left(z_k - \mathbf{R}_{(k,k+1:N_T)}\mathbf{d}_{(k+1:N_T)}\right) & \text{if } 1 \le k < N_T \\ r^{-1}_{k,k}z_k & \text{if } k = N_T \end{cases} \tag{4.11}$$

then from (4.9) we have

$$\xi'_k(\mathbf{d}_{(k:N_T)}) = \xi'_{k+1}(\mathbf{d}_{(k+1:N_T)}) + \gamma'_k(\mathbf{d}_{(k:N_T)})\,, \quad k = 1,\ldots,N_T \tag{4.12}$$

with $\xi'_{k+1}(\mathbf{d}_{(k+1:N_T)}) = 0 \quad \text{if} \quad k = N_T$. Now since $\gamma'_k(\mathbf{d}_{(k:N_T)}) \ge 0\,, \forall k, \mathbf{d}$, from (4.12), for any given $\mathbf{d}$, we get

$$\xi'_k(\mathbf{d}_{(k:N_T)}) \ge \xi'_{k+1}(\mathbf{d}_{(k+1:N_T)}) \tag{4.13}$$

Therefore a necessary condition for $\xi'_1(\mathbf{d}_{(1:N_T)}) \le C^2_{SD}$ is

$$\xi'_k(\mathbf{d}_{(k:N_T)}) \le C^2_{SD}\,, \quad k = 2,\ldots,N_T. \tag{4.14}$$

Using (4.12), (4.13) and (4.14), the SD algorithm solves (4.8) adopting a tree search strategy. The tree has N_T levels (excluding the root node) and is traversed from level $k = N_T$

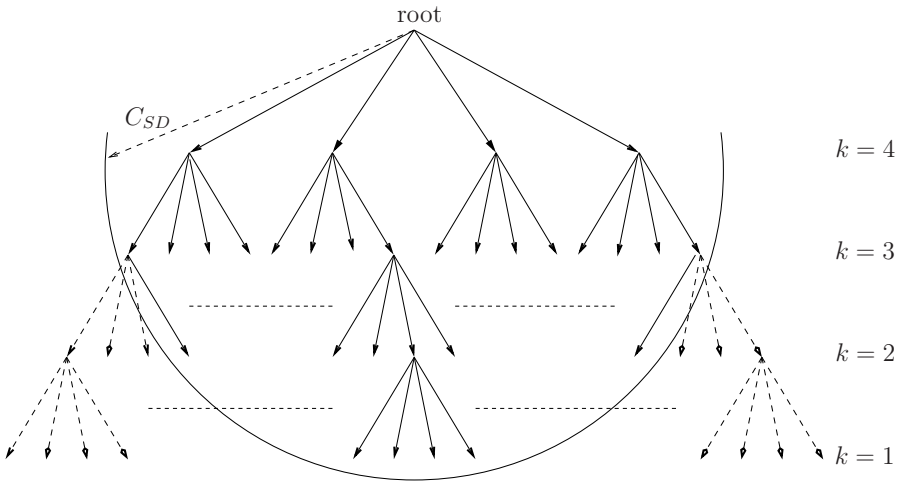

Fig. 4.1 Illustration of the SD search tree: $N_T = 4$, $M = 4$

to $k = 1$. The SD tree is illustrated in Fig. 4.1. If a parent node v_{k+1} associated with the partial vector $\mathbf{d}_{(k+1:N_T)}$ does not satisfy the sphere constraint, i.e $\xi'_{k+1}(\mathbf{d}_{(k+1:N_T)}) > C^2_{SD}$ then from (4.13), any child node emanating from v_{k+1} will also not satisfy the sphere constraint. Hence v_{k+1} and the entire subtree emanating from it can be pruned from the search tree since none of these nodes can lead to the ML solution. On the other hand, if a parent node v_{k+1} associated with the partial vector $\mathbf{d}_{(k+1:N_T)}$ is valid, i.e. $\xi'_{k+1}(\mathbf{d}_{(k+1:N_T)}) \leq C^2_{SD}$, then from (4.12), a child node v_k associated with the partial vector $\mathbf{d}_{(k:N_T)}$ is valid, i.e. $\xi'_k(\mathbf{d}_{(k:N_T)}) \leq C^2_{SD}$, if and only if

$$\gamma'_k(\mathbf{d}_{(k:N_T)}) \leq C^2_{SD} - \xi'_{k+1}(\mathbf{d}_{(k+1:N_T)})\,. \tag{4.15}$$

Using (4.10), (4.15) is equivalent to the following constraint on allowable values for the element d_k

$$|\zeta'_k(\mathbf{d}_{(k+1:N_T)}) - d_k|^2 \leq r^{-2}_{k,k}\left(C^2_{SD} - \xi'_{k+1}(\mathbf{d}_{(k+1:N_T)})\right)\,. \tag{4.16}$$

The classical depth first search SD algorithm with radius update and Schnorr-Euchner (SE) ordering for child nodes enumeration can now be summarized as follows [20]:

1. Create the empty list ACTIVE and place the root node in ACTIVE. Set $C^2_{SD} = \infty$.
2. Let $\mathbf{d}_{(k:N_T)}$ be the partial vector associated with the node v_k at the top of ACTIVE. *If* $\xi'_k(\mathbf{d}_{(k:N_T)}) > C^2_{SD}$, then remove v_k from ACTIVE and *Goto* step 3).

If $k = 1$, i.e we have reached a leaf node, then set

$$C_{SD}^2 = \xi_1'(\mathbf{d}_{(1:N_T)}), \quad \hat{\mathbf{x}}^{\mathrm{ML}} = \mathbf{d}_{(1:N_T)},$$

remove v_1 from ACTIVE and *Goto* step 3).

Find all the child nodes of v_k that satisfy

$$|\zeta_{k-1}'(\mathbf{d}_{(k:N_T)}) - d_{k-1}|^2 \leq r_{k-1,k-1}^{-2} \left(C_{SD}^2 - \xi_k'(\mathbf{d}_{(k:N_T)})\right).$$

Sort these child nodes with respect to $\gamma_{k-1}'(\mathbf{d}_{(k-1:N_T)})$ and place them in ACTIVE above v_k, with the top node being the one associated with the smallest value of $\gamma_{k-1}'(\mathbf{d}_{(k-1:N_T)})$. Remove v_k from ACTIVE.

3. If ACTIVE is empty then *Exit*, otherwise *Goto* step 2).

The SD algorithm has lower complexity than the exhaustive search approach and achieves ML performance. However, the number of nodes generated during the search is a random variable that depends on the operating SNR and the channel realization through $\mathbf{R}$. In fact, the expected complexity of SD is exponential in N_T for any finite SNR [13]. Observe now that for a given radius C_{SD} and a given parent node at level $k+1$ associated with the partial vector $\mathbf{d}_{(k+1:N_T)}$, from (4.16), the valid child nodes are those that fall within a circle centered at $\zeta_k'(\mathbf{d}_{(k+1:N_T)})$ with radius $r_{k,k}^{-1}\left(C_{SD}^2 - \xi_{k+1}'(\mathbf{d}_{(k+1:N_T)})\right)^{1/2}$. Thus, the smaller is $r_{k,k}$, then the larger is this radius and therefore a larger number of valid nodes may be generated. Hence channel matrix ordering prior to applying the SD algorithm can offer substantial complexity gains over the unordered case [11, 26]. Now let $\mathbf{P}$ be an N_T-dimensional column permutation matrix and let

$$\mathbf{HP} = \mathbf{Q_P R_P} \tag{4.17}$$

be the (thin) QR decomposition of $\mathbf{HP}$ where $\mathbf{Q_P} \in \mathbb{C}^{N_R \times N_T}$ has orthonormal columns and $\mathbf{R_P}$ is an N_T-dimensional upper triangular matrix with positive diagonal elements. Then observe that

$$\det\left(\mathbf{H}^H\mathbf{H}\right) = \det\left((\mathbf{HP})^H(\mathbf{HP})\right) = \det\left(\mathbf{R}_\mathbf{P}^H\mathbf{R_P}\right) = \prod_{k=1}^{N_T} r_{k,k}^{(P),\,2} \tag{4.18}$$

where $r_{k,k}^{(P)}$ is the k-th diagonal element of $\mathbf{R_P}$. Hence, the product of the diagonal elements of $\mathbf{R_P}$ is a constant independent of $\mathbf{P}$ and therefore the diagonal elements cannot all be

made simultaneously large. A commonly used ordering is the V-BLAST ordering rule which is given by [3, 7]

$$\mathbf{P}^{\text{V-BLAST}} = [\mathbf{e}_{p_1} \dots \mathbf{e}_{p_{N_T}}] \tag{4.19}$$

with

$$p_k = \arg \min_{j=1,\dots,k} (\mathbf{H}_k^H \mathbf{H}_k)^{-1}_{(j,j)} \ , \quad k = N_T, \dots, 1 \tag{4.20}$$

where $\mathbf{H}_{N_T} = \mathbf{H}$ and $\mathbf{H}_k$ is obtained from $\mathbf{H}_{k+1}$ by removing its p_{k+1}-th column. It can be shown that this strategy recursively maximizes $r_{k,k}^{(P)}$ from $k = N_T$ to $k = 1$ [55, 56]. Indeed the subtrees associated with nodes closer to the root node are bigger than those of nodes closer to the bottom of the tree. Hence larger values of $r_{k,k}^{(P)}$ for those layers can lead to a more efficient pruning of the tree. Furthermore, the V-BLAST ordering has the additional property that it maximizes the smallest diagonal element of $\mathbf{R_P}$ over all permutation matrices, i.e [4, 20]

$$\mathbf{P}^{\text{V-BLAST}} = \arg \max_{\mathbf{P}} \min_{k \in \{1,\dots,N_T\}} r_{k,k}^{(P)} \, . \tag{4.21}$$

4.2 The variable complexity MMSE-ISVTP tree search scheme

4.2.1 Variable complexity tree search stage

The MMSE-ISTP scheme solves (3.58) through an exhaustive search over a set $\mathcal{S}$ with cardinality $|\mathcal{S}| = M^N$, resulting in an inefficient implementation, especially for large values of M or N. Given the upper triangular structure of $\bar{\mathbf{R}}$, similar to the SD principle, we apply a radius constraint C_{SD} to the search set to provide additional complexity reductions. The radius constrained minimization now becomes $\hat{\mathbf{d}} = \arg \min_{\mathbf{d} \in \mathcal{S}''} \left(\xi_1(\mathbf{d}_{(1:N_T)}) \right)$ with $\mathcal{S}'' = \{\mathbf{d} \in \mathcal{S} : \xi_1(\mathbf{d}_{(1:N_T)}) \leq C_{SD}^2\}$ and $\xi_1(\mathbf{d}_{(1:N_T)})$ is defined in (3.60). Due to the negative term in (3.61), $\gamma_k(\mathbf{d}_{(k:N_T)})$ is not necessarily nonnegative. Therefore, from (3.60), the node associated with $\mathbf{d}_{(k+1:N_T)}$ cannot be pruned from the tree even if $\xi_{k+1}(\mathbf{d}_{(k+1:N_T)}) > C_{SD}^2$. To solve this issue, let

$$r_{\max}^2 = \max_{z \in \mathcal{A}} |z|^2 \tag{4.22}$$

and since $r_{\max}^2$ is a constant independent of $\mathbf{d}$, (3.58) can be rewritten as

$$\hat{\mathbf{d}} = \arg\min_{\mathbf{d}\in\mathcal{S}} \left(\left\| \bar{\mathbf{y}}_{(1:N_T)} - \bar{\mathbf{R}}\mathbf{d} \right\|^2 + \beta^2 \left(N_T r_{\max}^2 - \|\mathbf{d}\|^2 \right) \right) . \tag{4.23}$$

Now define $\hat{\xi}_k(\mathbf{d}_{(k:N_T)}) = \|\bar{\mathbf{y}}_{(k:N_T)} - \bar{\mathbf{R}}_{(k:N_T,k:N_T)}\mathbf{d}_{(k:N_T)}\|^2 + \beta^2 \left((N_T - k + 1) r_{\max}^2 - \|\mathbf{d}_{(k:N_T)}\|^2 \right)$, $k=1,\ldots,N_T$, so that (4.23) is equivalent to

$$\hat{\mathbf{d}} = \arg\min_{\mathbf{d}\in\mathcal{S}} \left(\hat{\xi}_1(\mathbf{d}_{(1:N_T)}) \right) . \tag{4.24}$$

It is straightforward to show that

$$\hat{\xi}_k(\mathbf{d}_{(k:N_T)}) = \hat{\xi}_{k+1}(\mathbf{d}_{(k+1:N_T)}) + \hat{\gamma}_k(\mathbf{d}_{(k:N_T)}) \tag{4.25}$$

with $\hat{\xi}_{k+1}(\mathbf{d}_{(k+1:N_T)}) = 0$ if $k = N_T$ and

$$\hat{\gamma}_k(\mathbf{d}_{(k:N_T)}) = \bar{r}_{k,k}^2 |\zeta_k(\mathbf{d}_{(k+1:N_T)}) - d_k|^2 + \beta^2 (r_{\max}^2 - |d_k|^2) , \quad k = 1,\ldots,N_T \tag{4.26}$$

with $\zeta_k(\mathbf{d}_{(k+1:N_T)})$ defined in (3.62). Thus from (4.24), we obtain the equivalent radius constrained minimization $\hat{\mathbf{d}} = \arg\min_{\mathbf{d}\in\tilde{\mathcal{S}}} \left(\hat{\xi}_1(\mathbf{d}_{(1:N_T)}) \right)$ with $\tilde{\mathcal{S}} = \{\mathbf{d} \in \mathcal{S} : \hat{\xi}_1(\mathbf{d}_{(1:N_T)}) \leq C_{SD}^2\}$. By the definition of $r_{\max}^2$ in (4.22), the second term in (4.26) is nonnegative, and therefore $\hat{\gamma}_k(\mathbf{d}_{(k:N_T)})$ is now nonnegative. If $\hat{\xi}_{k+1}(\mathbf{d}_{(k+1:N_T)}) > C_{SD}^2$, the node associated with $\mathbf{d}_{(k+1:N_T)}$ is pruned from the tree. Hence the MMSE-ISTP output can be found with any variable complexity tree search algorithm which solves exactly (2.2), using (4.26), (4.25) and the additional constraint that for any node v_{k+1} at the $k+1$-th level with $1 \leq k \leq L$, the only candidate child node to be considered is the one given by (3.64). The resulting algorithm will be referred to as MMSE-ISVTP. We stress here that while any exact ML tree search scheme like those from [14, 15, 18, 22] can be employed with MMSE-ISVTP, those that provide a tradeoff between complexity and ML performance by varying a set of parameters (e.g. [16, 19, 21]) are not suitable for MMSE-ISVTP as they may not preserve high SNR optimality.

For constant modulus alphabets, as PSK, i.e $|z|^2 = \sigma_s^2$, $\forall z \in \mathcal{A}$, in (4.23) we have $\beta^2\left(N_T r_{\max}^2 - \|\mathbf{d}\|^2\right)=0$, and thus can be omitted. Hence in this case, (4.23) becomes

$$\hat{\mathbf{d}} = \arg\min_{\mathbf{d}\in\mathcal{S}} \left(\left\| \bar{\mathbf{y}}_{(1:N_T)} - \bar{\mathbf{R}}\mathbf{d} \right\|^2 \right) . \tag{4.27}$$

Similarly, $\beta^2(r_{\max}^2 - |d_k|^2) = 0$, and thus can be omitted in (4.26). For arbitrary con-

stellations, the minimization problems in (4.27) and (4.23) are not equivalent. However, for each $\mathbf{d} \in \mathcal{S}$, the objective function in (4.23) adds $\beta^2 \left(N_T r_{\max}^2 - \|\mathbf{d}\|^2 \right) \geq 0$ to that in (4.27). Therefore a variable complexity search scheme that solves (4.27) can operate with a smaller sphere radius and thereby achieve additional complexity reductions, especially for large values of β (low SNR). Hence, we also consider a simplified algorithm that solves (4.27) rather than (4.23), referred to as Sub-MMSE-ISVTP.

4.2.2 Improved channel partition preprocessing

In step 2) of the MMSE-ISTP's channel partition stage (cf. section 3.2), V-BLAST ordering is applied to $\tilde{\mathbf{H}}_2$ only. This is justified by the fact that the error rate performance of the algorithm is invariant to the internal ordering of the columns of $\tilde{\mathbf{H}}_1$ defined in (3.18) (cf. section 2.5). However for a variable complexity implementation, the internal ordering of $\tilde{\mathbf{H}}_1$ can affect the overall cost. Thus for both Sub-MMSE-ISVTP and MMSE-ISVTP we propose to use V-BLAST ordering within both the columns of $\tilde{\mathbf{H}}_2$ and $\tilde{\mathbf{H}}_1$. This improved channel partition can be summarized as follows:

Algorithm: Improved channel partition

1. Same as step 1) of the MMSE-ISTP's channel partition of section 3.2.

2. Obtain $\left(\mathbf{B}_{N_T}^H \mathbf{B}_{N_T}\right)^{-1} = \left(\tilde{\mathbf{H}}^H \tilde{\mathbf{H}}\right)^{-1} = \tilde{\mathbf{R}}^{-1} \left(\tilde{\mathbf{R}}^{-1}\right)^H$ with $\tilde{\mathbf{H}}$, $\tilde{\mathbf{\Pi}}$ and $\tilde{\mathbf{R}}$ defined in (3.18). Then the column permutation matrix $\hat{\mathbf{\Pi}}^{\mathrm{VTP}} \in \mathbb{C}^{N_T \times N_T}$ is obtained as $\hat{\mathbf{\Pi}}^{\mathrm{VTP}} = [\mathbf{e}_{p_1} \ldots \mathbf{e}_{p_{N_T}}]$ with
$$p_i = \begin{cases} \arg\min_{l=L+1,\ldots,i} \left(\mathbf{B}_i^H \mathbf{B}_i\right)^{-1}_{(l,l)} & \text{if } i \geq L+1 \\ \arg\min_{l=1,\ldots,i} \left(\mathbf{B}_i^H \mathbf{B}_i\right)^{-1}_{(l,l)} & \text{otherwise} \end{cases}, \quad i = N_T, \ldots, 1$$
where $\mathbf{B}_{N_T} = \tilde{\mathbf{H}}$ and $\mathbf{B}_i$ is obtained from $\mathbf{B}_{i+1}$ by removing its p_{i+1}-th column. The algorithm of [48] is used to find $\hat{\mathbf{\Pi}}^{\mathrm{VTP}}$ efficiently.

3. Use the Givens QR algorithm from [52] to obtain
$$\bar{\mathbf{H}}^{\mathrm{VTP}} = \breve{\mathbf{H}} \bar{\mathbf{\Pi}}^{\mathrm{VTP}} = [\tilde{\mathbf{H}}_2 \hat{\mathbf{\Pi}}^{\mathrm{VTP}}_{(1:L,1:L)} \;\; \tilde{\mathbf{H}}_1 \hat{\mathbf{\Pi}}^{\mathrm{VTP}}_{(L+1:N_T,L+1:N_T)}] = \bar{\mathbf{Q}}^{\mathrm{VTP}} [\bar{\mathbf{R}}^{\mathrm{VTP},T} \mathbf{0}]^T \;,\; \bar{\mathbf{y}}^{\mathrm{VTP}} = \bar{\mathbf{Q}}^{\mathrm{VTP},H} \breve{\mathbf{y}} \quad (4.28)$$
with $\bar{\mathbf{\Pi}}^{\mathrm{VTP}} = \tilde{\mathbf{\Pi}} \begin{bmatrix} \hat{\mathbf{\Pi}}^{\mathrm{VTP}}_{(1:L,1:L)} & \mathbf{0} \\ \mathbf{0} & \hat{\mathbf{\Pi}}^{\mathrm{VTP}}_{(L+1:N_T,L+1:N_T)} \end{bmatrix}$ and $\bar{\mathbf{R}}^{\mathrm{VTP}} \in \mathbb{C}^{N_T \times N_T}$ is upper triangular with positive diagonal elements.

Theorem 3. *Let* $\bar{r}_{i,j}^{VTP} = \bar{\mathbf{R}}_{(i,j)}^{VTP}$. *Then we have:*

$$\min_{k\in\{1,\ldots,N_T\}} \bar{r}_{i,i}^{VTP} \geq \min_{k\in\{1,\ldots,N_T\}} \bar{r}_{i,i}\,. \tag{4.29}$$

Proof. From step 2) of the MMSE-ISTP and MMSE-ISVTP channel partitions, it is easily verified that $\hat{\mathbf{\Pi}}_{(1:L,1:L)}^{\mathrm{VTP}} = \hat{\mathbf{\Pi}}$. Thus (4.28) becomes

$$\bar{\mathbf{H}}^{\mathrm{VTP}} = [\tilde{\mathbf{H}}_2\hat{\mathbf{\Pi}} \;\; \tilde{\mathbf{H}}_1\hat{\mathbf{\Pi}}_{(L+1:N_T,L+1:N_T)}^{\mathrm{VTP}}] = \bar{\mathbf{Q}}^{\mathrm{VTP}}\,[\bar{\mathbf{R}}^{\mathrm{VTP},T}\,\mathbf{0}]^T\,. \tag{4.30}$$

Combining (4.30) with the relation $[\tilde{\mathbf{H}}_2\hat{\mathbf{\Pi}} \;\; \tilde{\mathbf{H}}_1] = \bar{\mathbf{Q}}\,[\bar{\mathbf{R}}^T\,\mathbf{0}]^T$ (cf. (3.24)), and using that $\bar{\mathbf{R}}^{\mathrm{VTP}}$ and $\bar{\mathbf{R}}$ have positive diagonal elements, from the uniqueness of QR decomposition [52], we obtain $\bar{\mathbf{R}}_{(1:L,1:L)}^{\mathrm{VTP}} = \bar{\mathbf{R}}_{(1:L,1:L)}$. In particular,

$$\min_{k\in\{1,\ldots,L\}} \bar{r}_{i,i}^{\mathrm{VTP}} = \min_{k\in\{1,\ldots,L\}} \bar{r}_{i,i}\,. \tag{4.31}$$

Furthermore, following similar steps as for the proof of the optimality of the V-BLAST ordering rule [4], we can show

$$\min_{k=L+1,\ldots,N_T} \bar{r}_{i,i}^{\mathrm{VTP}} \geq \min_{k=L+1,\ldots,N_T} \bar{r}_{i,i} \tag{4.32}$$

The combination of (4.31) and (4.32) yields $\min_{k\in\{1,\ldots,N_T\}} \bar{r}_{i,i}^{\mathrm{VTP}} \geq \min_{k\in\{1,\ldots,N_T\}} \bar{r}_{i,i}$. □

Now, it is well known that variable complexity tree search algorithms tend to generate a large number of nodes for layers associated with small values of the diagonal elements of $\mathbf{R}$ [11, 20, 26]. Hence the use of $\bar{\mathbf{R}}^{\mathrm{VTP}}$ rather than $\bar{\mathbf{R}}$ for the search stage can provide additional complexity reductions since the smallest diagonal element of the former is no smaller than that of the latter. Next we show that the layers associated with the N smallest diagonal elements of $\bar{\mathbf{R}}^{\mathrm{VTP}}$ are those closest to the root.

Theorem 4. $\max_{k=L+1,\ldots,N_T} \bar{r}_{k,k}^{VTP} \leq \min_{k=1,\ldots,L} \bar{r}_{k,k}^{VTP}$.

Proof. Let $\tilde{r}_{i,i} = \tilde{\mathbf{R}}_{(i,i)}$ with $\tilde{\mathbf{R}}$ defined in (3.18). Then using (3.23), we can show

$$\max_{k=L+1,\ldots,N_T} \tilde{r}_{k,k} \leq \min_{k=1,\ldots,L} \tilde{r}_{k,k}\,. \tag{4.33}$$

Then, from the optimality of the V-BLAST ordering rule [4], we obtain

$$\min_{k=1,\ldots,L} \bar{r}_{k,k}^{\mathrm{VTP}} \geq \min_{k=1,\ldots,L} \tilde{r}_{k,k}\,. \tag{4.34}$$

In addition, following similar steps as for the proof of (3.23), we can show

$$\max_{k=L+1,\ldots,N_T} \bar{r}_{k,k}^{\text{VTP}} \leq \max_{k=L+1,\ldots,N_T} \tilde{r}_{k,k} \,. \tag{4.35}$$

The combination of (4.33), (4.34) and (4.35) proves the theorem. □

This "poor" layer ordering that may lead to a large number of nodes being generated for the top N layers is however necessary for MMSE-ISVTP to guarantee optimal performance at high SNR while restricting the number of candidate child nodes per parent node to one for the lower L layers.

4.2.3 Cost of the channel partition step for the MMSE-ISVTP and Sub-MMSE-ISVTP schemes

Both MMSE-ISVTP and Sub-MMSE-ISTP are variable complexity schemes. However the channel partition step, that is identical for both schemes, has a fixed complexity that is analyzed in this section. The total complexity costs will be obtained through computer simulations in chapter 5. Following similar steps as in section 3.4.2, we can show that the total cost of the channel partition step for these schemes is

$$C_{\text{ISVTP}}^{\text{part}} = N_T \left(8N_T^2 + 8N_T N_R + 18N_R + \frac{45}{2} N_T - N + \frac{9}{2} \right) + N^2 - 15 \quad \text{flops} \,. \tag{4.36}$$

Comparing (3.75) to (4.36), we observe that the complexity increase induced by the improved channel partition step is fairly small (only $24NN_T^2$ flops, ignoring lower order terms).

4.3 Comparison with MMSE-SD and Sub-MMSE-SD

In [11,26], the SD algorithm was applied to the MMSE regularized channel matrix $\breve{\mathbf{H}}$. This scheme, referred to as Sub-MMSE-SD, essentially solves

$$\hat{\mathbf{d}}^{\text{Sub-SD}} = \arg \min_{\mathbf{d} \in \mathcal{A}^{N_T}} \|\breve{\mathbf{y}} - \breve{\mathbf{H}}\mathbf{d}\|^2 = \arg \min_{\mathbf{d} \in \mathcal{A}^{N_T}} \left(\|\mathbf{y} - \mathbf{H}\mathbf{d}\|^2 + \beta^2 \|\mathbf{d}\|^2 \right) \tag{4.37}$$

under a sphere radius constraint. Except for constant modulus alphabets, the solution to (4.37) differs in general from the ML solution of (2.2). Contrary to the conventional SD scheme that operates directly on $\mathbf{H}$, Sub-MMSE-SD is suitable for all system configurations and provides lower complexity. For over-determined systems, the performance loss entailed by Sub-MMSE-SD for non constant modulus constellations is very small [11]. However, as we shall see in section 5, this loss is more substantial for under-determined systems. This loss can be recovered by solving

$$\hat{\mathbf{d}}^{\text{SD}} = \arg \min_{\mathbf{d} \in \mathcal{A}^{N_T}} \left(\|\breve{\mathbf{y}} - \breve{\mathbf{H}}\mathbf{d}\|^2 + \beta^2 (N_T r_{\max}^2 - \|\mathbf{d}\|^2) \right) \tag{4.38}$$

instead of (4.37) under a sphere radius constraint. It is easily verified that the solution of (4.38) is the ML solution. We refer to this scheme as MMSE-SD. This modification of Sub-MMSE-SD was reported in [57, 58] where it was applied for generating soft outputs.

Contrary to the proposed Sub-MMSE-ISVTP and MMSE-ISVTP schemes, the Sub-MMSE-SD and MMSE-SD schemes can employ the V-BLAST ordering rule that puts the best layers closer to the root and therefore can generate fewer nodes than the proposed schemes at the top N levels. However, the Sub-MMSE-ISVTP and MMSE-ISVTP schemes operate on a set with cardinality upper bounded by M^N while the corresponding bound for the Sub-MMSE-SD and MMSE-SD schemes is M^{N_T}. Thus for poorly conditioned channels or low operating SNR, the proposed schemes can provide substantially lower complexity than the Sub-MMSE-SD and MMSE-SD schemes.

Chapter 5

Computer simulations results

In this chapter, we provide computer simulations results for the complexities and the bit-error-rate (BER) performances of the schemes discussed above. We consider uncoded QPSK, 16QAM and 64QAM with Gray code labeling. The detection schemes considered are Sel-MMSE-OSIC, Sub-MMSE-ISVTP, MMSE-ISVTP, Sub-MMSE-SD, MMSE-SD and SFSD. For each channel use, a new vector of N_T randomly generated symbols is transmitted, and the channel varies randomly and independently from one use to another. For each SNR point, the BER is averaged over a minimum of 100000 channel realizations, and a minimum of 200 errors are accumulated.

Since the cost of a variable complexity scheme is a random variable with a certain distribution, the average complexity is the criterion mostly used in the literature for complexity comparison. Indeed, when a large number of symbols are transmitted, the total decoding complexity is governed by the average complexity. However, to ensure that sufficient resources (e.g. memory) are available for the scheme to run to completion for all channel and noise realizations, the resource allocation must be dictated by the behavior under worst case scenarios instead of average ones (see. e.g. [20, 22]). Furthermore, variable

complexity schemes generally induce significant variations in throughput [14]. This non constant throughput is however undesirable in practical communications systems. Thus, in order to guarantee a minimum throughput, a limit on the maximum tolerable complexity is generally imposed [14, 59]. In such cases, the complexity distribution's tail behavior provides an indication to the probability that the considered scheme exceeds this limit (see. e.g. [60]). Hence, in addition to the mean, we also consider high complexity quantiles (see. Appendix D for the definition of quantiles). The 99.9% quantile is typically used in the literature (see. e.g. [29, 61]). Therefore we compare these schemes on the basis of their respective average and 99.9% quantile relative complexities, that is the ratio of their average or quantile complexities to the cost of the fixed complexity MMSE-ISTP scheme $C_{\text{MMSE-ISTP}}=C^{\text{partition}}_{\text{MMSE-ISTP}}+C^{\text{list}}_{\text{MMSE-ISTP}}$, with $C^{\text{partition}}_{\text{MMSE-ISTP}}$ and $C^{\text{list}}_{\text{MMSE-ISTP}}$ defined in (3.75) and (3.80). Hence the average and quantile relative complexities of MMSE-ISTP are 1. For each variable complexity scheme, a counter is used to count the number of FLOPS required by the decoder for each channel use. Since in a practical system channel partition has to be done only when the channel changes, then $C^{\text{partition}}_{\text{MMSE-ISTP}}$ has to be divided by the channel time coherency in symbols. In our numerical results below we treat the most unfavorable situation as far as complexity is concerned, that is when channel partition is done every transmitted vector. The comparison methodology is described in Appendix D. These schemes are all implemented here using the classical depth first SD algorithm with radius update and Schnorr-Euchner (SE) ordering for child nodes enumeration (see. section 4.1 and [14, 20]). The initial radius is set to ∞ in all cases. Both Sub-MMSE-SD and MMSE-SD employ the V-BLAST ordering rule in the preprocessing stage. Part of this chapter was published in [36].

5.1 BER and complexity results for space uncorrelated channels

5.1.1 BER results

Quasi-optimal performance of Sel-MMSE-OSIC and MMSE-ISVTP

In Fig. 5.1, we compare the BER performances of Sel-MMSE-OSIC, MMSE-ISVTP (which provides identical performance as MMSE-ISTP) and MMSE-SD (which provides exact ML performance) for space uncorrelated channels perfectly known at the receiver. The results for the $N_T = N_R = 6$ system with QPSK, 16QAM and 64QAM modulation are presented in Fig. 5.1a. For both Sel-MMSE-OSIC and MMSE-ISVTP, we set $N = N_{min} = 2$ so that theoretically both schemes should provide ML performance at high SNR. The numerical results show that Sel-MMSE-OSIC, MMSE-ISVTP and MMSE-SD all provide virtually same performance for the entire SNR range for all constellation sizes. Thus both Sel-MMSE-OSIC and MMSE-ISVTP can provide optimal performance not only asymptotically but actually at almost all SNR levels. Similar observations hold for the results presented in Fig. 5.1b which considers the under-determined $N_T = 8$, $N_R = 6$ system. In this case, we set $N = N_{min} = 3$. In summary, the significance of the results presented in Fig. 5.1 is two-fold: first, the theoretically predicted asymptotic optimality of the Sel-MMSE-OSIC and MMSE-ISVTP schemes for all system configurations over space uncorrelated channels is verified. Second, these two schemes are not only asymptotically optimal but they actually perform virtually same as ML detection at almost all SNR levels, a feature that could not be inferred from a diversity analysis.

Comparison between (Sub)-MMSE-ISVTP, (Sub)-MMSE-SD and SFSD

Fig. 5.2 presents BER results for space uncorrelated channels, perfectly known at the receiver for the $N_T = N_R = 8$ and the $N_T = 7$, $N_R = 6$ systems. These results confirm

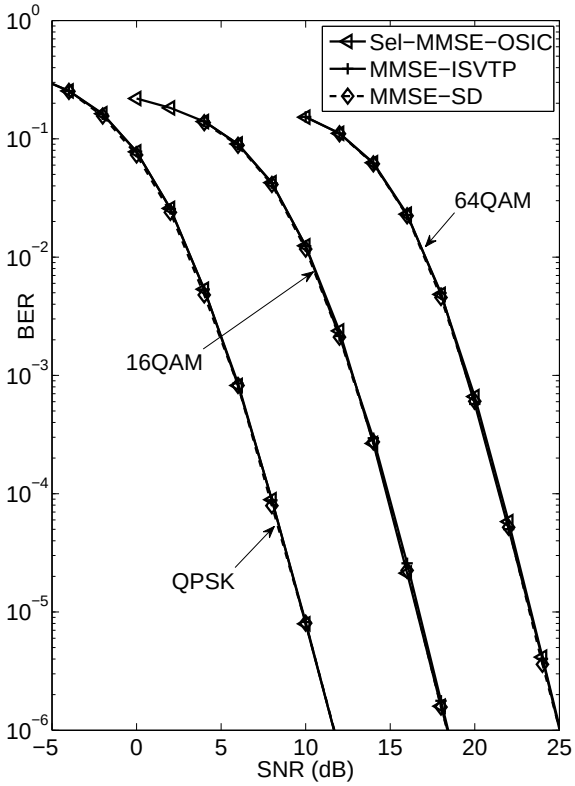

(a) $N_T = N_R = 6$, $N = 2$

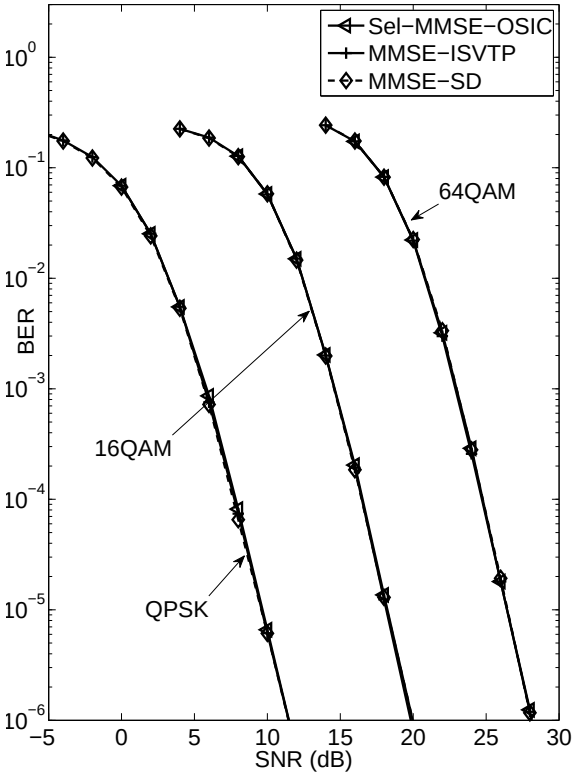

(b) $N_T = 8$, $N_R = 6$, $N = 3$

Fig. 5.1 Quasi-optimal performance for space uncorrelated channels, perfectly known at the receiver

the excellent performance of the MMSE-ISVTP scheme. In particular, for 64QAM, its performance is essentially indistinguishable from MMSE-SD over the entire SNR range for both systems. The Sub-MMSE-ISVTP and Sub-MMSE-SD schemes provide the same diversity gain and perform very close to MMSE-ISVTP and MMSE-SD. Indeed, for $N_T = N_R = 8$ system with 64QAM, compared to MMSE-ISVTP and MMSE-SD, both Sub-MMSE-ISVTP and Sub-MMSE-SD exhibit a performance degradation less than 0.2 dB at all SNR levels. For the $N_T = 7$, $N_R = 6$ system with 64QAM, this loss increases to about 0.4 dB. The SFSD scheme on the other hand exhibits a diversity loss with respect to MMSE-SD and MMSE-ISVTP and for the $N_T = N_R = 8$ system, the performance degradation with respect to MMSE-SD is approximately 1, 2.7 and 2 dB at a BER of 10^{-6} for QPSK, 16QAM and 64QAM respectively.

5.1.2 Complexity results

Relative complexity results for the N_T=N_R=8 system are presented in Fig. 5.3. Note that for QPSK, the results are presented for MMSE-ISVTP only since the MMSE-ISVTP and Sub-MMSE-ISVTP schemes are equivalent for constant modulus alphabets. The same applies also to MMSE-SD and Sub-MMSE-SD. For QPSK, the variable complexity schemes provide no significant complexity reductions over the fixed complexity MMSE-ISTP scheme (the reduction factor in average relative complexity is less than 1.25 for all SNR levels), and in fact, they exhibit slightly higher quantile relative complexities for a wide range of SNR. This is because for small constellation sizes, the total complexity is dominated by the complexity of the preprocessing stage. Thus variable complexity schemes which aim at reducing the cost of the search stage achieve very little gains in overall cost. Hence for small constellation sizes, allowing complexity variations does not provide any substantial complexity advantage over the fixed complexity approach. This is however no longer true

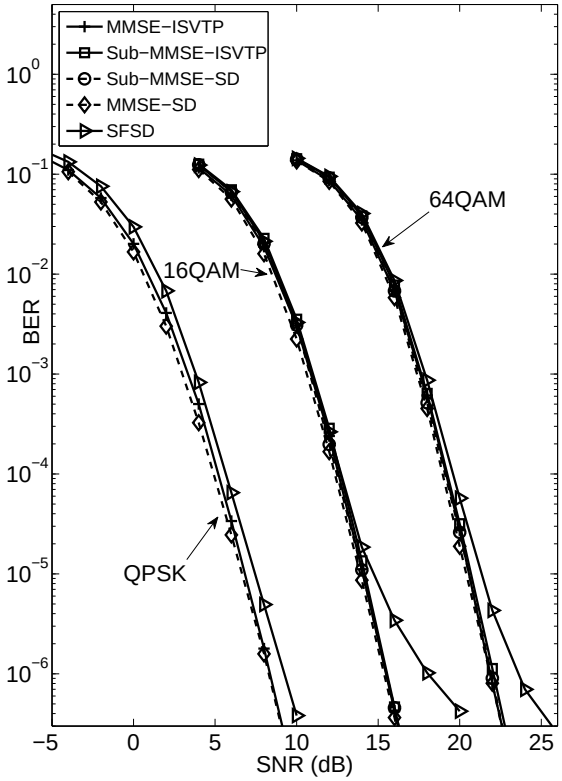

(a) $N_T = N_R = 8$, $N = 2$

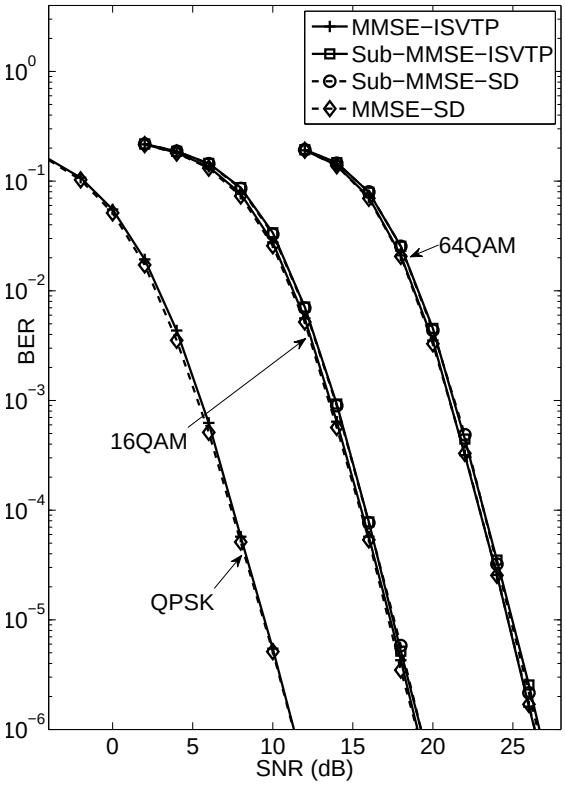

(b) $N_T = 7$, $N_R = 6$, $N = 2$

Fig. 5.2 BER comparison for space uncorrelated channels, perfectly known at the receiver

for larger constellations like 64QAM. Indeed at SNR=18 dB when BER=5×10^{-4}, MMSE-ISVTP lowers the average and quantile relative complexities with respect to MMSE-ISTP by a factor of 55 and 9 respectively. Compared to MMSE-SD, MMSE-ISVTP can provide significant complexity reductions. Although the complexity advantages decrease with SNR, MMSE-ISVTP still provides a reduction factor of 2 with respect to MMSE-SD in quantile relative complexity at SNR=18 dB when BER=5×10^{-4}. Regarding the average relative complexity, MMSE-ISVTP can provide significant reductions only for SNR$\leq$14 dB where BER$>10^{-2}$. Such a high BER is however of no practical interest for typical wireless communications systems. For lower BER the two schemes have similar average relative complexities. Both Sub-MMSE-ISVTP and Sub-MMSE-SD have significantly lower complexity than their MMSE-ISVTP and MMSE-SD counterparts. The two schemes have similar average relative complexities, and Sub-MMSE-ISVTP lowers the quantile relative complexity with respect to Sub-MMSE-SD by a factor of 2 at SNR=18 dB when BER=5×10^{-4}.

Fig. 5.4 presents the corresponding results for the $N_T = 7$, $N_R = 6$ system. Similar observations as for the N_T=N_R=8 system of Fig. 5.3 hold here except that for 64QAM, the average relative complexities of MMSE-ISVTP and Sub-MMSE-ISVTP can be slightly higher (by a factor only up to 1.3) than MMSE-SD and Sub-MMSE-SD. However, as a measure of complexity variability, we compare the ratio of quantile to average relative complexities for each scheme. At SNR=22 dB when BER=4×10^{-4}, this ratio is 6.5 and 6.3 for MMSE-ISVTP and Sub-MMSE-ISVTP respectively, while the corresponding numbers for MMSE-SD and Sub-MMSE-SD are respectively 15.3 and 15.9. Hence our proposed schemes show significantly lower complexity variability than MMSE-SD and Sub-MMSE-SD. This is appealing for practical implementations where large variations in complexity are undesirable.

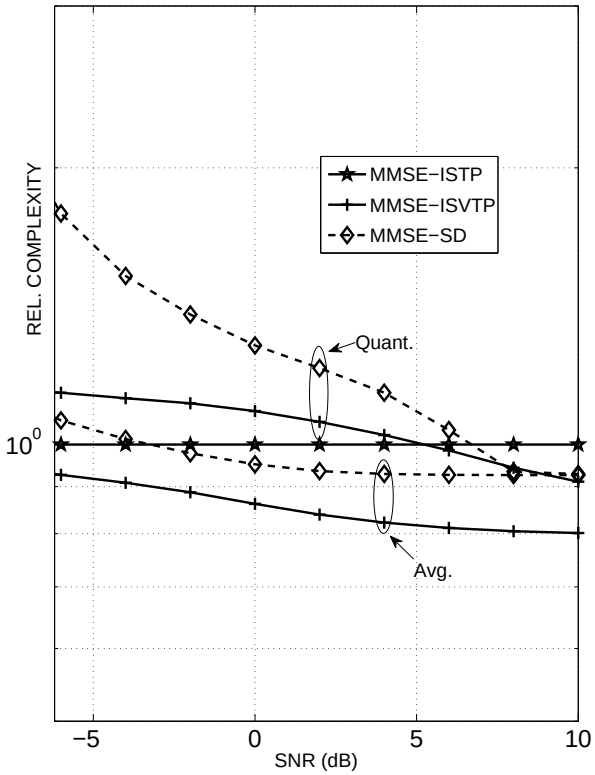

(a) QPSK

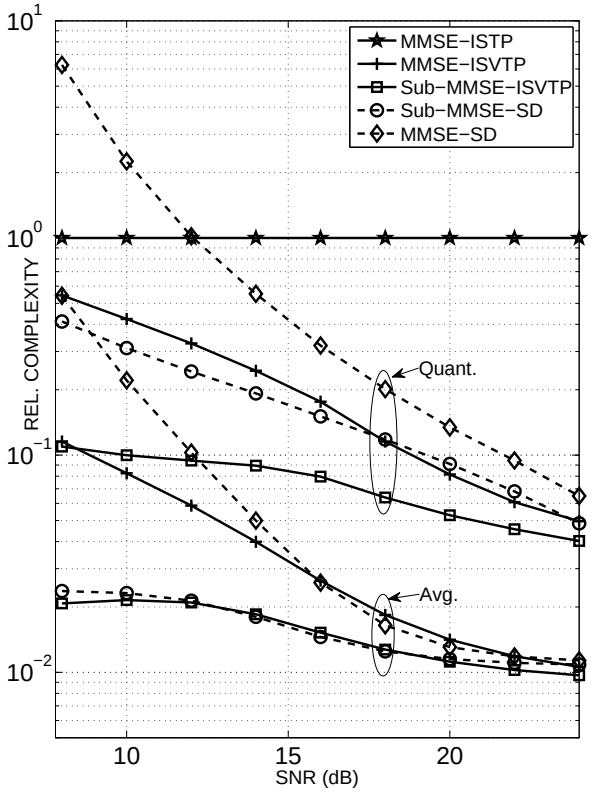

(b) 64QAM

Fig. 5.3 Relative complexities over space uncorrelated channels, perfectly known at the receiver, for $N_T = N_R = 8$, $N = 2$

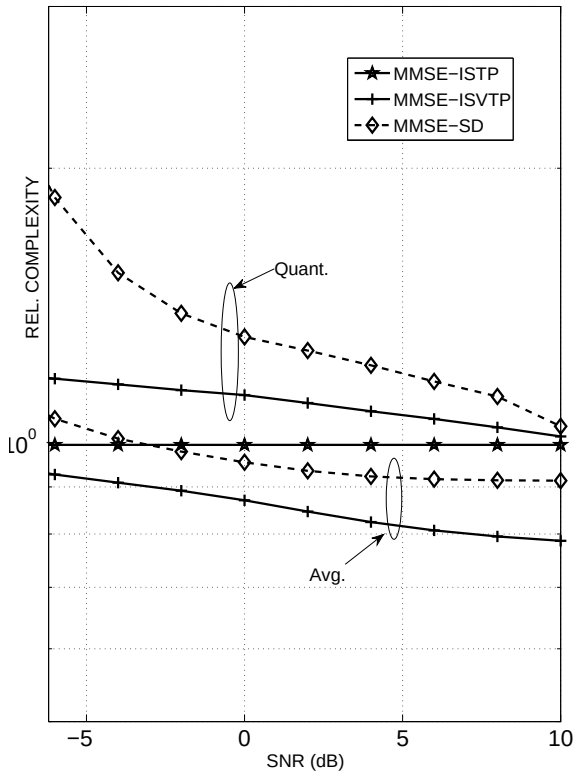

(a) QPSK

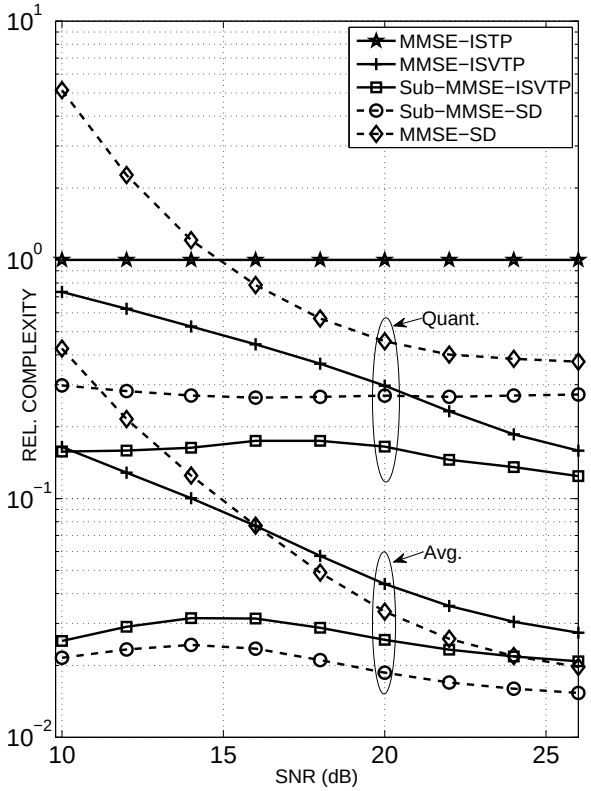

(b) 64QAM

Fig. 5.4 Relative complexities over space uncorrelated channels, perfectly known at the receiver, for $N_T = 7$, $N_R = 6$, $N = 2$

5.2 BER and complexity results for space correlated channels

We now investigate the impact of space correlation on the performances and complexities of the considered schemes. We adopt the single coefficient exponential correlation model of [62], and set the correlation coefficient r to 0.7.

5.2.1 BER results

The impact of space correlation on BER for the N_T=N_R=6 and the N_T=8, N_R=6 systems with 64QAM is presented in Fig. 5.5. Comparing the uncorrelated and correlated cases, we observe that space correlation entails a significant performance degradation for all schemes. However, this degradation is about 0.4 dB and 0.5 dB higher for MMSE-ISVTP than for MMSE-SD at a BER of 10^{-6} for N_T=N_R=6 and N_T=8, N_R=6 respectively. We also observe that for the N_T=8, N_R=6 system, the Sub-MMSE-SD and Sub-MMSE-ISVTP schemes have a performance loss of about 0.4 dB with respect to MMSE-SD and MMSE-ISVTP at almost all SNR levels for both uncorrelated and correlated channels. Thus the Sub-MMSE-ISVTP and Sub-MMSE-SD schemes can have non-negligible performance loss with respect to MMSE-ISVTP and MMSE-SD for under-determined systems. Regarding the SFSD scheme, the appropriate setting [53] found by computer simulations for N_T=N_R=6 with 64QAM is (1536, 1024, 512). The results show that SFSD entails a performance loss of 1.1 dB and 1.3 dB with respect to MMSE-SD at a BER of 10^{-6} for the uncorrelated and correlated cases respectively. Hence, the SFSD scheme performs worse than MMSE-ISVTP for BER$\leq 10^{-4}$ for both uncorrelated and correlated channels.

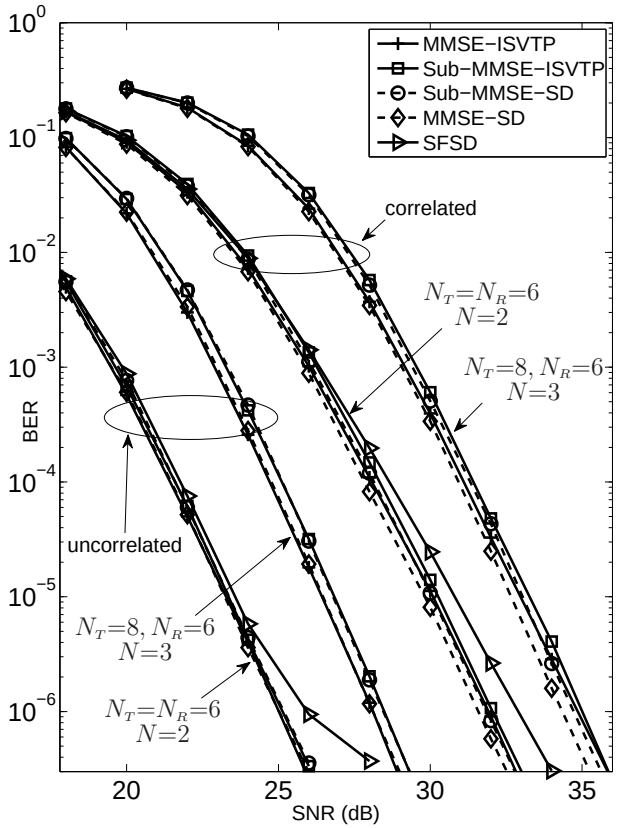

Fig. 5.5 Impact of space correlation on BER for 64QAM with perfectly known channels at the receiver: $r = 0.7$

5.2.2 Complexity results

The impact of space correlation on relative complexity is illustrated in Fig. 5.6 and Fig. 5.7. We observe that for the variable complexity schemes, space correlation entails a significant complexity increase. However, the relative complexities of MMSE-ISVTP and Sub-MMSE-ISVTP are more robust than those of MMSE-SD and Sub-MMSE-SD. Indeed from Fig. 5.6a, at SNR=20 dB when BER=6×10^{-4}, the MMSE-ISVTP and MMSE-SD schemes have same quantile relative complexities, while from Fig. 5.6b, at SNR=26 dB when BER=9×10^{-4}, MMSE-ISVTP lowers the quantile relative complexity with respect to MMSE-SD by a factor of 2. In addition, we compare the ratio of quantile to average relative complexities for each scheme. For uncorrelated channels, at SNR=20 dB when BER=6×10^{-4}, this ratio is 6.9 for both schemes, while for correlated channels at SNR=26 dB when BER=9×10^{-4}, it is 6.4 and 15 for MMSE-ISVTP and MMSE-SD respectively. Hence MMSE-ISVTP's complexity variability is more robust to space correlation than MMSE-SD. Similarly, from Fig. 5.7b, at SNR=30 dB when BER=4×10^{-4}, the ratio of quantile to average relative complexities for MMSE-ISVTP is 6 while MMSE-SD's is 19. In addition, the reductions in quantile relative complexity provided by MMSE-ISVTP over MMSE-SD increase at high SNR. Notice however that MMSE-SD lowers the average relative complexity with respect to MMSE-ISVTP by a factor of 1.8 at SNR=30 dB when BER=4×10^{-4}. To explain the increased robustness of MMSE-ISVTP over MMSE-SD, we recall that the cardinality of the search set for the former is M^N while that for the latter is M^{N_T}. Hence when the tree pruning becomes less efficient due to spatial correlation, MMSE-ISVTP can provide significant quantile relative complexity savings compared to MMSE-SD because of the much smaller cardinality of its search set.

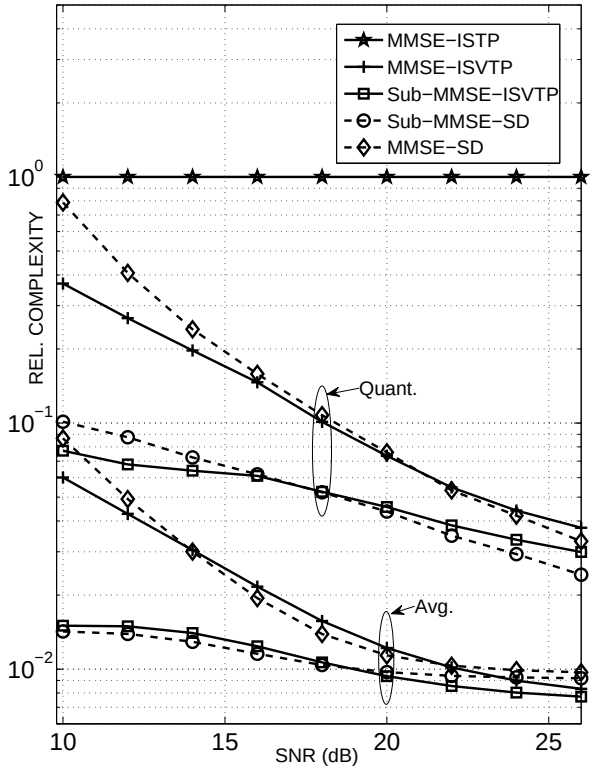

(a) uncorrelated

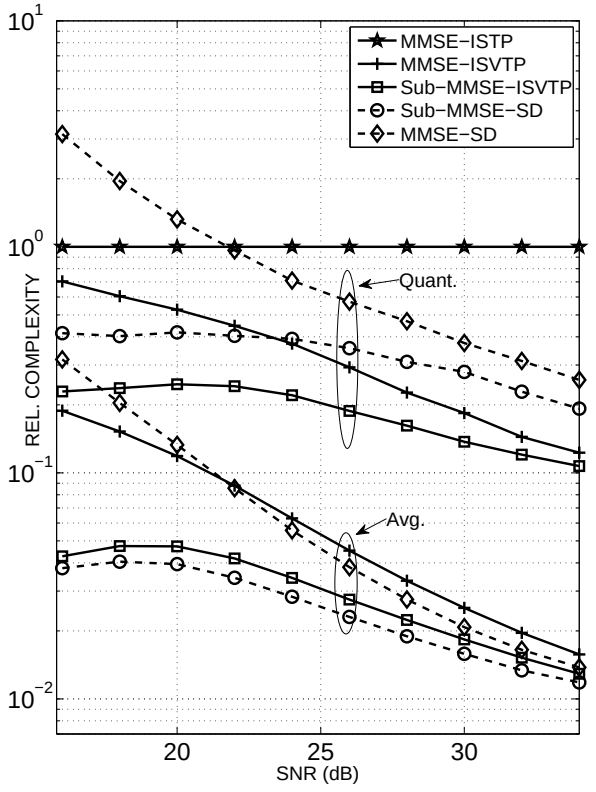

(b) correlated

Fig. 5.6 Impact of space correlation on complexity with perfectly known channels at the receiver: $N_T = N_R = 6$, $N = 2$, $r = 0.7$, 64QAM

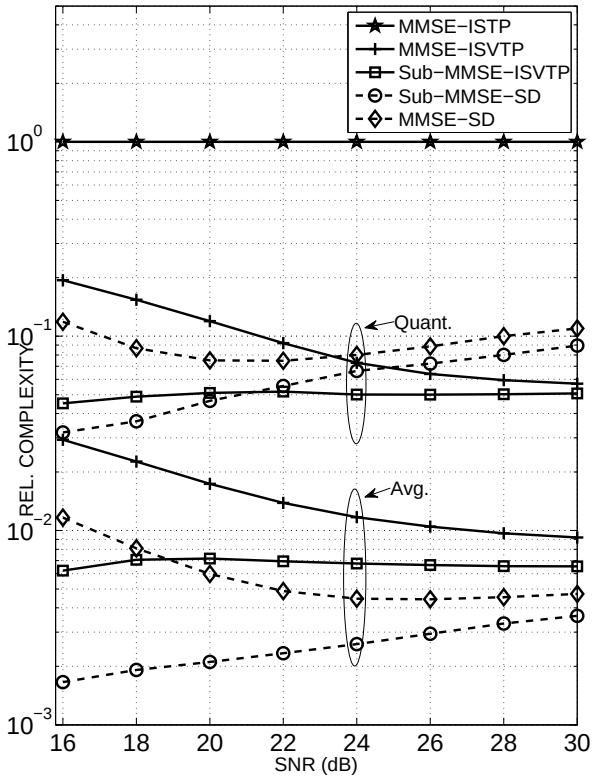

(a) uncorrelated

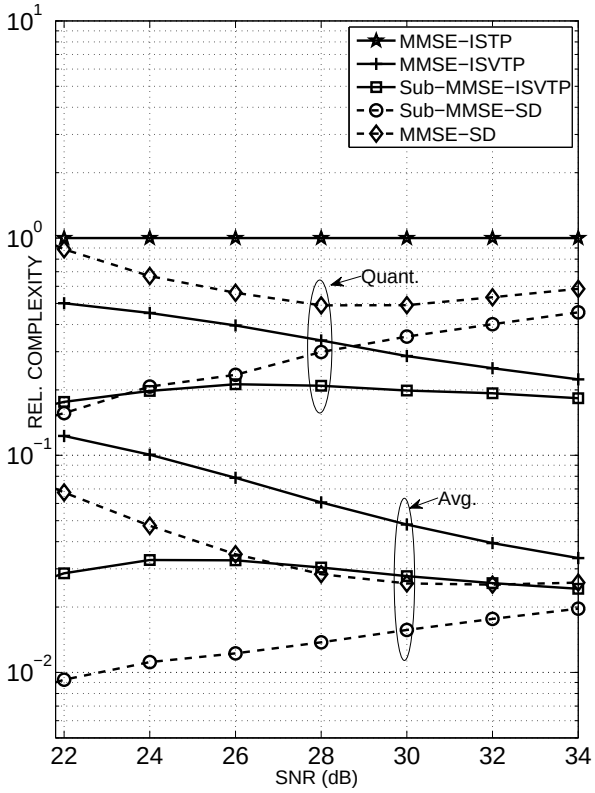

(b) correlated

Fig. 5.7 Impact of space correlation on complexity with perfectly known channels at the receiver: $N_T = 8$, $N_R = 6$, $N = 3$, $r = 0.7$, 64QAM

5.3 Effects of channel estimation errors

Now we study the effect of channel estimation errors on performance and complexity. We adopt the estimation error model of [63]. The entries of the error matrix are i.i.d zero-mean CSCG RVs with variance $\alpha^2\sigma_n^2$ (see. [63]). We set $\alpha^2 = 3$.

5.3.1 BER results

Fig. 5.8 presents BER results for the N_T=N_R=8 and the N_T=7, N_R=6 systems with 64QAM. Comparing Fig. 5.8 to Fig. 5.1, we observe that channel estimation errors cause an almost equal performance degradation for all schemes.

5.3.2 Complexity results

Relative complexity results are shown in Fig. 5.9. Comparing Fig. 5.9a to Fig. 5.3 we observe that the quantile complexity reductions provided by the MMSE-ISVTP and Sub-MMSE-ISVTP schemes over the MMSE-SD and Sub-MMSE-SD schemes increase significantly in presence of channel estimation errors. Indeed, at SNR=24 dB when BER=5×10^{-4}, MMSE-ISVTP lowers the quantile relative complexity with respect to MMSE-SD by a factor of 4.8. Furthermore, at such SNR, the quantile to average relative complexity ratio for MMSE-ISVTP is 6.4, while for MMSE-SD's is 27.1. Hence MMSE-ISVTP's complexity variability is more robust to channel estimations errors than MMSE-SD's. Similar observations hold for the results presented in Fig. 5.9b which considers the N_T=7, N_R=6 system.

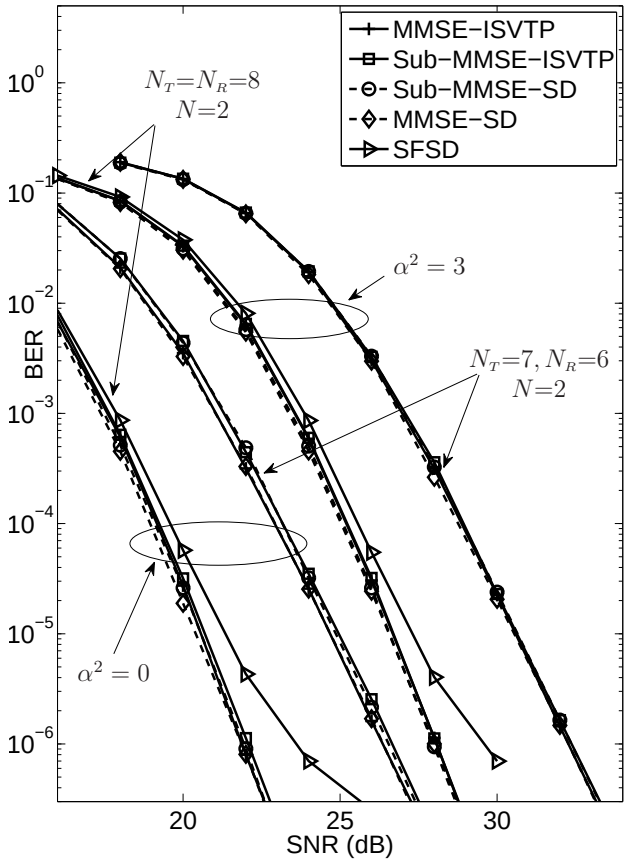

Fig. 5.8 Impact of channel estimation errors on BER for space uncorrelated channels, 64QAM

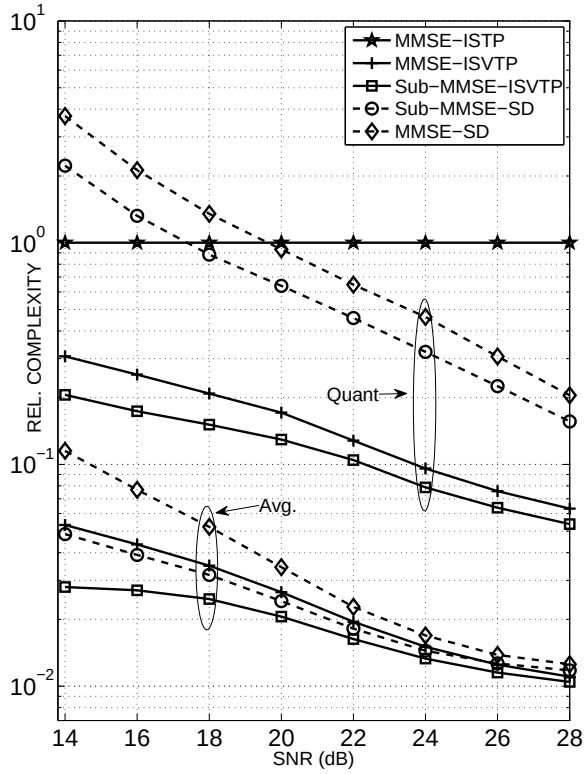

(a) $N_T = N_R = 8$, $N = 2$, $\alpha^2 = 3$, 64QAM

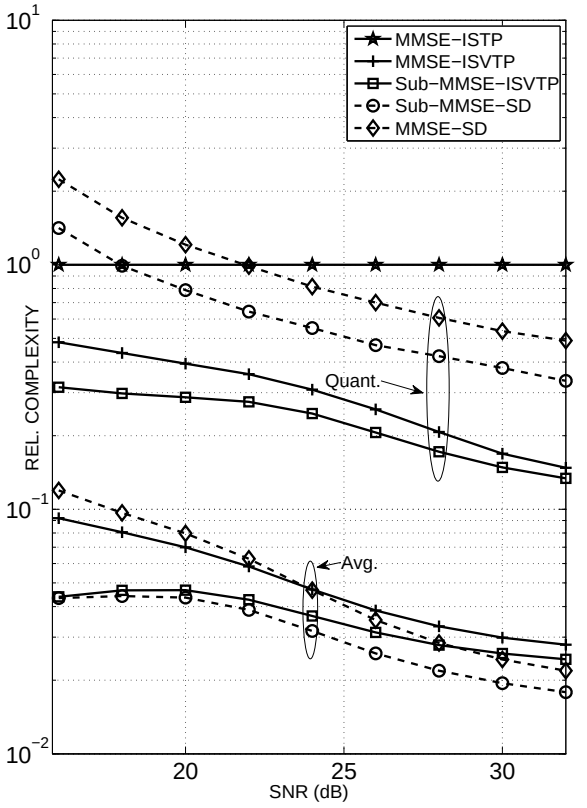

(b) $N_T = 7$, $N_R = 6$, $N = 2$, $\alpha^2 = 3$, 64QAM

Fig. 5.9 Impact of channel estimation errors on complexity for space uncorrelated channels

Chapter 6

Conclusion

In this thesis, we performed a detailed diversity analysis of list-based MIMO detectors that yield sufficient conditions for achieving optimal performance asymptotically for all system configurations on space uncorrelated channels. Specifically in the channel partition step, a diversity maximizing channel partition procedure must be employed and the parameter N should be no less than N_{min}, given by (2.61). For most practical cases, $N_{min} \leq 2$ and for large systems $N_{min} \approx \lfloor N_T \rfloor$. Hence for large systems, optimal performance at high SNR can be achieved with a list size that grows exponentially with $\lfloor N_T \rfloor$ only as opposed to N_T for an exhaustive ML receiver.

We also proposed the fixed complexity asymptotically optimal Sel-MMSE-OSIC and MMSE-ISTP algorithms. The latter provides substantial complexity reductions over the former in two ways: first it employs a simpler channel partition technique based on "incremental" antenna selection and second it employs an efficient tree based approach for candidates list generation. Simulations results reveal that both schemes perform indistinguishably close to ML over a large SNR range. The MMSE-ISTP scheme provides substantial complexity reductions FSD [23]. The SFSD algorithm [53] can lower complexity

with respect to MMSE-ISTP but it entails a significant performance loss at low BER. The MMSE-ISTP scheme is suitable for under-determined systems, and has lower complexity than MMSE-FSD, an MMSE extension of FSD applicable for under-determined systems.

This thesis also introduced the MMSE-ISVTP and Sub-MMSE-ISVTP schemes as variable complexity versions of MMSE-ISTP, that can provide significant complexity reductions for large constellation sizes. MMSE-ISVTP maintains the same performance as MMSE-ISTP while Sub-MMSE-ISVTP lowers the complexity further with respect to MMSE-ISVTP but incurs some performance loss. Simulations results show that MMSE-ISVTP and Sub-MMSE-ISVTP can provide lower quantile complexity than MMSE-SD and Sub-MMSE-SD. The complexity reduction provided by MMSE-ISVTP and Sub-MMSE-ISVTP increases with spatial correlation. However, spatial correlation also increases slightly the performance degradation for MMSE-ISVTP. Channel estimation errors also increase the complexity reduction provided by MMSE-ISVTP and Sub-MMSE-ISVTP over MMSE-SD and Sub-MMSE-SD. However, unlike spatial correlation, channel estimation errors induce an almost equal performance degradation for all schemes. In addition, for spatial correlation and channel estimation errors, MMSE-ISVTP and Sub-MMSE-ISVTP show significantly reduced variability compared to MMSE-SD and Sub-MMSE-SD. Hence, the proposed schemes are high performance low complexity MIMO detection algorithms, with increased complexity robustness against commonly encountered practical impairments such as spatial correlation and channel estimation errors.

This thesis has considered only uncoded transmission, however many practical systems employ some form of channel coding. In such cases, the MIMO detector is generally required to provide soft outputs as opposed to the hard decisions considered in this thesis. Hence an important direction for future work is to extend the proposed schemes to generate reliable soft outputs for coded MIMO transmission.

Appendix A

Useful lemma

Lemma 1. *If X and Y are two continuous random variables such that $Y \geq X$ with probability one then $Pr(Y \leq \alpha) \leq Pr(X \leq \alpha)$ with $\alpha \in \mathbb{R}$.*

Proof. Let X and Y be two continuous random variables with joint probability density function $p_{XY}(x, y)$. Then $Y \geq X$ with probability one means that $\iint_{y \geq x} p_{XY}(x, y)\, dx\, dy = 1$. Hence $p_{XY}(x, y) = 0$ in the region where $y < x$. Consider the following generalization: $p_{XY}(x, y) \leq p_{XY}(y, x)$ in the region where $y < x$. Define the three non overlapping regions:

$$\begin{aligned} \mathcal{R}_1 &= \{(x, y) : x \leq \alpha\,,\, y \leq \alpha\} \\ \mathcal{R}_2 &= \{(x, y) : x \leq \alpha\,,\, y > \alpha\} \\ \mathcal{R}_3 &= \{(x, y) : x > \alpha\,,\, y \leq \alpha\} \end{aligned}$$

with $\alpha \in \mathbb{R}$. Then,

$$\Pr(Y \leq \alpha) = \iint_{\mathcal{R}_1 \cup \mathcal{R}_3} p_{XY}(x, y)\, dx\, dy = \iint_{\mathcal{R}_1} p_{XY}(x, y)\, dx\, dy + \iint_{\mathcal{R}_3} p_{XY}(x, y)\, dx\, dy \tag{A.1}$$

and

$$\Pr(X \leq \alpha) = \iint_{\mathcal{R}_1 \cup \mathcal{R}_2} p_{XY}(x, y)\, dx\, dy = \iint_{\mathcal{R}_1} p_{XY}(x, y)\, dx\, dy + \iint_{\mathcal{R}_2} p_{XY}(x, y)\, dx\, dy\,. \tag{A.2}$$

But

$$\iint_{\mathcal{R}_3} p_{XY}(x,y)\,dx\,dy = \iint_{x>\alpha\,,\,y\leq\alpha} p_{XY}(x,y)\,dx\,dy \;\leq\; \iint_{y\leq\alpha\,,\,x>\alpha} p_{XY}(y,x)\,dy\,dx \tag{A.3}$$

$$= \iint_{\mathcal{R}_2} p_{XY}(x,y)\,dx\,dy\,. \tag{A.4}$$

Hence,

$$\Pr(Y\leq\alpha) \leq \iint_{\mathcal{R}_1} p_{XY}(x,y)\,dx\,dy + \iint_{\mathcal{R}_2} p_{XY}(x,y)\,dx\,dy = \Pr(X\leq\alpha)\,. \tag{A.5}$$

□

Appendix B

MMSE based Greedy QR selection algorithm

The Greedy QR algorithm is essentially a Householder based QR decomposition algorithm with column permutations. The algorithm permutes the columns of the input matrix $\mathbf{H}$ in such a way that the diagonal elements of $\mathbf{R}$ are successively maximized from $\mathbf{R}_{(1,1)}$ to $\mathbf{R}_{(N_T,N_T)}$. This algorithm was used in [52] to compute the QR decomposition of rank deficient matrices. Here, similar to [50, 51], it is used as a low complexity incremental antenna selection rule where the $L \leq N_T$ selected antennas correspond the first L columns of the output of the Greedy QR algorithm. Below, we present an MMSE criterion based extension of the Greedy QR of [50, 51].

Algorithm: MMSE based Greedy QR

Inputs: $\breve{\mathbf{H}}$, $\breve{\mathbf{y}}$
Outputs: $\tilde{\mathbf{p}}$, $\tilde{\mathbf{R}}$, $\tilde{\mathbf{y}}$

$\tilde{\mathbf{R}} = \breve{\mathbf{H}}$, $\tilde{\mathbf{y}} = \breve{\mathbf{y}}$, $\tilde{\mathbf{p}} = [1, 2, \ldots, N_T]^T$

for $i = 1, \ldots, N_T$

$\mathbf{norms}(i) = \|\tilde{\mathbf{R}}_i\|^2$

end

for $i = 1, \ldots, N_T$

$k_i = \arg\max_{l=i,\ldots,N_T} \mathbf{norms}(l)$

Exchange columns i and k_i in $\tilde{\mathbf{R}}$, and rows i and k_i in **norms** and $\tilde{\mathbf{p}}$

$\mathbf{x} = \tilde{\mathbf{R}}_{(i:N_R,i)}$

$\|\mathbf{x}\| = \sqrt{\mathbf{norms}}(i)$

$\mathbf{v} = \mathbf{x} - \|\mathbf{x}\|\mathbf{e}_1$

$\alpha = \dfrac{1}{\|\mathbf{x}\|(\|\mathbf{x}\| - x_1)}$

$\tilde{\mathbf{v}} = \alpha\mathbf{v}$

$\mathbf{z}^H = \mathbf{v}^H\tilde{\mathbf{R}}_{(i:N_R,i+1:N_T)}$

$\lambda = \mathbf{v}^H\tilde{\mathbf{y}}_{(i:N_R)}$

$\tilde{\mathbf{R}}_{(i,i)} = \|\mathbf{x}\|$

$\tilde{\mathbf{R}}_{(i+1:N_R,i)} = \mathbf{0}$

$\tilde{\mathbf{R}}_{(i:N_R,i+1:N_T)} = \tilde{\mathbf{R}}_{(i:N_R,i+1:N_T)} - \tilde{\mathbf{v}}\mathbf{z}^H$

$\tilde{\mathbf{y}}_{(i:N_R)} = \tilde{\mathbf{y}}_{(i:N_R)} - \lambda\tilde{\mathbf{v}}$

for $j = i + 1, \ldots, N_T$

$\mathbf{norms}(j) = \mathbf{norms}(j) - |\tilde{\mathbf{R}}_{(i,j)}|^2$

end

end

Appendix C

Quantization cost

Let $c = c_R + jc_I$ be the decision statistic, so that the decision $\hat{c}$ is given by

$$\hat{c} = \mathcal{M}(c) = \arg\min_{a \in \mathcal{A}} |c - a|^2 . \tag{C.1}$$

Now let $\mathcal{A}$ be a square QAM constellation of size $M = 2^{2k}$ (with k a positive integer), obtained from a PAM constellation $\mathcal{B}_{PAM}$ of size $\sqrt{M}$. It is then straightforward to show [64]

$$\hat{c} = \hat{c}_R + j\hat{c}_I , \tag{C.2}$$

with

$$\hat{c}_R = \arg \min_{a_R \in \mathcal{B}_{PAM}} |c_R - a_R|^2 \tag{C.3}$$

and

$$\hat{c}_I = \arg \min_{a_I \in \mathcal{B}_{PAM}} |c_I - a_I|^2 \tag{C.4}$$

Let the elements of $\mathcal{B}_{PAM}$ be denoted as $\{s_{-\sqrt{M}/2}, \ldots, s_{-1}, s_1, \ldots, s_{\sqrt{M}/2}\}$, with

$$s_i = -s_{-i} = d(2i-1) , \qquad i = 1, 2, \ldots, \sqrt{M}/2 , \tag{C.5}$$

where $2d$ is the minimum distance between adjacent points in the PAM constellation. The decision boundaries are vertical lines at $0, \pm 2d, \pm 4d, \ldots, \pm(\sqrt{M}/2 - 1)2d$. Define

$$\check{c}_R = \left\lfloor \frac{|c_R|}{2d} \right\rfloor . \tag{C.6}$$

$\check{c}_I$ is similarly defined. Then (C.3) is solved as follows:

If $c_R \geq 0$

$$\hat{c}_R = \begin{cases} s_{\sqrt{M}/2} & \text{if } \check{c}_R \geq \sqrt{M}/2 - 1 \\ s_{\check{c}_R+1} & \text{otherwise} \end{cases} \tag{C.7}$$

otherwise

$$\hat{c}_R = \begin{cases} s_{-\sqrt{M}/2} & \text{if } \check{c}_R \geq \sqrt{M}/2 - 1 \\ s_{-(\check{c}_R+1)} & \text{otherwise} \end{cases} \tag{C.8}$$

(C.4) is similarly solved. Clearly, the cost of obtaining $\hat{c}_R$ is the same as that of obtaining $\hat{c}_I$. Now since computing $|c_R|$ requires no floating points operations as it amounts at most to reversing the sign bit in the binary representation of c_R and since computing $\lfloor a \rfloor$ does not require floating points operations either since it only amounts to ignoring the decimal part of a, the computation of $\check{c}_R$ requires 1 flop (assuming that $2d$ is readily available). Then comparing $\check{c}_R$ to $\sqrt{M}/2 - 1$ requires 1 flop (assuming that $\sqrt{M}/2 - 1$ is readily available). And since a comparison with 0 requires only recovering the sign bit and thus costs 0 flop, the total cost of obtaining $\hat{c}_R$ is 2 flops. Hence the total cost of obtaining $\hat{c}$ is 4 flops.

Now in the special case where $M = 4$, i.e QPSK modulation, then $\sqrt{M}/2 - 1 = 0$ and since from (C.6) we have $\check{c}_R \geq 0$, in this case the decision rule simplifies to

$$\hat{c}_R = \begin{cases} s_1 & \text{if } c_R \geq 0 \\ s_{-1} & \text{otherwise} \end{cases} \tag{C.9}$$

$\hat{c}_I$ is similarly obtained. Thus in this case, the cost of obtaining $\hat{c}$ is 0 flop.

Appendix D

Comparison strategy for variable complexity algorithms

D.1 Quantiles estimation and confidence intervals

Let $X_1, \ldots, X_n$ be i.i.d samples from a common cumulative distribution function $F_X(.)$, and let $Y_1 \leq Y_2 \leq \cdots \leq Y_n$ be the corresponding order statistics. Then the p-th quantile η_p of F_X is defined as [65]:

$$\eta_p = \inf\{x : F_X(x) \geq p\}\,, \qquad 0 < p < 1\,. \tag{D.1}$$

It is shown in [65] that $F_X(\eta_p) = p\,, 0 < p < 1$ if and only if F_X is continuous. Thus assuming that F_X is continuous, η_p satisfies:

$$P(X \leq \eta_p) = F_X(\eta_p) = p \qquad 0 < p < 1 \tag{D.2}$$

The estimator $\hat{\eta}_p$ of η_p in terms of the order statistics is given by [65]

$$\hat{\eta}_p = Y_{\lceil np \rceil} \tag{D.3}$$

Using the central limit theorem [65], it can be shown that for sufficiently large n, we have

$$\Pr\left(\hat{\eta}_{p-\epsilon} \leq \eta_p \leq \hat{\eta}_{p+\epsilon}\right) \approx 1 - 2\alpha\,, \quad 0 < p - \epsilon < p < p + \epsilon < 1 \tag{D.4}$$

with

$$\epsilon = z_\alpha \sqrt{p(1-p)/n} \tag{D.5}$$

and z_α=$\mathbb{Q}^{-1}(\alpha)$ where $\mathbb{Q}(.)$ is the $\mathbb{Q}$-function. Similarly, it can also be shown that

$$\Pr\left(\eta_{p-\epsilon} \leq \hat{\eta}_p \leq \eta_{p+\epsilon}\right) \approx 1-2\alpha\,, \quad 0 < p-\epsilon < p < p+\epsilon < 1 \tag{D.6}$$

with ϵ defined in (D.5). Clearly ϵ>0 and we also must have $\epsilon < \min(p, 1-p)$ in order to ensure that $0<p-\epsilon<p<p+\epsilon<1$ as required in (D.4) and (D.6). Thus the sample size n should be chosen such that $\epsilon \leq \beta \min(p, 1-p)$ with $0 < \beta < 1$. Since

$$\frac{\epsilon}{p} \leq \frac{\epsilon}{\min\left(p, 1-p\right)} \leq \beta\,, \tag{D.7}$$

if $\beta \ll 1$, then $\frac{\epsilon}{p} \ll 1$ and from (D.6), we get $\Pr\left(\hat{\eta}_p \approx \eta_p\right) \approx 1-2\alpha$. Hence small values of β can improve the accuracy of $\hat{\eta}_p$. Given β, from (D.5) and (D.7), we obtain that the sample size n must satisfy:

$$n \geq \frac{z_\alpha^2}{\beta^2}\ \max\left(\frac{1-p}{p}\,,\ \frac{p}{1-p}\right)\,. \tag{D.8}$$

D.2 Variable complexity algorithms comparison strategy

The complexity X in flops associated with a varying complexity algorithm is a discrete random variable with support $\mathcal{B}$. Denote the elements of $\mathcal{B}$ as $b_1, b_2, \ldots, b_{|\mathcal{B}|}$, with b_i (i=$1, \ldots, |\mathcal{B}|$) a positive integer. Furthermore, letting $\Pr\left(X{=}b_i\right){=}t_i{>}0$, with $\sum_{i=1}^{|\mathcal{B}|} t_i{=}1$, the cdf F_X of X is given by $F_X(x) = \sum_{i:\, b_i \leq x} t_i$. Clearly this cdf is discontinuous at each $x = b_i$, i=$1, \ldots, |\mathcal{B}|$. In such a case, a given p may not belong to the range of F_X, i.e $F_X(x) \neq p$, $\forall x$, and thus we have [65]: $F_X(\eta_p) > p$. Furthermore, even if $F_X(\eta_p) = p$, F_X must be discontinuous at η_p and therefore the consistency of the estimator $\hat{\eta}_p$ is no longer guaranteed [65].

To alleviate these issues, let U be a continuous RV independent of X with a triangular pdf of support $[-1/2\,,\, 1/2]$,

$$f_U(u) = \begin{cases} -4|u| + 2 & -1/2 \leq u \leq 1/2 \\ 0 & \text{otherwise} \end{cases} \tag{D.9}$$

Then the corresponding cdf F_U is given by:

$$F_U(u) = \begin{cases} 0 & u \leq -1/2 \\ 1/2 + 2u(1-|u|) & -1/2 < u < 1/2 \\ 1 & u \geq 1/2 \end{cases} \tag{D.10}$$

U has the same distribution as the sum of two i.i.d RVs U^1 and U^2 uniformly distributed over the range $[-1/4\,,\,1/4]$. Both $f_U(u)$ and $F_U(u)$ are plotted in Fig. D.1.

Define the RV V as

$$V = X + U \tag{D.11}$$

where X is uniquely determined by V since $X = [V]$, with [.] standing for rounding to the nearest integer. Then, its cdf can be obtained as

$$F_V(v) = \begin{cases} F_X(v-1/2) + t_{k_v} F_U(v - b_{k_v}) & \text{if } |v-[v]| < 1/2 \text{ and } [v] = b_{k_v} \in \lfloor \\ F_X(v-1/2) & \text{otherwise} \end{cases} \tag{D.12}$$

that is a differentiable function of v. We thus compare the complexity of various algorithms on the basis of V rather than X. An illustrative example of $F_X(x)$ and the associated $F_V(v)$ is shown in Fig. D.2.

For each algorithm, we obtain n independent observations for X and U. We then construct n observations for V as $V_i = X_i + U_i\,,\, i = 1, \ldots, n$. Each U_i (i=1, $\ldots$, n) is obtained as $U_i = U_i^1 + U_i^2$ where U_i^1 and U_i^2 are i.i.d. RVs generated from a uniform distribution with support $[-1/4\,,\,1/4]$. The sample mean $\tilde{\mu}_V = n^{-1} \sum_{i=1}^{n} V_i$ is then obtained as an estimate of $\mathcal{E}[V]$. An estimate of η_p^V, the p-th quantile of V is obtained as $\tilde{\eta}_p^V = \tilde{V}_{\lceil np \rceil}$ where $\tilde{V}_1 \leq \cdots \leq \tilde{V}_n$ are the order statistics corresponding to $V_1, \ldots, V_n$. A typical value of p used in the literature is $p = 99.9\%$ (see. e.g. [29, 61]). Setting $\alpha = 2.5\%$ corresponds to a 95% confidence level, which is the level generally considered in the statistics literature (see. e.g. [65]). We also set $\beta = 10\%$ in (D.8) to obtain $n \geq 3.84 \times 10^5$. Hence in our simulations we use $n = 4 \times 10^5$.

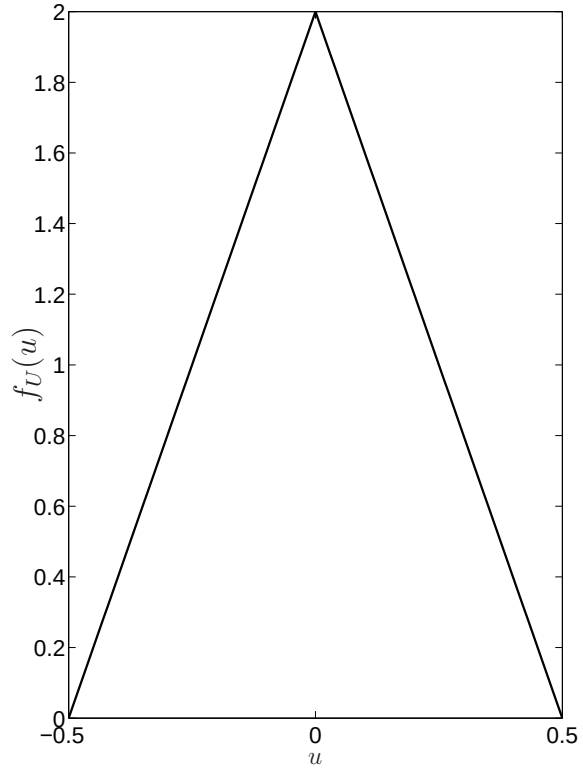

(a) $f_U(u)$

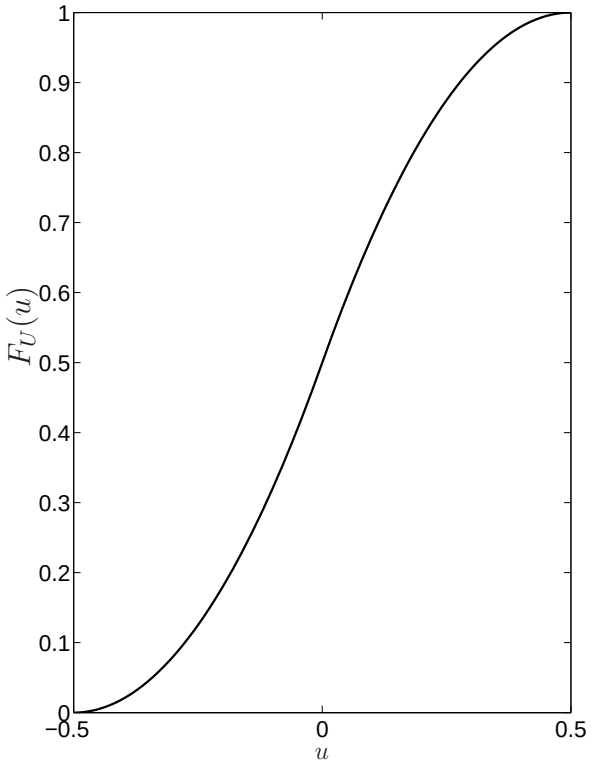

(b) $F_U(u)$

Fig. D.1 Plot of $f_U(u)$ and $F_U(u)$

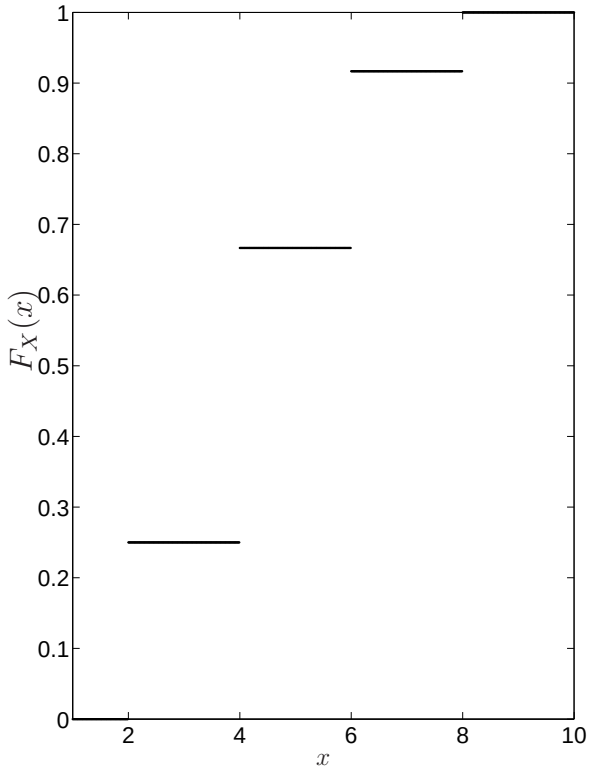

(a) $F_X(x)$

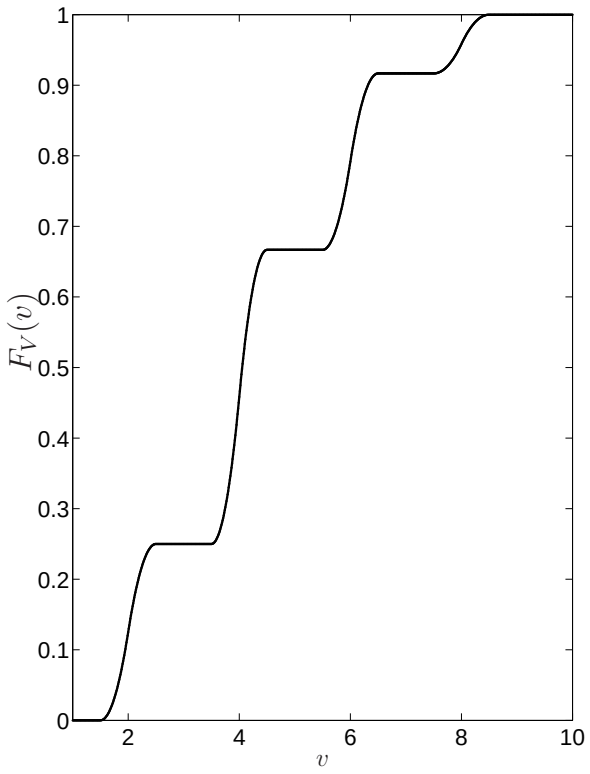

(b) $F_V(v)$

Fig. D.2 Illustrative example of $F_X(x)$ and associated $F_V(v)$

Appendix E

Computer simulations guide

In this section, we provide a brief overview of the computer simulation software provided with the attached CD. Directory BER contains all necessary source codes to simulate the BER performance of the Sel-MMSE-OSIC, MMSE-ISVTP, Sub-MMSE-ISVTP, MMSE-SD, Sub-MMSE-SD and SFSD schemes. The main system files for each of these schemes are respectively "Sel_MMSE_OSIC.c", "MMSE_ISVTP.c", "Sub_MMSE_ISVTP.c", "MMSE_SD.c", "Sub_MMSE_SD.c" and "SFSD.c". In each case, at the top of the file, a short paragraph that indicates how to set the required simulation parameters is provided. After setting up the parameters for the desired scheme, for example "MMSE_ISVTP.c", the next step is the compilation which is done using the following command:

gcc -o MMSE_ISVTP MMSE_ISVTP.c -lgsl -lgslcblas -lm

This command creates "MMSE_ISVTP" as an executable file. Note that our codes make extensive use the GNU Scientific Library (GSL) software package (version 1.10 or higher) which is available at www.gnu.org. The final step is to run the executable file using the following command

./ MMSE_ISVTP &

After running the executable file, the results are saved in the output file, which for our example, is "MMSE_ISVTP.txt". At the top of the output file, there is a short paragraph that describes the information (i.e SNR level, number of cumulated symbol errors, bit errors, channel realizations, etc...) stored in this file. These results can then be processed using a software like MATLAB to obtain the BER results figures presented in this thesis.

Directory COMPLEXITY contains all necessary source codes to measure the average and quantile complexities of the search stage of the MMSE-ISVTP, Sub-MMSE-ISVTP, MMSE-SD and Sub-MMSE-SD schemes. Similar to the BER case, the main system files for each of these schemes are respectively "MMSE_ISVTP.c", "Sub_MMSE_ISVTP.c", "MMSE_SD.c" and "Sub_MMSE_SD.c". Also similar to the BER directory, in each case, at the top of the file, a short paragraph that indicates how to set the required simulation parameters is provided. The compilation and running steps are done following the same procedure as described above. Finally, same as for the BER case, at the top of the output file, there is a short paragraph that describes the information (i.e SNR level, number of channel realizations, average complexity, quantile complexity, etc...) stored in this file. These results can then be added to the complexity of the preprocessing stage as derived in chapter 4 to obtain the total complexities.

References

[1] E. Telatar, "Capacity of multi-antenna Gaussian channels," *European Transactions on Telecommunications*, vol. 10, no. 6, pp. 585–595, Nov.-Dec. 1999.

[2] M. Kassouf and H. Leib, "Information rates for multi-dimensional modulation over multiple antenna wireless channels," *European Transactions on Telecommunications*, vol. 20, no. 5, pp. 463–481, Aug. 2009.

[3] P. Wolniansky, G. Foschini, G. Golden, and R. Valenzuela, "V-BLAST: An architecture for realizing very high data rates over the rich-scattering wireless channel," in *IEEE International Symposium on Signals, Systems and Electronics*, Pisa, Italy, Oct. 1998, pp. 295–300.

[4] G. J. Foschini, G. D. Golden, R. A. Valenzuela, and P. W. Wolniansky, "Simplified processing for high spectral efficiency wireless communication employing multi-element arrays," *IEEE J. Sel. Areas Commun.*, vol. 17, no. 11, pp. 1841–1852, Nov. 1999.

[5] L. Zheng and D. N. C. Tse, "Diversity and multiplexing: a fundamental tradeoff in multiple-antenna channels," *IEEE Trans. Inf. Theory*, vol. 49, no. 5, pp. 1073–1096, May 2003.

[6] A. Paulraj, *Introduction to Space-Time Wireless Communications*. Cambridge University Press, 2003.

[7] J. Benesty, Y. A. Huang, and J. Chen, "A fast recursive algorithm for optimum sequential signal detection in a BLAST system," *IEEE Trans. Signal Process.*, vol. 51, no. 7, pp. 1722–1730, Jul. 2003.

[8] S. Loyka and F. Gagnon, "Performance analysis of the V-BLAST algorithm: An analytical approach," *IEEE Trans. Wireless Commun.*, vol. 3, no. 4, pp. 1326–1337, Jul. 2004.

[9] N. Prasad and M. K. Varanasi, "Analysis of decision feedback detection for MIMO Rayleigh-fading channels and the optimization of power and rate allocations," *IEEE Trans. Inf. Theory*, vol. 50, no. 6, pp. 1009–1025, Jun. 2004.

[10] Y. Jiang, X. Zheng, and J. Li, "Asymptotic analysis of V-BLAST," in *IEEE GLOBECOM*, St. Louis, MO, USA, Nov. 2005, pp. 3882–3886.

[11] M. O. Damen, H. E. Gamal, and G. Caire, "On maximum-likelihood detection and the search for the closest lattice point," *IEEE Trans. Inf. Theory*, vol. 49, no. 10, pp. 2389–2402, Oct. 2003.

[12] B. M. Hochwald and S. ten Brink, "Achieving near-capacity on a multiple-antenna channel," *IEEE Trans. Commun.*, vol. 51, no. 3, pp. 389–399, Mar. 2003.

[13] J. Jaldén and B. Ottersten, "On the complexity of sphere decoding in digital communications," *IEEE Trans. Signal Process.*, vol. 53, no. 4, pp. 1474–1484, Apr. 2005.

[14] A. Burg, M. Borgmann, M. Wenk, M. Zellweger, W. Fichtner, and H. Bölcskei, "VLSI implementation of MIMO detection using the sphere decoding algorithm," *IEEE J. Solid-State Circuits*, vol. 40, no. 7, pp. 1566–1577, Jul. 2005.

[15] M. Stojnic, H. Vikalo, and B. Hassibi, "Speeding up the sphere decoder with H^∞ and SDP inspired lower bounds," *IEEE Trans. Signal Process.*, vol. 56, no. 2, pp. 712–726, Feb. 2008.

[16] B. Shim and I. Kang, "Sphere decoding with a probabilistic tree pruning," *IEEE Trans. Signal Process.*, vol. 56, no. 10, pp. 4867–4878, Oct. 2008.

[17] Z. Guo and P. Nilsson, "Algorithm and implementation of the K-Best sphere decoding for MIMO detection," *IEEE J. Sel. Areas Commun.*, vol. 24, no. 3, pp. 491–503, Mar. 2006.

[18] H. G. Kang, I. Song, J. Oh, J. Lee, and S. Yoon, "Breadth-first signal decoder: a novel maximum-likelihood scheme for multi-input-multi-output systems," *IEEE Trans. Veh. Technol.*, vol. 57, no. 3, pp. 1576–1584, May 2008.

[19] K.-C. Lai and L.-W. Lin, "Low-complexity adaptive tree search algorithm for MIMO detection," *IEEE Trans. Wireless Commun.*, vol. 8, no. 7, pp. 3716–3726, Jul. 2009.

[20] A. D. Murugan, H. E. Gamal, M. O. Damen, and G. Caire, "A unified framework for tree search decoding: rediscovering the sequential decoder," *IEEE Trans. Inf. Theory*, vol. 52, no. 3, pp. 933–953, Mar. 2006.

[21] T. An, I. Song, H. Kwon, Y. H. Kim, S. Yoon, and J. Bae, "Decoding with expected length and threshold approximated (DELTA): A near-ML scheme for multiple-input-multiple-output systems," *IEEE Trans. Veh. Technol.*, vol. 58, no. 7, pp. 3234–3246, Sep. 2009.

[22] Y. Dai and Z. Yan, "Memory-constrained tree search detection and new ordering schemes," *IEEE. J. Sel. Topics in Sign. Process.*, vol. 3, no. 6, pp. 1026–1037, Dec. 2009.

[23] L. G. Barbero and J. S. Thompson, "Fixing the complexity of the sphere decoder for MIMO detection," *IEEE Trans. Wireless Commun.*, vol. 7, no. 6, pp. 2131–2142, Jun. 2008.

[24] J. Jálden, L. G. Barbero, B. Ottersten, and J. S. Thompson, "Full diversity detection in MIMO systems with a fixed-complexity sphere decoder," in *IEEE ICASSP*, Apr. 2007, pp. 49–52.

[25] ——, "The error probability of the fixed-complexity sphere decoder," *IEEE Trans. Signal Process.*, vol. 57, no. 7, pp. 2711–2720, Jul. 2009.

[26] L. G. Barbero and J. S. Thompson, "Performance of the complex sphere decoder in spatially correlated MIMO channels," *IET, Communications*, vol. 1, no. 1, pp. 122–130, Feb. 2007.

[27] M.-T. Le, V.-S. Pham, L. Mai, and G. Yoon, "A low complexity branch-and-bound-based decoder for V-BLAST systems with PSK signals," *Elsevier Signal Processing.*, vol. 89, no. 2, pp. 197–205, Feb. 2009.

[28] X.-W. Chang, X. Yang, T. Le-Ngoc, and P. Wang, "Partial regularization approach for detection problems in underdetermined linear systems," *IET Commun.*, vol. 3, no. 1, pp. 17–24, Jan. 2009.

[29] D. W. Waters and J. R. Barry, "The Chase family of detection algorithms for multiple-input multiple-output channels," *IEEE Trans. Signal Process.*, vol. 56, no. 2, pp. 739–747, Feb. 2008.

[30] Z. Luo, M. Zhao, S. Liu, and Y. Liu, "Generalized parallel interference cancellation with near-optimal detection performance," *IEEE Trans. Signal Process.*, vol. 56, no. 1, pp. 304–312, Jan. 2008.

[31] P. Aggarwal, N. Prasad, and X. Wang, "An enhanced deterministic sequential Monte Carlo method for near-optimal MIMO demodulation with QAM constellations," *IEEE Transactions on Signal Processing*, vol. 55, no. 6, pp. 2395–2007, Jun. 2007.

[32] J. W. Choi, B. Shim, A. C. Singer, and N. I. Cho, "Low-complexity decoding via reduced dimension maximum-likelihood search," *IEEE Trans. Signal Process.*, vol. 58, no. 3, pp. 1780–1793, Mar. 2010.

[33] D. Radji and H. Leib, "Interference cancellation based detection for V-BLAST with diversity maximizing channel partition," *IEEE. J. Sel. Topics in Sign. Process.*, vol. 3, no. 6, pp. 1000–1015, Dec. 2009.

[34] ——, "Simplified detection for MIMO systems using diversity maximizing incremental channel partition," in *Proc. of IEEE VTC Fall 2010*, Ottawa, Canada, Sep. 2010, pp. 1–5.

[35] ——, "Bounded complexity tree search MMSE detection for MIMO systems using improved channel partition preprocessing," in *Proc. of IEEE CCECE 2011*, Niagara Falls, Canada, May 2011, pp. 708–712.

[36] ——, "Asymptotic optimal detection for MIMO communication systems employing tree search with incremental channel partition preprocessing," *Trans. on Emerging Telecom. Tech.*, vol. 3, no. 6, pp. 1000–1015, May 2012.

[37] Y. Li and Z. Q. Luo, "Parallel detection for V-BLAST system," in *IEEE ICC*, New York, NY, USA, May 2002, pp. 340–344.

[38] H. Sung, K. B. Lee, and J. W. Kang, "A simplified maximum likelihood detection scheme for MIMO systems," in *IEEE VTC*, Oct. 2003, pp. 419–423.

[39] Z. Lei, Y. Dai, and S. Sun, "A low complexity near ML V-BLAST algorithm," in *IEEE VTC-Fall*, Dallas, TX, USA, Sep. 2005, pp. 942–946.

[40] X. Zhu and R. D. Murch, "Performance analysis of maximum likelihood detection in a MIMO antenna system," *IEEE Trans. Commun.*, vol. 50, no. 2, pp. 187–191, Feb. 2002.

[41] D. Tse and P. Viswanath, *Fundamentals of wireless communication*. Cambridge University Press, 2005.

[42] H. Zhang, H. Dai, Q. Zhou, and B. L. Hughes, "On the diversity order of spatial multiplexing systems with transmit antenna selection: a geometrical approach," *IEEE Trans. Inf. Theory*, vol. 52, no. 12, pp. 5297–5311, Dec. 2006.

[43] R. W. H. Jr., S. Sandhu, and A. Paulraj, "Antenna selection for spatial multiplexing systems with linear receivers," *IEEE Commun. Lett.*, vol. 5, no. 4, pp. 142–144, Apr. 2001.

[44] J. Jaldén and B. Ottersten, "On the maximal diversity order of spatial multiplexing with transmit antenna selection," *IEEE Trans. Inf. Theory*, vol. 53, no. 11, pp. 4273–4276, Nov. 2007.

[45] Y. Jiang, M. K. Varanasi, and J. Li, "Performance analysis of ZF and MMSE equalizers for MIMO systems: An in-depth study of the high SNR regime," *IEEE Trans. Inf. Theory*, vol. 57, no. 4, pp. 2008–2026, Apr. 2011.

[46] D. Seethaler, H. Artés, and F. Hlawatsch, "Dynamic nulling and cancelling for efficient near-ML decoding of MIMO systems," *IEEE Trans. Signal Process.*, vol. 54, no. 12, pp. 4741–4752, Dec. 2006.

[47] S.-R. Lee, S.-H. Park, S. W. Kim, and I. Lee, "Enhanced detection with new ordering schemes for V-BAST systems," *IEEE Trans. Commun.*, vol. 57, no. 6, pp. 1648–1651, Jun. 2009.

[48] Y. Shang and X.-G. Xia, "On fast recursive algorithms for V-BLAST with optimal ordered SIC detection," *IEEE Trans. Wireless Commun.*, vol. 8, no. 6, pp. 2860–2865, Jun. 2009.

[49] A. Gorokhov, D. A. Gore, and A. J. Paulraj, "Receive antenna selection for MIMO spatial multiplexing: theory and algorithms," *IEEE Transactions on Signal Processing*, vol. 51, no. 11, pp. 2796–2807, Nov. 2003.

[50] Y. Jiang and M. K. Varanasi, "Spatial multiplexing architectures with jointly designed rate-tailoring and ordered BLAST decoding-Part I: diversity-multiplexing tradeoff analysis," *IEEE Trans. Wireless Commun.*, vol. 7, no. 8, pp. 3252–3261, Aug. 2008.

[51] ——, "The RF-chain limited MIMO system-Part I: optimum diversity-multiplexing tradeoff," *IEEE Trans. Wireless Commun.*, vol. 8, no. 10, pp. 5238–5247, Oct. 2009.

[52] G. H. Golub and C. F. V. Loan, *Matrix compuations*, 3rd ed. John Hopkins University Press, 1996.

[53] C. Xiong, X. Zhang, K. Wu, and D. Yang, "A simplified fixed-complexity sphere decoder for V-BLAST systems," *IEEE Commun. Lett.*, vol. 13, no. 8, pp. 582–584, Aug. 2009.

[54] L. G. Barbero and J. S. Thompson, "Rapid prototyping of a fixed-throughput sphere decoder for MIMO systems," in *IEEE ICC*, Istanbul, Turkey, Jun. 2006.

[55] D. Wübben, J. Rinas, R. Böhnke, V. Kühn, and K.-D. Kammeyer, "Efficient algorithm for detecting layered space-time codes," in *Proc. ITG Conference on Source and Channel Coding*, Berlin, Germany, Jan. 2002, pp. 399–405.

[56] X.-W. Chang and C. C. Paige, "Euclidean distances and least squares problems for a given set of vectors," *Applied Numerical Mathematics*, vol. 57, pp. 1240–1244, 2007.

[57] Y. Dai and Z. Yan, "A modified MMSE-SD soft detector for coded MIMO-OFDM systems," in *Proc. IEEE. Int. Symp. Circuits Syst. (ISCAS)*, Seattle, Washington, USA, May 2008, pp. 312–315.

[58] C. Studer and H. Bölcskei, "Soft-input soft-output single tree-search sphere decoding," *IEEE Trans. Inf. Theory*, vol. 56, no. 10, pp. 4827–4842, Oct. 2010.

[59] C. Studer, A. Burg, and H. Bölcskei, "Soft-output sphere decoding: algorithms and VLSI implementation," *IEEE Journal on Selected Areas in Communications*, vol. 26, no. 2, pp. 290–300, Feb. 2008.

[60] D. Seethaler, J. Jaldén, C. Studer, and H. Bölcskei, "On the complexity distribution of sphere decoding," *IEEE Transactions on Information Theory*, vol. 57, no. 9, pp. 5754–5768, Sep. 2011.

[61] D. L. Milliner, E. Zimmermann, J. R. Barry, and G. Fettweis, "A fixed-complexity smart candidate adding algorithm for soft-output MIMO detection," *IEEE. J. Sel. Topics in Sign. Process.*, vol. 3, no. 6, pp. 1016–1024, Dec. 2009.

[62] A. van Zelst and J. Hammerschmidt, "A single coefficient spatial correlation model for multiple-input multiple-output (MIMO) radio channels," in *Proc. of 27th General Assembly of Int. Union of Radio Science (URSI)*, Aug. 2002, pp. 17–24.

[63] E. G. Larsson, "Diversity and channel estimation errors," *IEEE Trans. Commun.*, vol. 52, no. 2, pp. 205–208, Feb. 2004.

[64] J. G. Proakis, *Digital Communications*, 4th ed. Boston, USA: McGraw-Hill, 2001.

[65] A. W. van der Vaart, *Asymptotic Statistics*. Cambridge University Press, 1998.